

# Modelling of cavern convergence and brine permeation after plug & abandonment of deep salt caverns.

By  
Sander Jacob Maat

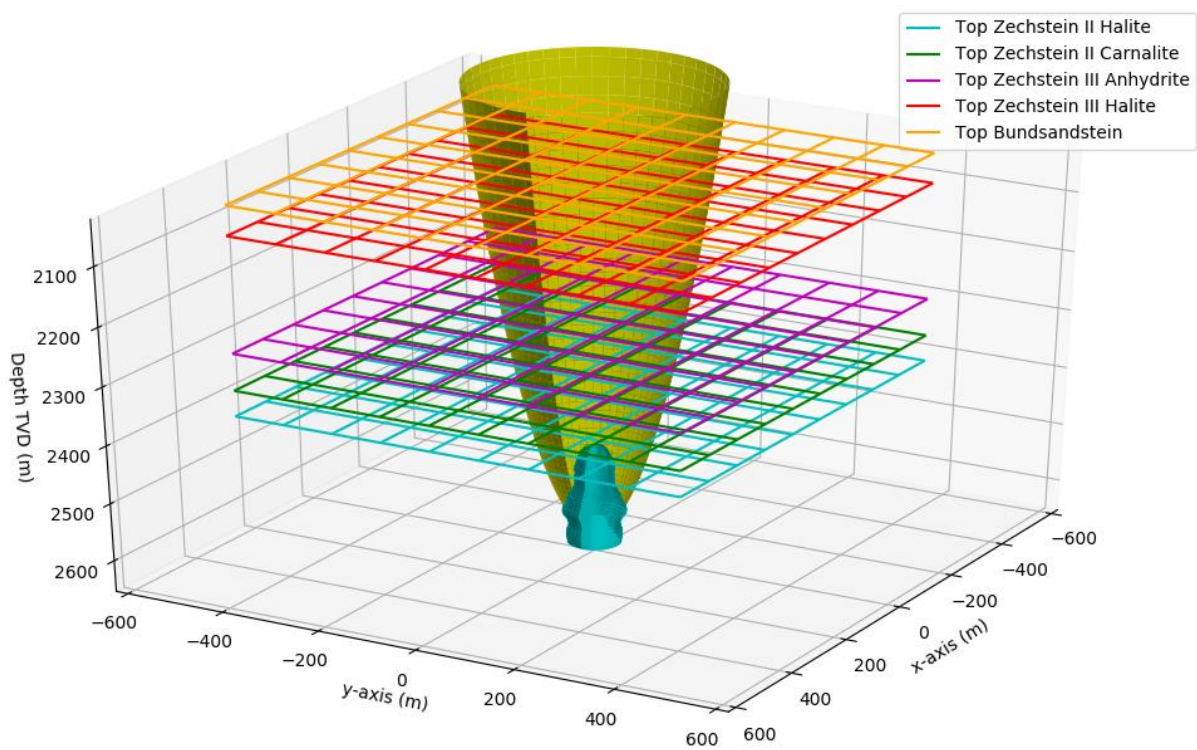


Figure 0.1 Impression of BAS-4 Cavern (in cyan) and permeation model (in yellow).



# Modelling of cavern convergence and brine permeation after plug & abandonment of deep salt caverns.

By

S.J. Maat

in partial fulfilment of the requirements for the degree of  
**Master of Science**  
in Applied Earth Sciences  
of the European Mining, Minerals and Environmental Programme  
at the Delft University of Technology,  
to be defended publicly on June 27, 2023

Supervisor:	Dr. M.W.N. Buxton,	TU Delft
Thesis committee:	Dr. M.W.N. Buxton, Dr. ir. D.M.J Ngan-Tillard, Prof. dr. B. Lottermoser Dr. W. Solowski	TU Delft (CEG, Resource Engineering) TU Delft (CEG, Geo-Engineering) RWTH Aachen University Aalto University
Advisors:	Ir. T.A. Chorus, Ir. V.J. de Ruiter, Ir. R. Mastaler,	Well Engineering Partners B.V. Well Engineering Partners B.V. Frisia Zout B.V.

An electronic version of this thesis is available at <http://repository.tudelft.nl/>.



## Preface

This thesis presents the results of research conducted by Sander Maat on modelling of cavern convergence and brine permeation after plug & abandonment of deep salt caverns. The research was conducted under the supervision of Mike Buxton and Dominique Ngan-Tillard (TU Delft), Tijmen Chorus and Volkert de Ruiter (Well Engineering Partners (WEP) B.V.), Robert Mastaler (Frisia Zout B.V.) and was completed as a requirement for the degree in Master of Applied Earth Sciences (European Mining Course) at TU Delft.

Title	:	Modelling of cavern convergence and brine permeation after plug & abandonment of deep salt caverns.	
Author	:	Sander Maat	
Date	:	27-06-2023	
Supervisor	:	Dr. M.W.N. Buxton	TU Delft
Thesis committee	:	Dr. M.W.N. Buxton, Dr. D.M.J Ngan-Tillard, Prof. Dr. B. Lottermoser Dr. W. Solowski	TU Delft (CEG, Resource Engineering) TU Delft (CEG, Geo-Engineering) RWTH Aachen University Aalto University
Advisors	:	Ir. T.A. Chorus, Ir. V.J. de Ruiter, Ir. R. Mastaler,	Well Engineering Partners B.V. Well Engineering Partners B.V. Frisia Zout B.V.
Address	:	Section of Resource Engineering Department of Geosciences & Engineering Delft University of Technology Stevinweg 1 2628CN Delft The Netherlands	

*All rights reserved.  
No parts of this publication may be reproduced,  
Stored in a retrieval system, or transmitted,  
In any form or by any means, electronic,  
Mechanical, photocopying, recording, or otherwise,  
Without the prior written permission of the  
Section for Resource Engineering*

## Contents

Preface.....	5
List of Figures.....	8
List of tables .....	10
Abstract .....	12
1. Introduction.....	14
1.1 Introduction on topic and study.....	15
1.2 Research questions.....	16
1.3 Objectives .....	16
1.4 Research design.....	17
1.5 Out of scope .....	18
2. Cavern history and literature review.....	19
2.1 History of Frisia caverns .....	19
2.2 Literature review .....	20
2.3 Synthesis of literature .....	23
3. Convergence model.....	24
3.1 Measuring and modelling a cavern .....	24
3.2 Review of squeeze models .....	28
3.3 Model description .....	33
3.4 Model results for BAS-4.....	35
4. Sensitivity analysis of convergence model.....	38
4.1 Base case and deviations.....	38
4.2 Results sensitivity analysis.....	41
Discussion of sensitivity analysis .....	48
4.3 Conclusion on sensitivity analysis .....	49
5. Intermediate conclusions and recommendations convergence model.....	50
5.1 Conclusions convergence model.....	50
5.2 Recommendation on parameters and final cases.....	50
6. Brine permeation model .....	52
6.1 Concepts review permeation .....	52
6.1.1 Detailed description of geology, rock types and leakage mechanisms.....	52
6.1.2 Permeation shapes.....	55
6.2 Model description .....	58

6.2.1	Cone model .....	59
6.2.2	Paraboloid model .....	60
6.2.3	Adjusted paraboloid model .....	61
6.3	Modelling results for BAS-4.....	63
6.3.1	Cone Model .....	63
6.3.2	Paraboloid model .....	63
6.3.3	Adjusted paraboloid model .....	64
6.4	Permeability of halite .....	65
6.5	Discussion on other permeation mechanisms .....	68
6.5.1	Threshold pressure deficit for cavern convergence .....	68
6.5.2	Preferential flow due to heterogeneities .....	68
6.5.3	Stringers/floaters in salt formations .....	68
6.6	Comparison to other models.....	69
6.7	Subsidence bowl.....	70
7.	Sensitivity analysis of brine permeation model .....	73
7.1	Base case and deviations.....	73
7.1.1	Variability base case model .....	73
7.1.2	Variations on base case model .....	74
7.2	Results sensitivity analysis.....	77
7.2.1	Variability base case model .....	77
7.2.2	Variations on base case model.....	77
7.3	Discussion on sensitivity analysis .....	79
7.3.1	Variability base case model .....	79
7.3.2	Variations on base case model.....	80
8.	Intermediate conclusion on permeation model .....	81
9.	Discussion .....	82
10.	Conclusion and recommendations.....	84
10.1	Conclusion .....	84
10.2	Recommendations.....	85
11.	References.....	86
12.	Appendices .....	89

## List of Figures

Figure 0.1 Impression of BAS-4 Cavern (in cyan) and permeation model (in yellow).....	1
Figure 1.1 Representation of lithostratigraphic column of the barradeel concession (WEP, 2014) .....	14
Figure 1.2 Illustration of salt cavern.....	14
Figure 1.3 Content of research design .....	17
Figure 2.1 Map of concession and well of Frisia (retrieved from nlog.nl on 7-2-23).....	19
Figure 2.2 Timeline of relevant research done .....	23
Figure 3.1 Cavern with sonar tool .....	24
Figure 3.2 Cavern with sonar tool and obstruction.....	25
Figure 3.3 3D interpolation of BAS-4 cavern from sonar measurement.....	25
Figure 3.4 Sonar tool assembly (extracted from flodim.fr).....	25
Figure 3.5 Pressures related to the cavern for BAS-4 .....	26
Figure 3.6 Example of 4-layer cavern .....	27
Figure 3.7 Strain rate per day vs Pressure deficit (8-30MPa) of all different models.....	29
Figure 3.8 Squeeze per year vs Pressure deficit (0-8MPa) of all different models graph and table.....	30
Figure 3.9 Linear and Nonlinear part of WEP model separated (high pressure deficit) .....	31
Figure 3.10 Linear and Nonlinear part of WEP model separated (low pressure deficit) .....	31
Figure 3.11 Synoptic View of Laboratory Creep Test Results on Waste Isolation Pilot Plant Salt in Relation to Findings From Creep Tests on Various Salt Specimens at Low Deviatoric Stresses (Bérest et al., 2019)31	
Figure 3.12 (a) Deformation map for rock salt drawn at a constant temperature of 60 °C in log grain size vs. log stress space. (b) Deformation map at constant grain size (d = 5mm) drawn in log strain rate vs. log stress space. (van Oosterhout et al., 2022).....	32
Figure 3.13 BAS-4 Base case 3D cavern.....	35
Figure 3.14 Slice volume over time .....	36
Figure 3.15 Cumulative permeation and cavern volumes over time .....	37
Figure 4.1 Cavern squeeze and permeation of slice thickness analysis.....	41
Figure 4.2 Cavern squeeze and permeation of slice width analysis.....	42
Figure 4.3 Cavern squeeze and permeation of pressure deficit analysis.....	43
Figure 4.4 Cavern squeeze and permeation of specific weight lithosphere analysis.....	44
Figure 4.5 Cavern squeeze and permeation of specific weight brine analysis.....	45
Figure 4.6 Cavern squeeze and permeation of nonlinear part squeeze model analysis .....	46
Figure 4.7 Cavern squeeze and permeation of linear part squeeze model analysis.....	47
Figure 6.1 Core of BAS-1 at a depth of 2320m, red arrows point at thin anhydrite layers between the halite.....	52
Figure 6.2 Cross section made with the DGMdeep v5.0 mode, retrieved from dinoloket.nl on 21-3-2023 .....	53
Figure 6.3 Different possible brine leakage mechanisms implemented from (Brouard Consulting, 2019b; Lux, 2010; WEP, 2010, 2021).....	53
Figure 6.4 Impression of knotted cone permeation model .....	55
Figure 6.5 Impression of sunken paraboloid model.....	56
Figure 6.6 Impression of adjusted paraboloid model .....	57
Figure 6.7 Cone model on cavern BAS4 .....	59
Figure 6.8 Paraboloid model on BAS-4 Cavern.....	60
Figure 6.9 Adjusted paraboloid model on BAS-4 Cavern .....	61

Figure 6.10 Criteria for permeability of rock salt (Rokahr et al., 2002) .....	65
Figure 6.11 Subsidence with distance from the cavern .....	72
Figure 7.1 Sensitivity analysis horizontal flow Zechstein-II Halite .....	75
Figure 7.2 Sensitivity case horizontal flow Carnallite.....	76
Figure 7.3 West-East (Left) and North-South (Right) cross section of Zechstein over BAS-4 cavern (DGM-Deep model, extracted 2-5-2023). .....	79
Figure 12.1 Shut in pressure data top BAS-2 cavern and lithostatic pressure at top of cavern .....	89
Figure 12.2 Comparison to WEP model and production data up to a deficit of 12 MPa.....	90
Figure 12.3 Recent echo measurement of BAS-4 Cavern .....	92
Figure 12.4 BAS-4 Base case 2D cavern after 0 years .....	93
Figure 12.5 BAS-4 Base case 2D cavern after 1000 years .....	94
Figure 12.6 BAS-4 Base case 2D cavern after 2000 years .....	94
Figure 12.7 BAS-4 Base case 3D cavern after 0 years .....	95
Figure 12.8 BAS-4 Base case 3D cavern after 1000 years .....	96
Figure 12.9 BAS-4 Base case 3D cavern after 2000 years .....	96
Figure 12.10 Stack plot of layers over the first 1000 years .....	97
Figure 12.11 Stack plot of layers over 5000 years.....	97
Figure 12.12 Line plot of layers over the first 1000 years.....	98
Figure 12.13 Line plot of layers over 5000 years .....	98
Figure 12.14 Cavern permeation rates over time for slice thickness cases .....	99
Figure 12.15 Cavern and permeation volume over time for slice thickness cases .....	99
Figure 12.16 Cavern permeation rates over time for slice width cases.....	100
Figure 12.17 Cavern and permeation volume over time for slice width cases.....	100
Figure 12.18 Cavern permeation rates over time for pressure deficit cases.....	101
Figure 12.19 Cavern and permeation volume over time pressure deficit cases.....	101
Figure 12.20 Cavern and permeation volume over time for specific weight lithosphere cases.....	102
Figure 12.21 Cavern permeation rates over time for specific weight lithosphere cases.....	102
Figure 12.22 Cavern permeation rates over time for specific weight brine cases.....	103
Figure 12.23 Cavern and permeation volume over time for specific weight brine cases.....	103
Figure 12.24 Cavern permeation rates over time for nonlinear part squeeze model cases.....	104
Figure 12.25 Cavern and permeation volume over time for nonlinear part squeeze model cases.....	104
Figure 12.26 Cavern permeation rates over time for linear part squeeze model cases.....	105
Figure 12.27 Cavern and permeation volume over time for linear part squeeze model cases.....	105
Figure 12.28 Permeation model vertical flow Zechstein-II Halite .....	109
Figure 12.29 Permeation model vertical flow Zechstein-II Carnallite.....	110

## List of tables

Table 3.1 Example of cavern dimension input .....	33
Table 3.2 Input variables for base case of BAS-4 .....	35
Table 4.1 Results of Slice Thickness sensitivity analysis.....	41
Table 4.2 Results of Slice Width sensitivity analysis.....	42
Table 4.3 Results of Pressure Deficit sensitivity analysis. ....	43
Table 4.4 Results of specific weight lithosphere sensitivity analysis .....	44
Table 4.5 Results of specific weight brine sensitivity analysis. ....	45
Table 4.6 Results of nonlinear part squeeze model sensitivity analysis .....	46
Table 4.7 Results of linear part squeeze model sensitivity analysis.....	47
Table 5.1 Changes in input values for the P10,P50 and P90 cases .....	51
Table 5.2 Time for 0.11 Mm <sup>3</sup> of brine to permeate and permeation rate for the P10, P50 and P90 cases	51
Table 6.1 Top of layers and cavern.....	58
Table 6.2 Porosity inputs for each layer in base case .....	58
Table 6.3 Brine storage capacity and rock volume per layer cone model .....	60
Table 6.4 Brine storage capacity and rock volume per layer paraboloid model.....	61
Table 6.5 Base case a and b factors of adjusted paraboloid model.....	61
Table 6.6 Brine storage capacity and rock volume per layer adjusted paraboloid model.....	62
Table 6.7 Time in year for each layer to fill up in cone model. ....	63
Table 6.8 Time in year for each layer to fill up in paraboloid model. ....	63
Table 6.9 Time in year for each layer to fill up in adjusted paraboloid model. ....	64
Table 6.11 Permeabilities for models and corresponding effective pressures (permeabilities in m <sup>2</sup> ) .....	66
Table 6.12 Cavern permeation rates using permeability for top half of cavern in m <sup>3</sup> /year. ....	66
Table 6.13 Cavern permeation rates using permeability for whole of cavern in m <sup>3</sup> /year.....	67
Table 6.10 Subsidence predictions P50 case together with permeation rates (converted brine) .....	72
Table 7.1 Porosities tested in sensitivity analysis. ....	74
Table 7.2 Case for pressure increase when Zechstein-III Anhydrite is reached.....	78
Table 7.3 Case for pressure increase when Zechstein-III Halite is reached. ....	78
Table 7.4 Results case for more horizontal flow in the Zechstein-II Halite.....	78
Table 7.5 Results case for more horizontal flow in the Zechstein-II Carnallite.....	78
Table 12.1 GeoDelft squeeze model parameters.....	91
Table 12.2 WEP squeeze model parameters.....	91
Table 12.3 BAS-4 Base case 2D cavern after 500 years.....	93
Table 12.4 BAS-4 Base case 3D cavern after 500 years.....	95
Table 12.5 Permeation model sensitivity analysis top height Zechstein-II Halite.....	106
Table 12.6 Permeation model sensitivity analysis top height Zechstein-II Carnallite.....	106
Table 12.7 Permeation model sensitivity analysis top height Zechstein-III Anhydrite .....	106
Table 12.8 Permeation model sensitivity analysis top height Zechstein-III Halite.....	107
Table 12.9 Permeation model sensitivity analysis porosity Zechstein-II Halite .....	107
Table 12.10 Permeation model sensitivity analysis porosity Zechstein-II Carnallite .....	107
Table 12.11 Permeation model sensitivity analysis porosity Zechstein-III Anhydrite.....	108
Table 12.12 Permeation model sensitivity analysis porosity Zechstein-III Halite .....	108
Table 12.13 Volumes of base case adjusted paraboloid model (for comparison).....	109
Table 12.14 Model parameters sensitivity analysis vertical flow Zechstein-II Halite .....	109

Table 12.15 Permeation volumes sensitivity analysis vertical flow Zechstein-II Halite ..... 109  
Table 12.16 Model parameters sensitivity analysis vertical flow Zechstein-II Carnallite ..... 110  
Table 12.17 Permeation volumes sensitivity analysis vertical flow Zechstein-II Carnallite ..... 110

## Abstract

Frisia Zout B.V. extracts salt from the subsurface by means of solution mining in the north-western part of The Netherlands. The caverns are situated in the Zechstein-II Halite at a depth of around 2.5 km. Because of this depth and the low operating pressure (around 60% of lithostatic pressure) the salt creep within the cavern is high. Once a cavern is at the end of its lifetime it is decommissioned and shut in. During the shut-in period the cavern blanket fluid is removed and replaced with brine and gets time to equalize in pressure and temperature with its surroundings before being permanently abandoned. At the time of abandonment there is still a small pressure deficit (cavern brine at 98% of lithostatic pressure at roof of cavern). At this pressure deficit there is, in theory, still some salt creep because of the difference in pressure between the cavern brine and surrounding salt walls induced by lithostatic pressure. Since the cavern is closed and still creeps, the brine will escape by means of permeation through the surrounding salt walls and roof. At this point an equilibrium is reached between the cavern convergence and the brine permeation around the cavern.

This research aims to get a better understanding of the cavern convergence and permeation processes after abandonment. For this, a cavern convergence- and brine permeation model is made. Next to this the potential surface subsidence due to the migration of brine to more permeable layers is investigated. In the convergence model, the cavern is modelled as a stack of cylinders and a Norton-Hoff power law squeeze model is applied to the cavern. The squeeze model consists of 2 parts, a linear and a nonlinear part. The nonlinear part is most significant during the production phase and in these high-pressure deficits the squeeze model is fitted on the available production data. Recent creep tests on salt samples under lower pressure deficits (Bérest et al., 2019) have confirmed that the linear part becomes the most significant in the low-pressure deficit region and have shown that the linear creep is smaller than the linear component of existing squeeze model used for production.

Next to this a sensitivity analysis was done on the convergence model by varying the input variables of the model. The parameters that have a large uncertainty and have a large impact on the model were the linear part of the squeeze model and the width of a slice. To give a range of outputs of the convergence model a P10, P50 and P90 scenario is created where these are percentiles from the input range of the sensitivity analysis. The outcome of the convergence model at a cavern size of  $1\text{Mm}^3$  suggests a yearly cavern convergence of around of 5, 103 and  $2313\text{ m}^3/\text{year}$  for the P10, P50 and P90 cases respectively.

Since there is an equilibrium between the cavern convergence and the brine permeation, the output of the convergence model (convergence rate) can be used as an input for the permeation model (permeation rate). For the permeation model, different paraboloid shapes are fitted on each layer and are filled with brine from the converging cavern. Once all the salt layers are filled in, the brine reaches more permeable layers and can freely flow over a larger area. The permeation model is run with the P10, P50 and P90 convergence model scenarios as an input and predicts that the system fills after 26, 588 and 12,363 years respectively. At this point there could be some subsidence because the brine can freely flow over a larger area in the more permeable layers above the Zechstein. This subsidence is  $0.016\text{ mm/year}$  for the P50 case after 588 years. A negligible amount compared to unrelated subsidence processes.

To conclude the cavern convergence rates (even the P10 at  $5\text{m}^3/\text{year}$ ) are high compared to the permeability of salt according to the Darcy flow law (around  $17\text{ l/year}$ ). This could have multiple explanations. From the cavern perspective, the cavern convergence rates could be lower. This could be because of a threshold pressure for salt creep to occur (van Oosterhout et al., 2022) or because of some inaccuracies in the linear component of the squeeze model. Future research could focus on determining the creep rates of salt under low-pressure deficits. From the permeation perspective, other permeation paths next to permeability could be at play as well. In the cavern there could be permeation via anhydrite alterations or via micro fractures created during the production phase of the cavern. It would be good to look at these permeation processes in the future. Next to this the secondary porosity of the salt remains a question as well. A good understanding of this porosity is needed to assess the storage capacity of the overlying salt layers before the brine enters more permeable zones.

## 1. Introduction

Frisia Zout B.V. (abbreviated as Frisia in this report) operates multiple caverns from Harlingen (North-West Friesland), The Netherlands. Frisia uses the process of solution mining to extract salt from the Zechstein-II Halite layer that extends from roughly 2400 to 3100 meters, shown in figure 1.1 (not to scale). Solution mining is the process of injecting fresh water into the subsurface, dissolving the salt and producing the brine. The salt in place is replaced with this brine and a cavern is created. This brine is then evaporated at the surface to get the solid salt out. This mining of the salt caverns at Frisia is done by a single well with 2 inner tubing's (figure 1.2). The last cemented casing (in yellow) contains a blanket fluid, this blanket fluid is a fluid that can not dissolve the salt. The blanket prevents the cavern from expanding upwards and makes sure that a stable roof is created. The inner tube (dark blue) is where the freshwater is injected; salt dissolves in this water and is produced as brine in the outer tubing (light blue).

The lithostratigraphic column of where the caverns are situated is shown in figure 1.1. As discussed, the salt is mined from the Zechstein-II Halite. On top of that there is a carnallite layer with an approximate thickness of 40 meters, overlying the carnallite is an anhydrite layer with a thickness of approximately 60 meters. Overlying the anhydrite is the Zechstein III halite with a thickness of 200 meters. On top of that is the bundsandstein. This is a roughly 100-meter-thick sandstone layer with significantly higher porosity. Once the brine can exit the salt layer it can freely flow over these higher permeable layers. Note that this sandstone layer is not clean. There are clays and other imperfections present in this layer but it does have a much higher porosity and permeability than the salt layer below. On top of these layers are several other layers, the complete lithostratigraphic column off all the other layers is shown in figure 1.1. In addition to the high depth of the cavern, it is also important to mention its size. Frisia's caverns have a height of up to 200 meters and a width of over 100 meters. For comparison, the highest building in The Netherlands (Zalmhaventoren, Rotterdam) has approximately the same height but only a third of the width.

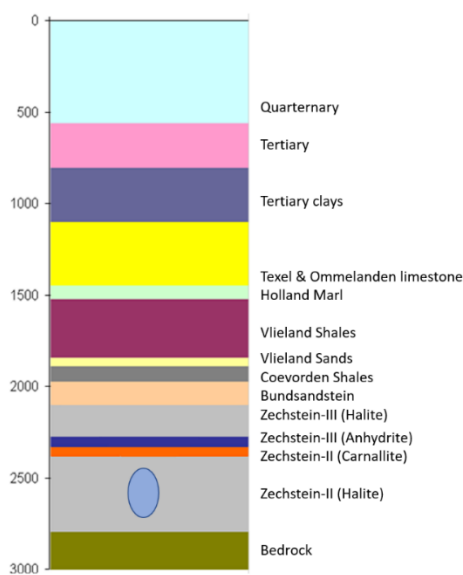


Figure 1.1 Representation of lithostratigraphic column of the barradeel concession (WEP, 2014)

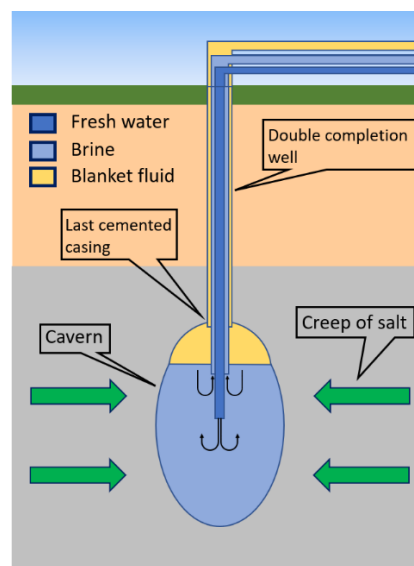


Figure 1.2 Illustration of salt cavern

## 1.1 Introduction on topic and study

The caverns are at a great depth and operated at a fluid pressure of 60% of lithostatic pressure. Due to this pressure difference, the salt creeps in the direction of the cavern. This leads to the 'squeeze' of the salt (green arrows in figure 1.2). Once the cavern has reached its final volume the salt squeeze allows steady state production, meaning that the salt can be produced at the cavern closure rate and therefore the caverns keep the same size or slowly close in.

Existing models are accurate for the production phase of such a cavern and assume that the salt is governed by a Norton-Hoff constitutive law, i.e., that it behaves as a perfectly viscoplastic or viscoelastic material with a viscosity varying with a linear and nonlinear component as a function of the applied stress. These models have been validated with available field data and are considered as accurate. When the cavern reaches its mining limits (surface subsidence and cavern size) or when the cavern reaches the last cemented casing because it slowly moves upwards, it is decommissioned. The blanket fluid is removed and the cavern is shut in. The reduction in pressure differences between the cavern brine and cavern walls leads to extremely low cavern squeeze rates. There is no data to validate the squeeze model for the shut-in phase of a cavern because the cavern convergence rates become much lower than is possible to measure. After the pressure and temperature in the cavern is stabilized the cavern is abandoned.

The cavern still tends to 'squeeze' since there is still a pressure deficit. However, the cavern is closed so the only way for the brine to escape is via permeation through the cavern walls and roof. Permeation is the process of a fluid moving through the voids of a rock mass. Salt is often considered impermeable, but under high pressures and temperatures salt becomes slightly permeable. After the decommissioning of a cavern, the cavern pressure rises and an equilibrium between the cavern squeeze and brine permeation is reached (Brouard Consulting, 2019a).

The current permeation model (WEP, 2010) assumes that the shape of the permeation front is an upside-down knotted cone with an angle of 45 degrees. Using this assumption, the time it takes for the brine to permeate through the sequence of impermeable evaporite layers above the cavern (the Zechstein-II Halite, Zechstein-II Carnallite, Zechstein-III Anhydrite and the Zechstein-III Halite, see figure 1.1) and reach the overlaying permeable layer (the Bundsandstein, see figure 1.1) is estimated.

If the brine stays within the salt formations around the cavern, no surface subsidence is present. When brine permeates from the salt layer to the sandstone above, the brine can flow away and can cause potential additional subsidence. The rate of this subsidence at the surface can be predicted with the convergence and permeation model.

## 1.2 Research questions

The research can be divided into 2 parts, the squeeze model and the permeation model. From these models, it is possible to predict long term cavern development and brine permeation after plug and abandonment. This leads to the main research question:

- What are the cavern convergence rates in an abandoned cavern and in what timeframe will the brine permeate through the salt layers above the cavern and permeate out of the Zechstein to the overlying layers?

Since the research is divided in 2 parts, the convergence model and the permeation model, 2 separate sets of sub-questions can be defined.

Convergence model:

- What are the current concepts and techniques for measuring cavern convergence?
- How does the Norton-Hoff based model perform in low pressure deficits?
- What is the impact of varying model inputs on the output of the convergence model?

Permeation model:

- What are the aspects of the current permeation model and what does previous research suggest about permeation fronts of brine?
- What variations can be made on parameters in the permeation model and how do these variations impact the outputs of the permeation model?
- At what time and rate is the outflow of brine into the sandstone layer above?
- What is the final additional surface subsidence and subsidence rate in the different models?

## 1.3 Objectives

From the research questions several objectives can be defined, these are:

- Build a new cavern convergence model for the cavern after abandonment.
- Test out the sensitivity of the convergence model by sensitivity analysis.
- Build new permeation models, use the output from the convergence model (brine permeation) as input for the permeation model.
- Test out the sensitivity of the new permeation model.
- Consider various aspects of the new permeation model and model different scenarios.
- Investigate permeation paths and potential subsidence.

## 1.4 Research design

The research is designed and sketched in figure 1.3.

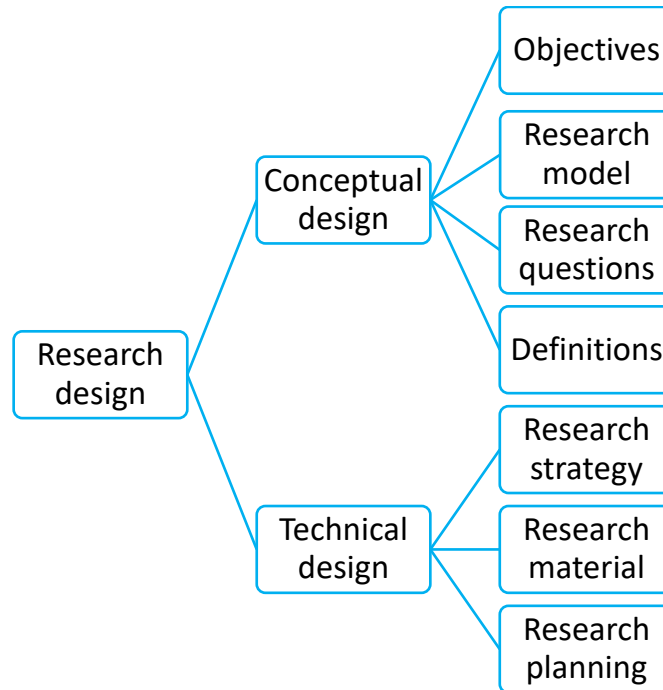


Figure 1.3 Content of research design

A summary of each of the items is listed below:

- Objectives
  - o The objective of this study is to get a better understanding of the convergence and permeation processes of a deep cavern after plug and abandonment.
- Research model
  - o First existing concepts and models are reviewed. With that in mind an improved model is created. The new model is tested by varying the input parameters. This will be done for both the convergence and permeation aspects of the cavern.
- Research questions
  - o The main research question is: What are the cavern convergence rates in an abandoned cavern and in what timeframe will the brine permeate through the salt layers above the cavern and permeate out of the Zechstein to the overlying layers? All the research questions are defined in chapter 1.2.
- Research strategy
  - o Cavern history and literature review of research
  - o Construction of convergence model
  - o Sensitivity analysis of convergence model
  - o Construction of permeation model
  - o Sensitivity analysis of permeation model

- Research material
  - o Relevant data for thesis are the cavern dimensions and lithology, squeeze model and parameters defined by lab tests and drilling operations. For the permeation model the rock properties of the different salt layers are used together with recent research on cavern abandonment.
- Research planning
  - o A brief planning of activities is made in the research proposal.

### 1.5 Out of scope

This study has limited time constraints; therefore, certain elements will not be assessed in the research.

First, the thermal expansion will not be considered; this has less relevance to the long-term processes of the cavern. After shut-in the brine takes 10-15 years to reach equilibrium with the rock temperature. Part of this time is still during the shut-in period of a cavern and will therefore not be relevant for the long-term modelling after plug and abandonment (Brouard Consulting, 2019b).

There is already research done on the carnallite layer that overlies the cavern. When halitic brine reaches the carnallite layer a chemical reaction occurs where the halite brine converts to a carnallitic brine. During this conversion a volume expansion takes place. This will be considered in the modelling, but not in detail. The report done by Well Engineering Partners (WEP, 2010) presents a sensitivity analysis on this expansion and Well Engineering Partners (WEP, 2014) explored more in depth scenarios modelling different possibilities such as cavern creation or roof collapse.

Surface subsidence is only briefly considered. The objective of the thesis is to get a better understanding of the cavern convergence and brine permeation processes. Although subsidence is not expected to happen for a long time after abandoning the cavern, if it does happen, the subsidence would be over a long time with a low rate. On top of that the subsidence can occur over such a wide area that other non-related subsidence processes (e.g., shallow settling of layers) could be more significant as well. Surface subsidence is therefore not likely to be significant and won't be considered in depth.

Lastly, the sump of a cavern will not be considered. The sump is the bottom part of a cavern. Within the timeframe of when a cavern starts producing and ends producing the cavern moves upwards closing the bottom part (the sump). The Zechstein-II layer consists of roughly 95% salt. The other 5% of insoluble materials will stay inside the cavern and build up in the sump. The residual pore volume in the sump is not significant compared to the total cavern volume. The sump has much lower convergence rates since it is already compacted during production.

## 2. Cavern history and literature review

In this chapter the history of the Frisia caverns is explained. Next the relevant available research on salt caverns is discussed. Finally, the chapter is concluded with a synthesis of the available literature.

### 2.1 History of Frisia caverns

Frisia operates multiple caverns in The Netherlands, the wells and concessions of Frisia are shown in figure 2.1. The Barradeel and Barradeel II concessions have caverns (BAS caverns) that are shut in or plugged and abandoned. The Havenmond concession currently has 1 well and is producing.

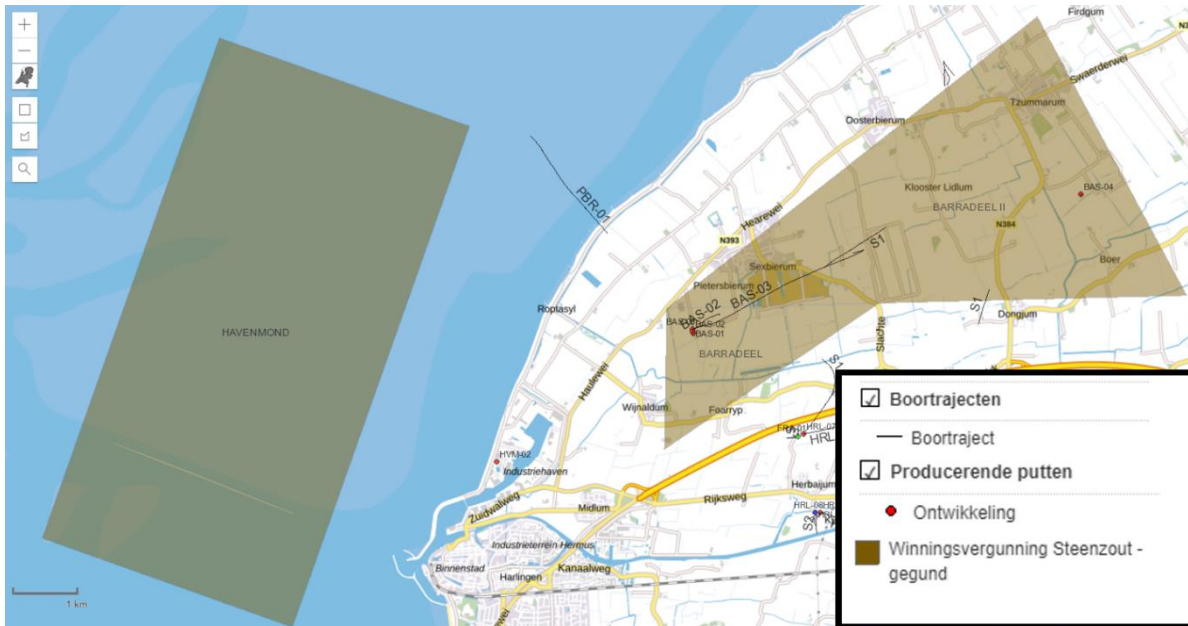


Figure 2.1 Map of concession and well of Frisia (retrieved from nlog.nl on 7-2-23)

The caverns/wells of Frisia are BAS-1, BAS-2, BAS-3, BAS-30, BAS-4 and HVM-2. Of those caverns BAS-2, BAS-3 and BAS-30 are currently plugged and abandoned. BAS-1 and BAS-4 are shut in of which BAS-1 is in preparation for plug & abandonment. HVM-2 is currently the only producing salt cavern. Currently, Frisia produces roughly 1 million tons of salt per year. The size of the caverns ranges between 200,000 m<sup>3</sup> and 1,000,000 m<sup>3</sup>.

Previous models were made for the abandonment of BAS-3 (Lux, 2010; WEP, 2010), these will be discussed in chapter 6.6. For the new models, the input parameters from BAS-3 will be used and outputs checked against those generated with the old model for BAS-3. The permeation model will also be checked with the BAS-3 model. However, for the different scenarios of the squeeze model and permeation model, the input data of BAS-4 will be used.

As can be seen in figure 2.1, BAS-4 is a relatively standalone cavern. It is further away from the other BAS caverns and therefore has little to no interference with them. BAS-1 and BAS-2 are close together, the same goes for BAS-3 and BAS-30. With a size of around 1 Mm<sup>3</sup>, BAS-4 is also a bigger cavern compared to the other caverns.

BAS-4 was drilled in 2004 and taken into production in 2006. The cavern produced salt until 2021 when the shut-in happened. The mining limits permit for onshore caverns was expiring by the end of 2021. Currently, the cavern is being monitored and will be abandoned in around 10 years.

## 2.2 Literature review

Numerous studies have been done on salt solution caverns. All caverns start with brine production but for some, the purpose of the cavern changes and they become a storage cavern for instance. Not all caverns are the same as well; they are in different geological settings or at different depths. Studies on caverns with other uses than salt production or in other geological settings have little relevance to this research since this study investigates the post-abandonment behaviour of caverns used purely for salt production and caverns that are at a much greater depth compared to other caverns. This chapter consists of a brief history of relevant research done on salt caverns. A short timeline summary of the research discussed in this chapter is shown in figure 2.2.

Research done for this thesis consists of theory research and field tests. An example of a field study is 'A salt cavern abandonment test' (Bérest et al., 2001). Here an 18-month test by not releasing any pressure from the well head was done. In this way the cavern could find an equilibrium pressure. This equilibrium is reached when the cavern creep (squeeze) is equal to the brine permeation through the cavern walls and ceiling. Therefore, the cavern still squeezes and the brine escapes due to permeability in the salt. This permeation prevents the pressure build-up in the cavern and equalizes to the cavern brine pressure. The study concluded that salt formation permeability must be considered when modelling cavern abandonment. When large pressures build up, fracture creation can happen which is a scenario that is evaluated often. This is mostly because of a thermal effect or if there are tectonic forces on a cavern. This is not taking place in Frisia caverns. However, having a shut-in phase of the cavern to understand the processes is important before abandoning the cavern completely. This research will continue this concept. However, in this research it is assumed that the cavern is already equalized with its surroundings and tries to give a better insight on the longer-term post-abandonment processes.

On the long-term abandonment there is also research done. Well Engineering Partners prepares abandonment risk analysis reports for each of the caverns operated by Frisia. For the BAS-3 cavern, a model for cavern convergence and permeation was set up as well. (WEP, 2010) describes important aspects of cavern abandonment including modelling of the cavern after plug and abandonment. An analysis of various aspects with different scenarios is done. A basic setup for the convergence model and permeation model is made in (WEP, 2010) using a nonlinear, low linear and high linear model for the convergence. For the permeation model, a knotted cone on top of the cavern is used to accumulate the brine over time and a breakthrough time to the sandstone layer above is estimated. WEP elaborated on the first report in (WEP, 2014). It revised some concepts and gave a second opinion on the model. This MSc graduation research continues this work done by WEP to gain a better understanding of the post abandonment cavern processes.

Continuing the long-term behaviour, long-term numerical modelling for salt caverns is done as well. A generic model for predicting the long-term behaviour of a cavern after abandonment is made in (Thoraval et al., 2015). The paper provides information about the evolution of abandoned salt caverns from numerical simulations. Issues with analytical models are that they rely on several simplifications such as pure homogenous layers or perfect cavern shapes (cylindrical or spherical). The numerical modelling considers the brine warming, cavern creep closure, permeation of brine, brine leaks and additional dissolution. In the end, a general numerical model came out that could simulate the processes well comparing the outcomes to monitoring data from a cavern. Another conclusion was that the outcomes of the simulations heavily depend on the inputs such as volume, shape and specific salt parameters. The research done in this report will not cover numerical modelling; an analytical model will

be used to model the cavern processes. Since the inputs of the caverns after abandonment are hard to measure a thorough sensitivity analysis will be done on the new models proposed in this research.

Another study also looked into the processes of a cavern after abandonment. (Brouard et al., 2017) describes what happens to a cavern after its being sealed and abandoned. It discussed factors that contribute to cavern pressure evolution, one of which is a salt mass creep. The report states that the processes can be described by a Norton-Hoff power law. The Norton-Hoff power law also forms the basis for the models used by WEP. (Brouard et al., 2017) also describes salt permeability. Here it is stated that for short-term periods it is not significant but becomes more important in the longer term. The report concludes that factors like cavern compressibility, brine thermal expansion and leak offs can be assessed accurately. However, in the processes of squeeze and permeation uncertainties remain. This research will try to give a better insight into the cavern squeeze and permeation by creating new models and conducting a sensitivity analysis on them. The input parameters will be defined from available data considering their inaccuracies.

A large study on caverns was done recently, and summarized in *Conclusions and Recommendations KEM-17* (Brouard Consulting, 2019b). The study was conducted upon request of the State Supervision on Mines (SodM) with the objective: *“to be able to predict the occurrence of cavern instability and uncontrolled subsidence (including sinkholes) and to define and supervise cavern risk management protocols ensuring that cavern instability and uncontrolled subsidence risks stay at acceptable levels during operation and after abandonment.”* The research was divided into 3 parts, namely: microscale, cavern scale and salt dome scale. The research was very broad (including research less relevant on this topic as well). The most important part for this research is the cavern scale report *Cavern Scale* (Brouard Consulting, 2019a). This separate report consists of a literature research and has multiple conclusions, the most relevant for this research being that *“A vast majority of authors agreed that evolution of a shut-in cavern is governed by three main phenomena”* (Brouard Consulting, 2019a). These 3 are brine warming, creep closure and brine permeation. When the brine warming can be neglected, the cavern squeeze and permeation balance each other and an equilibrium pressure is reached. It should be noted, that for deep caverns (>1000m) the equilibrium pressure is higher and the risk of fracturing should also be considered. The risk of fracturing was assessed in (WEP, 2021), by analysing the pressures in around the cavern it was concluded that fracturing around the cavern is an unlikely scenario. In terms of subsidence, it states that it's hard to predict how brine leakage to an overlying porous layer can cause surface subsidence. However, real life examples suggest an increase of subsidence in certain scenarios. In these scenarios the caverns had issues with well that weren't abandoned properly or already instable situations that escalated and caused subsidence. Furthermore, the report suggests a shut-in phase long enough to let the cavern temperature settle, gather information and monitor pressure before permanently sealing the cavern. Frisia operated caverns are at a great depth and are kept open for a period of 5-15 years after production. In this shut-in phase the cavern processes and pressures are constantly monitored and most of the warming of the cavern happens in this period. In this way as much data as possible is gathered before abandoning the cavern. This data can be used for the post abandonment modelling of the cavern and assures that for the first part of the shut-in no over pressures occurs and the pressure equalizes. After it is shown that the cavern pressures and temperatures equalize the cavern can be abandoned safely.

The microscale report (Brouard Consulting, 2019c) has some views on brine permeation. The brine permeation around the cavern is evaluated results of analyses conducted on cores of the BAS-1 are presented. The core analyses focused on grain sizes of the salt. Grain size in salt is important for the closure rate of the salt. Fine grained salt has faster closure rates than coarse grained salt. In general

pressure solution (linear creep) is dominant in cold fine-grained salts under low loads whereas dislocation creep (nonlinear creep) is more dominant in coarse grained salts under high loads. The dominant deformation mechanism is usually determined by grain size alone, but the type of salt and temperature also matter (Brouard Consulting, 2019c). The conclusion relevant for this report was that geomechanical modelling can be improved by using constitutive equations based on microphysical models and data obtained from laboratories. Next to the core analyses, another part of the microscale report was about permeation around the cavern. Here the conclusion on brine permeation around the cavern is that permeation will be strongly heterogenous and localized. During the production phase of the cavern there is a high-pressure deficit and pressures change constantly, therefore the salt around the cavern can become weaker and microfractures can occur. This will lead to localized higher permeabilities. The principles of the permeation processes around the cavern proposed here will be considered while making the permeation model.

As was discussed in the literature review, a Norton-Hoff power law can be used to model the behaviour of salt. This model is defined by several parameters. Since the caverns of Frisia are at an extreme depth, the conventional parameters used for salt do not fit the field data from Frisia caverns. Therefore, WEP defined a new model that better fit data from Frisia caverns (WEP, 2020). This model is currently used for operational caverns but will be evaluated since the model is fitted with data in high-pressure deficits. While in the abandonment phase of a cavern, there is a low-pressure deficit compared to the lithostatic pressure. If the model is still correct in low-pressure deficits will be assessed by other literature and by looking at the permeation processes around the cavern.

As was suggested by the KEM-17 report more research was needed to extend current models and support them by laboratory data. In the same year salt samples were tested at a low pressure deficit (Bérest et al., 2019). In these tests it was shown that at lower pressure deficits the strain rate drops significantly and show more linear behaviour compared to the nonlinear behaviour on high pressure deficit regions, indicating that pressure solution creep (linear) becomes dominant in the low-pressure deficit region. More recently a model was made for a threshold pressure for pressure solution creep to occur (van Oosterhout et al., 2022). According to this model the pressure solution creep comes to a halt somewhere between a deficit of 0.07-0.9 MPa. However, this phenomenon has yet to be observed in laboratory/field tests.

### 2.3 Synthesis of literature

Studies have been conducted in the field of salt cavern abandonment (see figure 2.2). Since the caverns of Frisia are very deep, the post-abandonment behaviour of the Frisia caverns is unique and little literature is available. The different studies do agree on the basic principles and dominating processes in salt caverns after production ends. The model currently in place can be improved by implementing a more accurate model of the cavern and studying the permeation behaviour on the layers above the cavern. Since the behaviour (mainly convergence and permeation) of salt caverns after abandonment is hard to measure the research done suggests more research into these cavern processes. After the sealing of a cavern, it's impossible to gather more data and since the processes of a brine-filled cavern take over a very long time there are not a lot of examples of previous caverns. On top of that, Frisia has the deepest caverns in the world making available research less relevant. Frisia caverns are at a much higher depth with a high salt creep compared to other caverns. This study tries to get a better understanding of the convergence and permeation processes of caverns after plug and abandonment by making more accurate models based on available data (such as cavern measurements/data, geology and rock properties) supported by recent studies discussed in chapter 2.2.

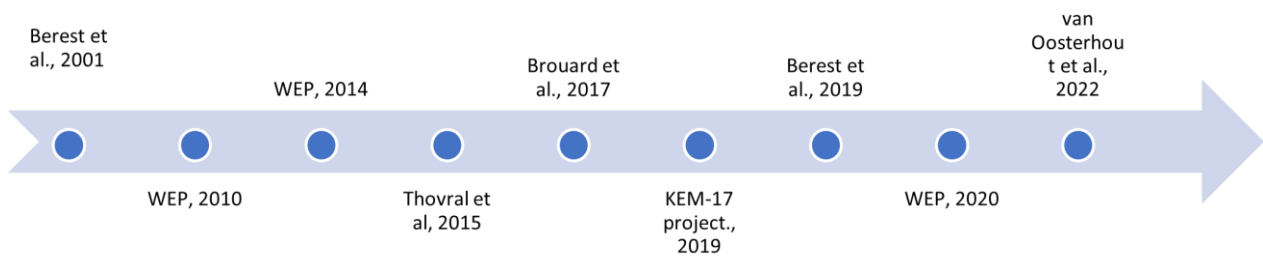


Figure 2.2 Timeline of relevant research done

### 3. Convergence model

This chapter will explain how the model is set up and what simplifications are made. Model parameters will be discussed and how they come to be. The model built will be described and with all parameters in place a base case model will be run and presented.

#### 3.1 Measuring and modelling a cavern

The basic principle of cavern production was explained in the introduction. This is a simplified view of the cavern, however. A cavern has a highly heterogeneous surface and through a cavern lifetime a cavern changes a lot in shape. When drilled, the last cemented casing is put at a sufficient depth below the carnallite to give a safe margin to make sure the cavern brine does not come into contact with the carnallite above during production. This last cemented casing is the most outer casing which holds the blanket fluid. The inner tubing's are drilled to a much larger depth. When the inner tubing's are installed, the cavern is created. In the beginning years of production, the cavern is not produced at steady state yet. This happens when the cavern is grown to where the cavern convergence is equal to the salt dissolution by mining. Before steady state mining, the cavern is growing and the salt is produced at a higher rate than the cavern convergence. In the beginning years the cavern is at a deeper depth than the last cemented casing holding the blanket fluid. Through the cavern's lifetime the cavern must move upwards because insoluble materials build in the bottom of the cavern and create a sump. Thereby the cavern backfills itself. This can be done by removing some blanket fluid allowing the brine to leach out the upper parts of the cavern. If it reaches the last cemented casing the cavern hits the end of its lifetime. This sump squeezes and closes during the lifetime of the cavern. The contents of the sump consist of for instance anhydrite and other impurities in the salt formation which can't be dissolved in the sodium chloride brine. Around 95% of the formation is sodium chloride and the other 5% consists of insoluble material. The salt layers are on a slight angle as well. The salt layers around Frisia caverns are dipping at an angle of around 20° to the Southwest.

The previous mentioned points make the cavern more complicated to operate and contribute to the caverns final shape. From a sonar measurement, a 3D figure can be made from a cavern. During a sonar measurement the cavern production of brine is stopped and a sonar tool is lowered into the cavern via the inner injection string. The position of this string is generally in the lower part of a cavern. The sonar measurement consists of 2 parts. First the sonar tool goes down into the cavern and partially sticks out of the tubing. From this point the tool can start sending sound waves through the cavern, as shown in figure 3.1. The red arrows are the sonar tool sending a sound signal out and the green arrows are reflections of the cavern wall that are sent back. The distance to the wall can then be calculated using the brine velocity. Secondly the sonar tool goes back into the tubing and does a series of horizontal shots at a certain interval. In these shots the tool is in the injection string so this noise must be filtered out.

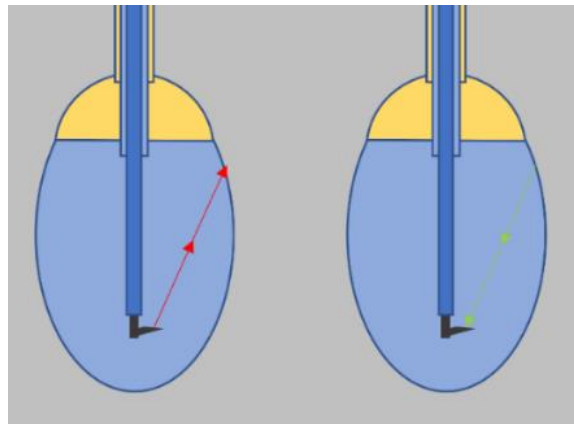


Figure 3.1 Cavern with sonar tool

An example of a sonar string assembly is shown in figure 3.4. Next to the sonar tool there are other measuring and stabilizing tools attached on the string to accurately measure the cavern. The sonar tool scans points by a predetermined interval and a point cloud is generated and interpolated to build a 3D representation of a cavern as shown in figure 3.3. Here it is possible to see that the cavern is not a perfect cylinder or sphere like shape. The cavern walls have a highly heterogenous surface and changes with time depending on where to production and injection strings are.

Since the sonar tool measures the cavern from a stationary point, the tool cannot see everything. An example of this is shown in figure 3.2. Here the cavern has a thicker part at the top (in purple), the sonar tool has a blind spot above the thicker part on the top of the cavern and cannot measure the cavern above it. This is one example of an inaccuracy that could lead to an incorrect cavern volume. This can be partially solved by the horizontal shots but these have to be filtered for the tubing as well. Especially in the upper part of the cavern where the sonar tool has to filter out both the injection and production tubing.

The sonar string has a lot of sensors measuring its location, pressure, temperature, rotation, etc. These sensors help to make the sonar measurement more accurate but all have their inaccuracies too. Finally, it is expected that the actual cavern volume is varies by  $\pm 5\%$  compared to the output of the cavern volume from the sonar measurement. This should be considered in the modelling of a cavern.

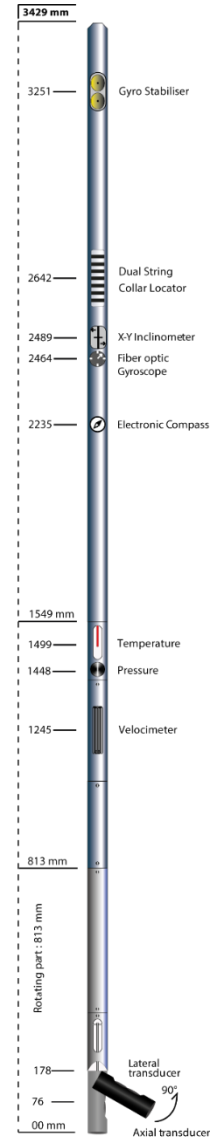


Figure 3.4 Sonar tool assembly (extracted from flodim.fr)

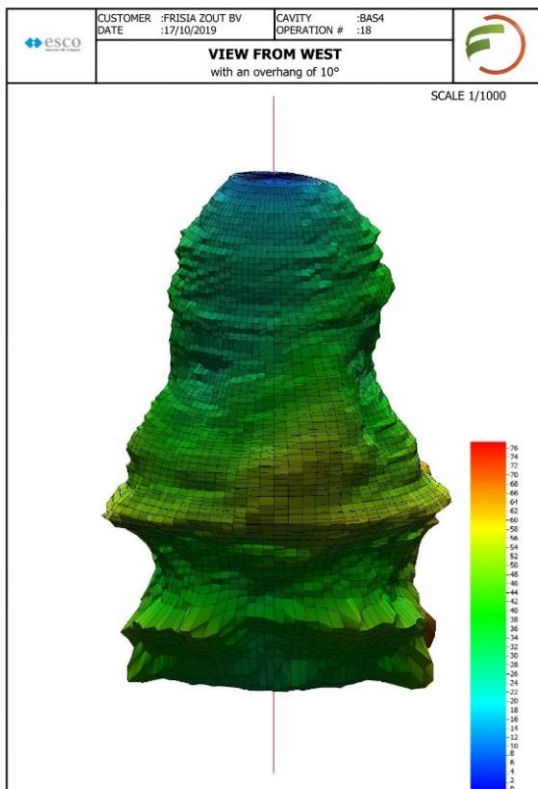


Figure 3.3 3D interpolation of BAS-4 cavern from sonar measurement

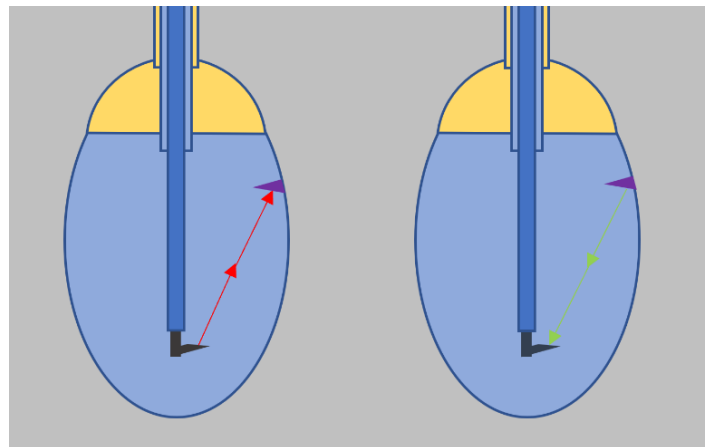


Figure 3.2 Cavern with sonar tool and obstruction

As explained in the introduction the salt can be produced at steady state once the cavern reaches its final shape. At steady state production the cavern squeeze is equal to the produced salt. Since there are almost no horizontal tectonic forces in The Netherlands (horizontal pressure ratio is around 1.07), the squeeze is driven from the lithostatic pressure pushing on the salt formation and thereby the cavern. As explained in the introduction the caverns of Frisia are the deepest in the world. At these pressures and temperatures, the salt can deform viscoplastic or viscoelastic. To give an idea of these pressures, the relevant wellhead pressures together with the lithostatic gradient are plotted in figure 3.5.

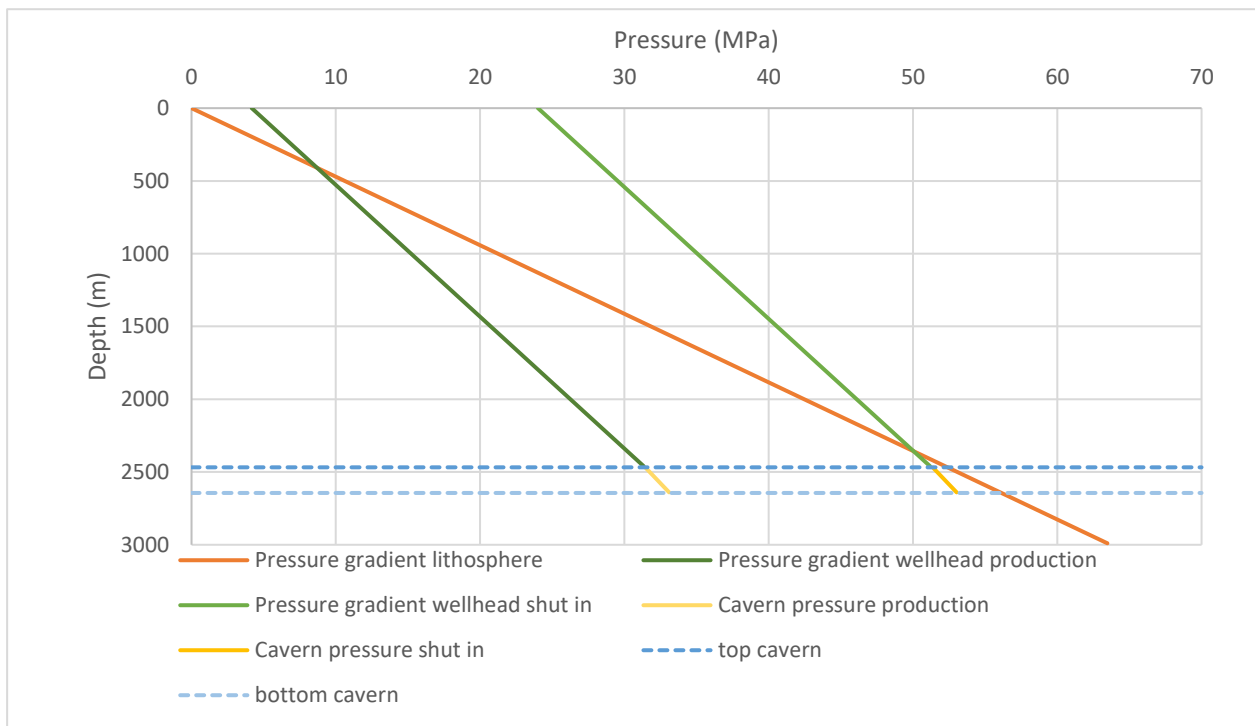


Figure 3.5 Pressures related to the cavern for BAS-4

Pressures are plotted against depth. For reference, the top cavern and bottom cavern depth are plotted by the dashed lines. Next, the pressure gradient of the lithosphere is plotted. The lithostatic specific weight around the area is  $2.164 \text{ g/cm}^3$ . Secondly the pressure curves for production and the shut in phase are plotted. These pressures are measured at the well head. These are the pressures at the outer most casing, for ease this is taken as water. As shown by the yellow lines, the pressures in the cavern deviate slightly. Here the pressure is out of the casing and is influenced by the cavern. How this pressure is calculated will be explained in chapter 3.2. The difference between the pressure of the brine during production and the lithostatic pressure is around 20MPa, this pressure difference allows the salt to creep and thereby allows for steady state production. The pressure gradient during shut in phase is slightly different. This is because the blanket fluid is replaced by water and has therefore a different gradient.

For this research its important to consider the pressures at the shut in phase. This is the phase where no production is happening anymore and the cavern is monitored before abandonment. After production ends the pressure rises until the pressure stabilizes to the pressure at shut in phase. At the top of the cavern this pressure stabilizes at around 51MPa. The pressure of the lithosphere at the top of the cavern is around 52MPa. Dividing the cavern pressure with the lithostatic pressure gives the pressure ratio at the top of the cavern. This comes to around 98%, this is not the case yet for BAS-4 since this well is only

recently shut in, but the other caverns have shown the similar behaviour. One of these caverns is the BAS-2 cavern. The wellhead pressure data of BAS-2 is shown in appendix 1. Here it is shown how the pressure stabilizes at 98% of lithostatic pressure. For modelling purposes, it is assumed that brine pressure of BAS-4 is already at 98% of lithostatic pressure.

The objective is to model the cavern after abandonment. As discussed in the introduction the cavern will be modelled as a 'layered cake' model. In practice this means that the average cavern width will be taken at a set interval (thickness) and the volume of a slice will be modelled as a cylinder. All these cylinders are then stacked and a model of the cavern is created from the sonar measurement at the point of abandonment. An example of a 4-layer cavern is given in figure 3.6.

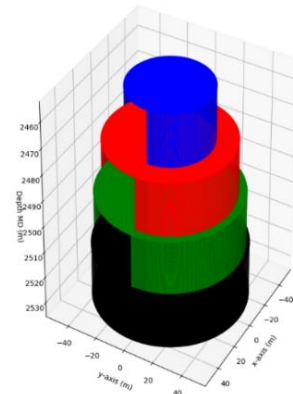


Figure 3.6 Example of 4-layer cavern

In the model the cavern convergence is governed by the pressure deficit between the brine and cavern walls. It is assumed that the pressure around the cavern is isotropic. As discussed in the literature review the cavern can be modeled using a Norton-Hoff power law (the squeeze model). The formula is as follows:

$$Q_{squeeze} = V_{cavern}(A_1\sigma^{n_1} + A_2\sigma^{n_2})$$

Equation 1

Where  $Q_{squeeze}$  is the squeeze rate per day ( $m^3/day$ ),  $V_{cavern}$  is the cavern volume  $m^3$ ,  $A_1$  is the nonlinear creep coefficient ( $MPa^{-n_1}day^{-1}$ ),  $\sigma$  the pressure deficit between the cavern brine pressure and the lithostatic pressure,  $n_1$  the nonlinear exponent,  $A_2$  is the linear creep coefficient ( $MPa^{-n_2}day^{-1}$ ) and  $n_2$  the linear exponent. The cavern volume from abandonment phase can be inserted together with the pressure deficit and a squeeze rate can be calculated. The model is described exactly in chapter 3.3. How the squeeze model and its parameters are defined will be explained in chapter 3.2.

When comparing figure 3.2 with 3.6 it is clear that the model will have some simplifications. Some related to the physical shape, some related to the cavern convergence and salt creep. As discussed before the cavern has a heterogeneous surface. On this surface there are forces as well. In the model the forces are assumed to be isotropic. Only the width of a slice will change and not the height, therefore the height of the cavern does not change in the modelling. The model is run over a long time (thousands of years), in this long time some vertical forces could be at play as well. These won't be modelled. The horizontal forces don't have to come from all directions as well. It could be that the horizontal forces on the cavern are slightly different in different directions. This could lead to the cavern squeezing in an ellipse like form. This is not considered as well, and the cavern converges cylindrically.

With all these considerations in mind, a multi layer cake model will be made to model the cavern as accurately as possible for after abandonment. The model will have its simplifications, the influence of these simplifications will be tested in the sensitivity analysis.

### 3.2 Review of squeeze models

As discussed in the previous section, a layered 'cake' model will be built to model the cavern more accurately. A layered system is needed because the pressure deficit in the cavern changes with depth. For each slice, the convergence rate can be calculated using a formula derived from the Norton-Hoff power law. The Norton-Hoff power law is a model used to describe the time-dependent deformation behaviour (strain) of materials under stress. The Norton-Hoff power law is shown in equation 2 below.

$$\dot{\varepsilon} = A\sigma^n$$

Equation 2

Where  $\dot{\varepsilon}$  is the strain rate, A is a constant,  $\sigma$  is the stress and n is the exponent. For the cavern processes, 2 types of deformation can happen, viscoplastic and viscoelastic. The viscoplastic part is the dislocation creep. Dislocation creep can be described by the Norton-Hoff power law, with the stress exponent (n) being greater than 1. The meaning of the power component is that the salt will deform faster under higher stress. Dislocation creep occurs under a high-stress deficit. This process is most relevant under the production phase of the cavern since the cavern is operated under around 60% of the lithostatic pressure. This viscoplastic behaviour will be referred to as the nonlinear component since the exponent is higher than 1.

The viscoelastic behaviour is the pressure solution. Pressure solution is a process that occurs under high stresses. With the cavern being at a depth of around 2.5km there is a high lithostatic pressure. This viscoelastic behaviour is when n=1 and the equation becomes linear. This is the process of salt creep from farther away from the cavern and becomes more relevant for the shut-in of the cavern. This viscoelastic behaviour will be referred to as the linear component.

The salt formation has both a viscoplastic and a viscoelastic behaviour. Next to stress, the grain size and temperature of the salt is important. This leads equation 3 where the all the relevant factors are combined into one squeeze formula.

$$Q_{squeeze} = V_{cavern} (A_1 (e^{E_a/RT}) \sigma^{n_1} + A_2 (e^{E_a/RT}) \sigma^{n_2})$$

Equation 3

Where  $Q_{squeeze}$  is the squeeze rate per day ( $m^3/day$ ),  $A_1$  is the nonlinear creep coefficient ( $MPa^{-n_1}day^{-1}$ ),  $E_a$  is the activation energy (J/mol), R the gas constant, T the temperature in Kelvin,  $\sigma$  the pressure deficit between the cavern brine pressure and the lithostatic pressure,  $n_1$  the nonlinear exponent,  $A_2$  is the linear creep coefficient ( $MPa^{-n_2}day^{-1}$ ) and  $n_2$  the linear exponent.

Since the cavern is assumed to be uniform temperature and that the temperature is only relevant for the first part of the abandonment and not for the long timescale,  $E_a/RT$  can assumed to be 0. Since  $n_2$  is the linear exponent, this can be set to 1. This simplifies the equation to the following:

$$Q_{squeeze} = V_{cavern} (A_1 \sigma^{n_1} + A_2 \sigma)$$

Equation 4

Previous research (WEP, 2014) used 2 types of models, a high linear and low creep model. The parameters for the low and high linear creep models were defined by GeoDelft (Pruiksma & Luger, 2005) for use on Frisia caverns and are shown in appendix 3. In previous modelling a pure nonlinear model was used for the cavern convergence after abandonment and the linear part was set at 0 (WEP, 2010). However, since the linear part becomes dominant in lower stress deficits, using a pure nonlinear model is not correct. However, the GeoDelft models have shown to not perfectly represent the squeeze behaviour of Frisia caverns during operations. Well Engineering Partners proposed a revised squeeze model with the parameters fitted with data from Frisia caverns (WEP, 2020). This model is currently being used in the production phase of caverns and includes both linear and nonlinear components. In this revised formula an extra parameter was added to redefine the nonlinear creep coefficient  $A_1$  as follows:

*Equation 5*

Where  $\beta_t$  is the system compressibility factor, this value can be achieved by compressibility tests on an operational cavern or by the following formula:

$$\beta_t = f \frac{1 + \nu}{E}$$

*Equation 6*

Where  $f$  is the cavern shape factor with 1.5 for a spherical cavern and 2 for a cylindrical cavern,  $\nu$  is the Poisson ratio and  $E$  is the bulk modulus. This addition together with a change in the values for  $A_1$ ,  $n_1$ ,  $A_2$ , and  $n_2$  made the new WEP squeeze model. The parameters are shown in appendix 4.

To give an idea of the different models and how they behave at different pressure deficits (cavern operation vs shut-in) the following graphs are made. The plotted graphs are all based on the same squeeze formula shown in equation 4. The only thing that changes are the squeeze parameters shown in Appendix 3 and 4. The graphs shown in figure 3.7 are the low linear and high linear models prepared by GeoDelft (Pruiksma & Luger, 2005) and the WEP model with a low shape factor and high shape factor in the high pressure deficit region.

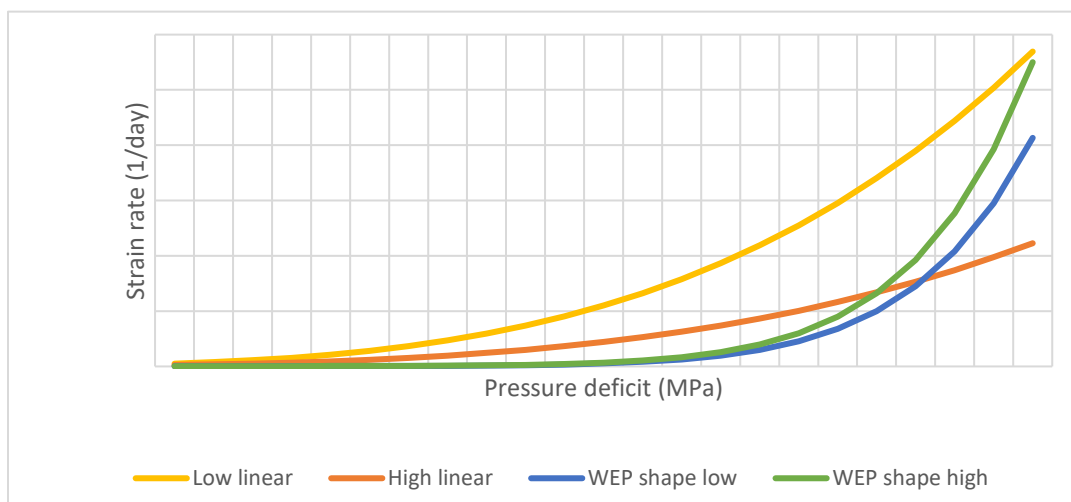


*Figure 3.7 Strain rate per day vs Pressure deficit (8-30MPa) of all different models*

Figure 3.7 shows the higher deficit ranges (8-24MPa). For reference, the lithostatic pressure is around 50MPa and a cavern is operated at around 30MPa. This gives a pressure deficit of 20MPa, the WEP model was fitted to this data or when the cavern is temporarily out of production and the cavern pressure increases (reducing the pressure deficit to a maximum 10 MPa). This model gives an accurate representation of the production data up to around a deficit of 10 MPa (example shown in appendix 2) and is used for the production phase of the cavern and is preferred over the other models.

However, the higher-pressure deficits are not of interest in this study. The question is how the squeeze behaves at lower pressures. Before the cavern is abandoned the pressure deficit is between 1-3MPa. As shown in figure 3.8 the differences between the models become smaller. To show the effective volumes that get squeezed the graph shown for a cavern volume of 1Mm<sup>3</sup> and the squeeze is shown per year.

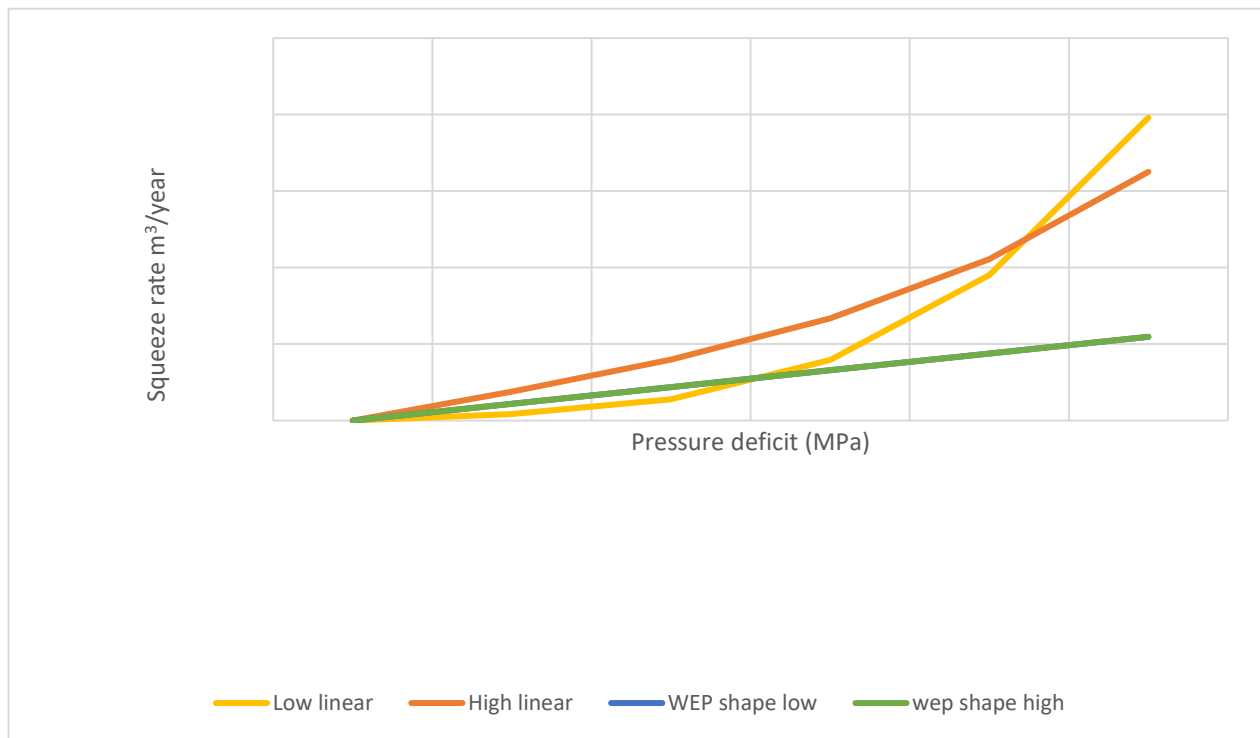


Figure 3.8 Squeeze per year vs Pressure deficit (0-8MPa) of all different models graph and table

In figure 3.8 it is seen that the models are more similar to each other in the low-pressure deficit region. This can be seen in Figures 3.10 and 3.11 as well where the linear and nonlinear part of the models are separated. In figure 3.10 the lower pressure deficit region is shown. Here it is visible that the nonlinear part has almost no significance. Figure 3.11 shows the opposite, here the higher-pressure deficit region is selected and it is visible that the linear part has little contribution to the total squeeze.

Remember that the caverns of Frisia are at an extreme depth with high lithostatic pressure. When the cavern reaches lower pressure deficits the pressure solution (linear component) will become dominant. During operation, there is a large pressure deficit and the dislocation creep (nonlinear component) becomes dominant. In the base modelling the WEP model parameters will be used, these parameters show the best match to field data from Frisia operated caverns.

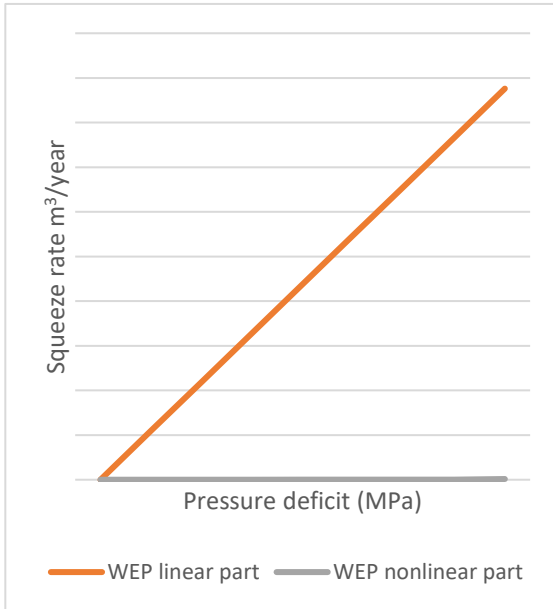


Figure 3.10 Linear and Nonlinear part of WEP model separated (low pressure deficit)

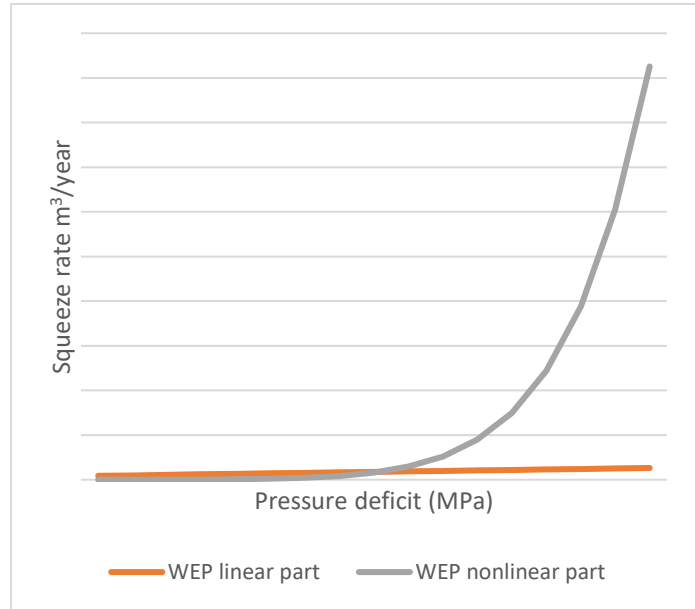


Figure 3.9 Linear and Nonlinear part of WEP model separated (high pressure deficit)

However, since the WEP parameters are calibrated to the production stage of a cavern and therefore where the nonlinear part of the model is mostly dominant. The linear part of the model is less significant in this stage and becomes significant in the abandonment phase of a cavern. Therefore, the WEP model should be checked and be considered in the sensitivity analysis.

According to different studies the strain rate at low-pressure deficits becomes lower. The value in the WEP model is in between the values of the high and low GeoDelft models. According to (WEP, 2014) these values are quite high. In this study different values are debated. More recently in the KEM-17 project (Brouard Consulting, 2019c) new ideas about the salt creep are proposed. More recently testing on low pressure deficits on salt samples was done (Bérest et al., 2019) and a threshold pressure for salt creep to occur was investigated (van Oosterhout et al., 2022).

In this testing a deformation mechanism map is made as shown in figure 3.11. In this deformation map it is seen that the behaviour of salt at a pressure deficit of below 5 MPa becomes different and almost linear. However, it should be noted as well that there is little data to validate these strain rates in this region. The deformation map related to a threshold pressure for salt creep is shown in figure 3.12

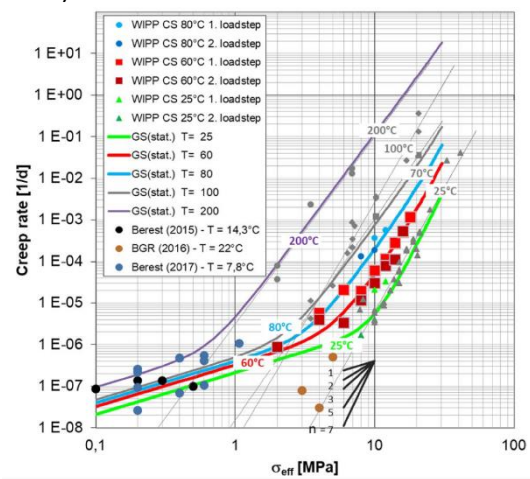


Figure 3.11 Synoptic View of Laboratory Creep Test Results on Waste Isolation Pilot Plant Salt in Relation to Findings From Creep Tests on Various Salt Specimens at Low Deviatoric Stresses (Bérest et al., 2019)

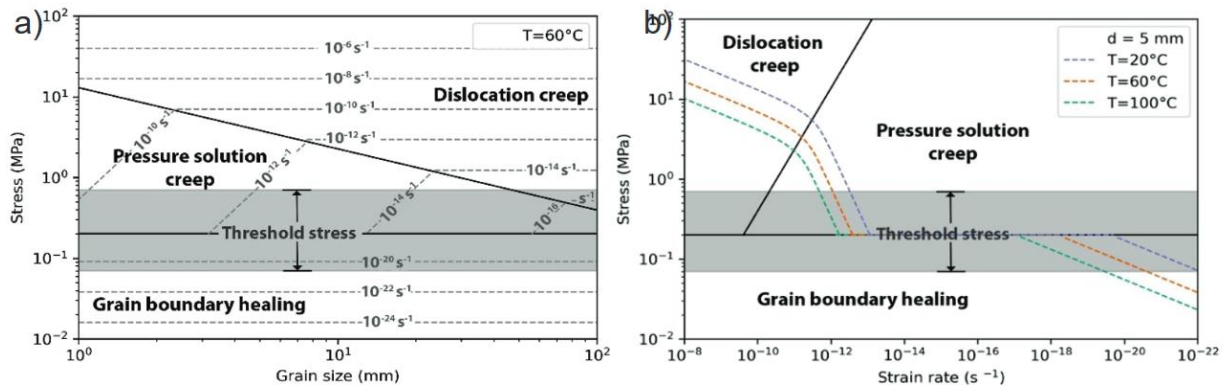


Figure 3.12 (a) Deformation map for rock salt drawn at a constant temperature of 60 °C in log grain size vs. log stress space. (b) Deformation map at constant grain size ( $d = 5\text{mm}$ ) drawn in log strain rate vs. log stress space. (van Oosterhout et al., 2022)

The study on very slow creep tests on salt samples (Bérest et al., 2019), performed tests in a salt mine of salt samples over the period of multiple years. The samples are from different mines/wells. Most relevant here is the Avery Island mine since it consists of a relatively pure halite at 98% (Bérest et al., 2019). The samples showed a transient creep response for over roughly 8 months. After that, the strain rates were calculated over a period of 10 days. The results of the test give slightly higher strain rates compared to the results from modelling a threshold pressure for salt creep to occur (van Oosterhout et al., 2022). The conclusions here were that in the higher stress deficit region (above 5 MPa), the salt shows a nonlinear behaviour indicating for dislocation creep while in the lower pressure deficit region (below 5 MPa), the creep becomes linear indicating a slow pressure solution creep.

To try to apply this to Frisia caverns several factors are important. First the grain size and temperature of salt is important. For the halite II in BAS caverns the grain size is around 5-20mm and the temperature can be taken at 100°C. Secondly the pressure deficit in the BAS-4 cavern is 1MPa at the top of the cavern and 2.7MPa at the bottom part of the cavern. So, when abandoned, according to the model the pressure deficit in the cavern is above the threshold and pressure solution creep will occur. However, a range for the linear component can still be extracted from the deformation mechanism map in this research. Recalculated from the Norton-Hoff power law and only considering the linear creep (since the nonlinear creep becomes insignificant) using  $A_2 = \dot{\epsilon}/\sigma$  and being conservative the  $A_2$  component ranges somewhere between  $1.44 \cdot 10^{-8}$  and  $1.44 \cdot 10^{-9} \text{MPa}^{-1}\text{day}^{-1}$ .

The value of  $A_2$  is different between different papers. The actual value of  $A_2$  might never be known since the cavern will be abandoned by that point or when still shut in, the cavern measurements (such as sonar) have a higher inaccuracy than the convergence rates itself. For reference, the BAS-4 cavern has a volume of  $1 \text{Mm}^3$ , 5% inaccuracy from the sonar measurement then means a difference in  $50,000 \text{m}^3$  in volume. According to the WEP model, at the lower pressure deficits the convergence model gives a yearly permeation rate of around  $2,200 \text{m}^3/\text{year}$ . On top of that comes the fact that the situation at Frisia is unique with the caverns being at such a high depth. It is therefore questionable how applicable these tests are and if they can be extrapolated to Frisia caverns. The effect of the ranging values of  $A_2$  will be evaluated in the sensitivity analysis.

### 3.3 Model description

For a model to work there are several input variables needed to generate an output. The convergence model has 2 input files. One file for the cavern dimensions (depth and width of a slice) and one file for the other relevant input variables.

An example of the input file for the cavern dimensions is given in table 3.1. Here the middle of a slice is taken (in this example the average of 2434m and 2454m). The same is done for cavern width, the average between the 2 widths is taken. With this the slice volume is calculated via the formula for a cylinder:  $V = H * \pi * (D/2)^2$ , where V is the volume in m<sup>3</sup>, H is the height of a slice in m and D is the width of a slice in m. The slice centre is taken as the average depth (2424m in the example). Note that the final amount of slices n is n-1.

Slice	Depth of layer top (m)	Width (m)
1	2434	56
2	2454	84
3	2474	94
4	2494	98
5	2514	98

Table 3.1 Example of cavern dimension input

Next, some other parameters need to be calculated. An important parameter is the pressure deficit as it is used as a main input of the squeeze formula. The pressure deficit at the top of the cavern can be calculated by subtracting the lithostatic pressure from the brine pressure and is shown in the formula below.

$$\sigma_t = (D_t * g * \rho) - (c * D_t * g * \rho)$$

Equation 7

Where  $\sigma_t$  is the pressure deficit in MPa at the top of the cavern, the first part is the lithostatic pressure and the second part is the cavern brine pressure where,  $D_t$  is cavern top depth in meter, g is the gravitational constant in m/s<sup>2</sup>,  $\rho$  is the specific weight in kg/m<sup>3</sup> and c is the pressure coefficient. In the case for Frisia caverns the lithostatic gradient is 2.164 g/cm<sup>3</sup>, the gravitational constant is set at 9.81 m/s<sup>2</sup> and the pressure coefficient for Frisia caverns is 98%. This number is empirically determined by the monitoring of caverns that are shut in. Once production is over the caverns have a shut-in period before plug and abandonment. In this period the cavern pressure will rise and reaches an equilibrium at 98% of the lithostatic pressure (shown as well in appendix 1). This leads to a pressure deficit of around 2% in the top of the cavern. Multiple abandonment tests with Frisia caverns have shown the cavern to stabilize at this pressure. As explained in the literature review the pressure equalizes at this number when the cavern squeeze rate is equal to the brine permeation rate out of the cavern.

At the deeper parts of the cavern there is a higher-pressure deficit. Here the lithostatic gradient follows the salt gradient, but compared to the brine pressure the pressure deficit becomes higher with depth. This is because the brine has a lower specific weight. So, for calculating the pressure deficit at a specific height in the cavern a slight deviation from the formula is needed as shown below.

$$\sigma_s = \sigma_t + (\rho - \rho_{NaCl}) * (D_s - D_t) * g$$

Equation 8

Where  $\sigma_s$  is the pressure deficit of a slice in MPa,  $\rho_{NaCl}$  is the specific weight of saturated brine and  $D_s$  depth of a slice in meters.  $\sigma_s$  is then used as the input for the squeeze model shown in equation 4.

$$Q_{squeeze} = V_{cavern} (A_1 \sigma_s^{n_1} + A_2 \sigma_s^1) * 365.25$$

Equation 9

Where  $Q_{squeeze}$  is the squeeze rate per year ( $m^3/year$ ),  $V_{cavern}$  is the the cavern volume in  $m^3$ ,  $A_1$  is the nonlinear creep coefficient ( $MPa^{-n_1}day^{-1}$ ),  $\sigma$  the pressure deficit between the cavern brine pressure and the lithostatic pressure,  $n_1$  the nonlinear exponent,  $A_2$  is the linear creep coefficient ( $MPa^{-1}day^{-1}$ ) and  $n_2$  the linear exponent. The model is run per year so it is multiplied by 365.25. The parameters  $A_1$ ,  $n_1$ ,  $A_2$  and  $n_2$  are all kept constant and the formula is taken per year. The values of these parameters were discussed in chapter 3.2.

The model calculates the cavern volume over time per slice. For the first year the squeeze is assumed 0 and the cavern volume of a slice from the most recent sonar measurement is inserted in  $V_{cavern}$ . With this the squeeze rate per year can be calculated and is subtracted from the cavern slice volume before repeating the steps again and inserting the newly established volume in the squeeze model. This is repeated for a set time. Once the model completed the squeeze for the first slice it continues to the next slice and repeats the entire process. The model outputs the cavern volume, permeation volume and permeation rate. This data can then be analysed and used for imaging the changing 3D geometry of the cavern from the latest echo measurement and as an input for the permeation model (explained in chapter 6).

### 3.4 Model results for BAS-4

As discussed in chapter 3.3 the model has 2 inputs, the cavern dimensions and an input parameters file. For the cavern dimensions the most recent sonar measurement on BAS-4 is used, this is lastly done in 2019. The cavern is not purely cylindrical as the model; therefore, the mean radius is used as an input. The mean radius of the cavern from the echo measurement is shown in appendix 5. For the layered cake model, a width is taken every 4 meters giving a total of 45 layers for BAS-4. How this simplification of the cavern changes the output of the model will be tested in the sensitivity analysis.

The model starts in the year 2023 and runs until the year 7023 (5000 years). The other relevant input variables are given in table 3.2. The model is run and a 3D plot is created as shown in figure 3.12.

Gravitation	Top cavern	Specific weight lithosphere	Pressure coefficient	Specific weight brine
9.81 m <sup>2</sup> /s	2468 m	2.164 g/cm <sup>3</sup>	0.98	1.2 g/cm <sup>3</sup>

Table 3.2 Input variables for base case of BAS-4

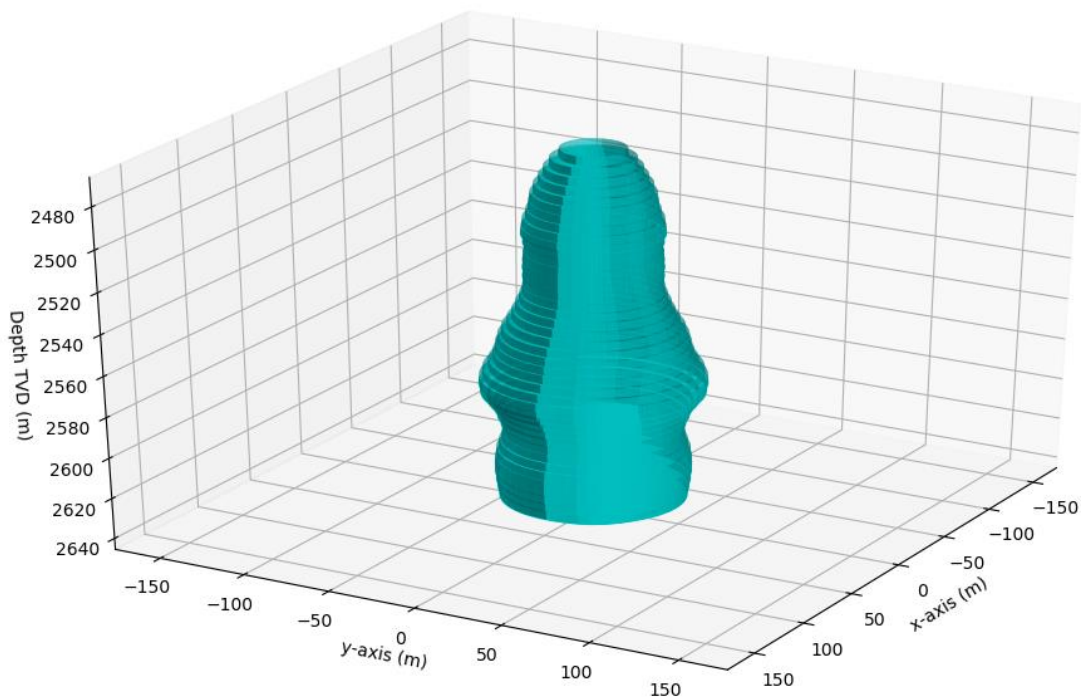


Figure 3.13 BAS-4 Base case 3D cavern

The cavern displayed in figure 3.13 is the cavern at its beginning state after abandonment with the sizes taken from its most recent echo measurement. The model measures a cavern volume of 986,287m<sup>3</sup> and the echo measurement results give a cavern volume of 971,587m<sup>3</sup>. The model overshoots the cavern measurement by 1.5%, the effects of this inaccuracy will be assessed in the sensitivity analysis in chapter 4.

With this volume and shape as a start and the input variables, the pressure deficit for each slice is calculated. At the top of the cavern this is around 1MPa. Going down the pressure deficit increases slightly up to 2.7MPa in the bottom of the cavern. The squeeze is driven mostly from the bottom of the cavern. Previous research (WEP, 2014) even suggests a pressure deficit of 0 MPa at the top of the cavern and that the squeeze is purely driven from the bottom part of a cavern. However, recent data shows that the pressure rises to around 98% of lithostatic pressure leaving around 1 MPa of deficit at the top of the cavern. This number will be tested in the sensitivity analysis.

The change in pressure deficit along the cavern can be seen by looking at 2D or 3D plots from later times (appendix 6). It is possible to see the bottom part of the cavern squeezes 'faster' than the top part because of the higher-pressure deficit in the bottom part of the cavern. This effect can also be seen in figure 3.14. Here the slices are plotted from top to bottom and it is possible to see the squeeze in the lower parts is higher. However, it should be noted that this is not only because of the higher-pressure deficit. As the cavern gets deeper it also gets wider and thus has a higher volume. Therefore, the bottom layers have more volume that gets squeezed. The stacked plot created shows the first 1000 years, the plot over the full modelled 5000 years can be found in appendix 6. With the WEP squeeze model parameters, in around 300 years the cavern roughly halves in size.

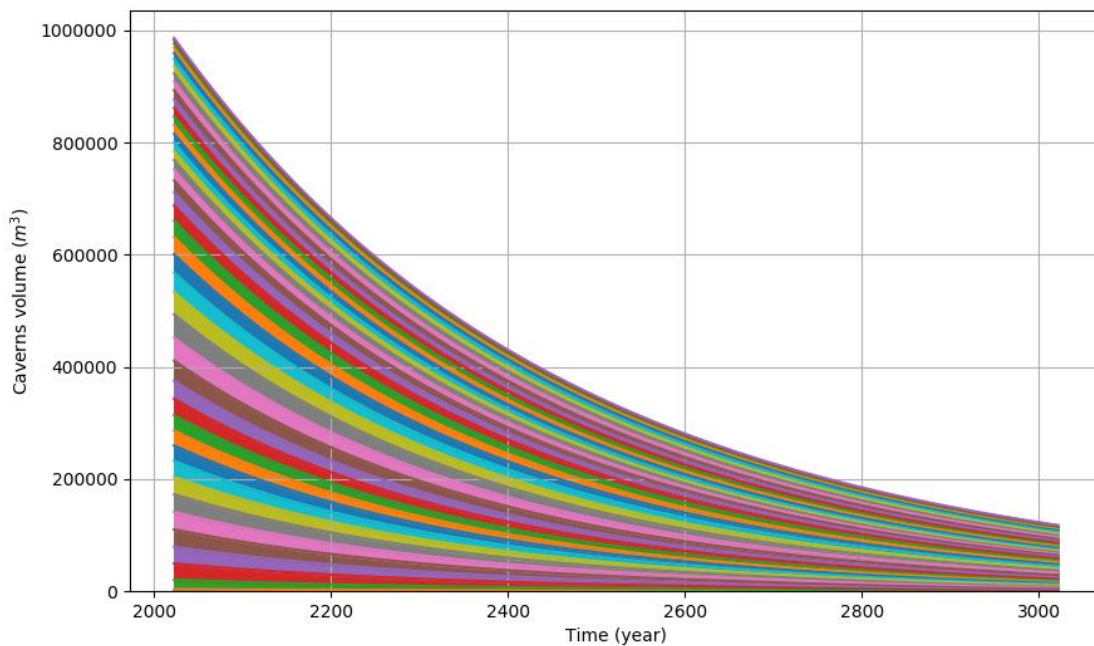


Figure 3.14 Slice volume over time

Lastly a plot of the total cavern volume and permeation volume is shown in figure 3.15. Here the full model is shown over 5000 years. After 5000 years the cavern converged to a volume of  $146\text{m}^3$ , almost fully closed. The permeation volume is the opposite of the cavern volume since it is assumed that once the cavern reaches an equilibrium between the cavern shrinking and brine leaving the cavern. The volume that is lost to the salt convergence is equal to the permeated volume. This is the final output of the convergence model. The permeation rate will be used as an input for the permeation model. The setup of this model is explained in chapter 6.

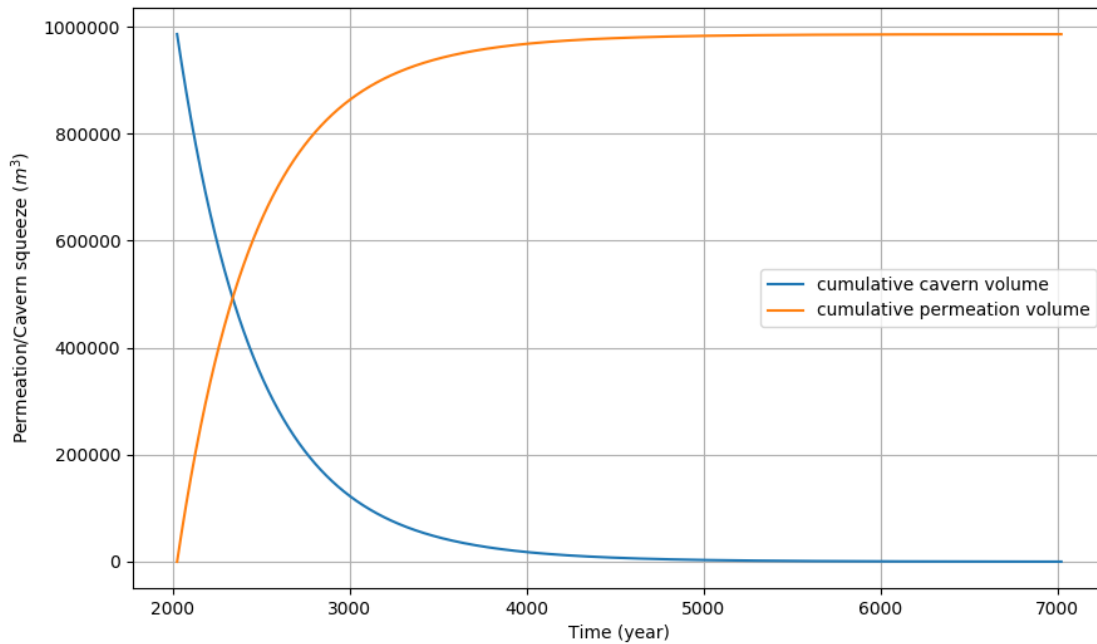


Figure 3.15 Cumulative permeation and cavern volumes over time

## 4. Sensitivity analysis of convergence model

To test out the model and check its parameters a sensitivity analysis is performed. For all important parameters a separate test will be performed, and the results will be analysed and discussed. In the end a new model is recommended with improved variables.

### 4.1 Base case and deviations

The base case is defined in the previous chapter, in this chapter the deviations from the base case are presented. What different parameters and how much they deviate from the base case depends on the parameter tested.

#### **Slice thickness**

Slice thickness is an important factor. In the case of a pressure deficit of 0 MPa the cavern squeeze is purely dictated from the bottom part of the cavern. If there are for instance only 2 slices, only the middle depths are taken for the pressure deficit between the brine and salt walls. This may result into inaccuracies in the modelling. Therefore, varying the slice thicknesses and thereby number of slices will be tested. The base case has 45 slices with a thickness of 4 m per slice. The following deviations will be tested:

- Thickness 2m, 90 slices
- Thickness 4m, 45 slices (base case)
- Thickness 6m, 30 slices
- Thickness 12m, 15 slices
- Thickness 18m, 10 slices
- Thickness 36m, 5 slices

#### **Slice Width**

The slice width is relevant since this is used as an input for the squeeze model. A higher slice volume directly leads to a higher squeeze. The start point of the convergence model is based on the most recent echo measurement available. As discussed in chapter 3.1 these sonar measurements have their limits and some uncertainties to the finale volume is expected. Next to this, converging the average cavern width from a sonar measurement to the cavern model has its limitations as well and an error is expected. For the base case model there was a 1.5% error in total cavern volume compared to the results of the sonar measurement. As explained in chapter 3.1 the measured cavern volume has an inaccuracy of  $\pm 5\%$ . Since the cavern width has a squared relation to the volume an increase of cavern volume by 5% means an increase of  $\sqrt{5\%}$  on the cavern width. To test out how these inaccuracies influence to the outcome of the model the following cases are run. The slice width will be altered by the following percentages:

- -3% cavern width
- -1.5% cavern width
- +0% cavern width (base case)
- +1.5% cavern width
- +3% cavern width

## Pressure deficit

An important factor is the pressure deficit at the top of the cavern. From the formula for calculating squeeze (shown again below), the amount of squeeze comes from constant factors and from the pressure deficit at a certain point ( $\sigma$ ). There are 2 factors that contribute to this squeeze, the pressure deficit at the top of the cavern and the pressure deficit generated from the difference in specific weight between the brine and salt walls.

$$Q_{squeeze} = V_{cavern}(A_1\sigma^{n_1} + A_2\sigma^{n_2})$$

In previous modelling the pressure deficit was taken between 95% of lithostatic pressure (WEP, 2010) and later research suggested no pressure deficit at the top of the cavern and that the squeeze model is purely driven from the bottom parts of the cavern (WEP, 2014). However, over the last 10 years multiple caverns have shown the cavern brine pressures show to stabilize at around 98% of lithostatic pressure. This data comes from shut in tests on Frisia caverns where no pressure is released from the cavern. 98% is used in the base case as an input for the cavern pressure relative to the lithostatic pressure. This pressure deficit, in theory, will stay constant after abandonment because there is an equilibrium between cavern squeeze and brine permeation. The 98% pressure at the top of the cavern or 2% pressure deficit is used as the base case. To see how a change in pressure deficit influences the cavern convergence rates the following cases will be evaluated (pressure deficit)

- 0%
- 0.5%
- 1%
- 1.5%
- 2% (base case)
- 2.5%
- 3%

## Specific weight lithosphere

The specific weight of the lithosphere at the caverns is well known because of multiple drillings of wells in the area. However, there could be slight inaccuracies in the provided data. Therefore, the specific weight of the lithosphere will be slightly adjusted to see the effects on the outcome of the model. The following cases will be considered (in g/cm<sup>3</sup>):

- 2.15
- 2.16
- 2.164 (base case)
- 2.17
- 2.18

## Specific weight brine

The brine is situated at around 2.5km depth under harsh conditions. Under these conditions the solubility and density of the brine can change. The density of a fluid rises with an increase of pressure and lowers with an increase of temperature. However, the salt solubility doesn't change significantly under pressure but does change under different temperatures. An increase in temperature of brine

increases the solubility of salt in water. After abandonment the temperature of the brine is equalized with the cavern walls in a range between 95-105°C (after 10-20 years of equalizing). The density of saturated brine is determined at 1.20g/cm<sup>3</sup>. This value might change as cavern conditions and the pressure and temperature in a cavern changes. A change in temperature or pressure only slightly changes the density of the saturated brine. Therefore, the following cases will be tested (in g/cm<sup>3</sup>):

- 1.19
- 1.20 (base case)
- 1.21

### **Nonlinear part squeeze model**

Lastly, both the nonlinear and linear parts of the WEP squeeze model will be tested. As explained in chapter 3.1, in the low-pressure deficit region the linear part is the most significant and the nonlinear part has very little significance. To assess out if an increase or decrease of the nonlinear part has an effect the following cases will be considered. Note that an increase on both  $A_1$  and  $n_1$  will be done at the same time.

- +20%
- 0% (base case)
- -20%

### **Linear part squeeze model**

Previous research proposed different values for the linear part,  $A_2$ , of the squeeze model (note that  $n_2$  always stays at 1 here since it is the linear part of the model). As discussed in chapter 3.2, more recently other tests and research have come with different values for the linear component (Bérest et al., 2019; van Oosterhout et al., 2022). The values in the range from  $10^{-6}$  are from the (WEP, 2020) and GeoDelft (Pruiksma & Luger, 2005) models. The values from  $10^{-7}$ - $10^{-8}$  are from the slow salt creep tests (Bérest et al., 2019) and the values in the lowest ranges are from the threshold value for salt creep model in the most favourable scenario for low salt creep (van Oosterhout et al., 2022). To assess out how these variations on the  $A_2$  component change the convergence rate the following cases will be evaluated (in MPa<sup>-1</sup>day<sup>-1</sup>).  $5 \cdot 10^{-6}$

- $3 \cdot 10^{-6}$  (base case)
- $1 \cdot 10^{-6}$
- $7 \cdot 10^{-7}$
- $4.2 \cdot 10^{-7}$
- $1.4 \cdot 10^{-7}$
- $7 \cdot 10^{-8}$
- $4.2 \cdot 10^{-8}$
- $1.4 \cdot 10^{-8}$
- $7 \cdot 10^{-9}$
- $5 \cdot 10^{-9}$

## 4.2 Results sensitivity analysis

In this chapter the results of the sensitivity analysis are presented. According to the previous study the total volume that can be accumulated in the overlying layers before exiting the Zechstein is 0.11 million m<sup>3</sup> (WEP, 2014). After the brine exits the salt formations it can freely flow over the area and extra subsidence could occur. To give a feeling of the time frame, this volume will be used as a reference in the sensitivity analysis and is presented in every case to analyse when the brine potentially exits the Zechstein and flows into the overlying sandstone layers. According to the subsidence theory at this point there might be some subsidence. This will be discussed in chapter 6.7. Next to that the time to reach 50% of original cavern volume is calculated and presented as well. Lastly the permeation rate at the first year after abandonment is shown for each analysis. Depending on the case extra parameters are presented if relevant.

### Slice thickness

Varying the slice thickness has an impact on the modelling, but all the scenarios are close to each other. At 5 slices the cavern volume starts to change significantly which can be seen in figure 4.1 where the cavern volume and permeated volume is shown over time for all the cases. At all the other analyses the cavern shows similar behaviour with only slight differences in permeation rate at the start and cavern volume at start. For 15 slices and more the deviation from the measured cavern volume is similar. Since the cavern volume is linked to the squeeze rate, the permeation rate at the start of the abandonment is slightly different as can be seen in table 4.1. The time to reach the certain volumes only changes slightly as well.

Case (# of slices)	Slice Thickness (m)	Cavern volume (start, m <sup>3</sup> )	Time to reach 50% cavern volume (years)	Time for 0.11M m <sup>3</sup> to accumulate (years)	Permeation rate at start (m <sup>3</sup> per year)
5	36	871,966	323	62	1,891
10	18	960,977	320	55	2,111
15	12	981,100	314	53	2,196
30	6	984,768	314	53	2,202
45 (Base Case)	4	986,400	314	53	2,206
90	2	992,713	314	52	2,224

Table 4.1 Results of Slice Thickness sensitivity analysis

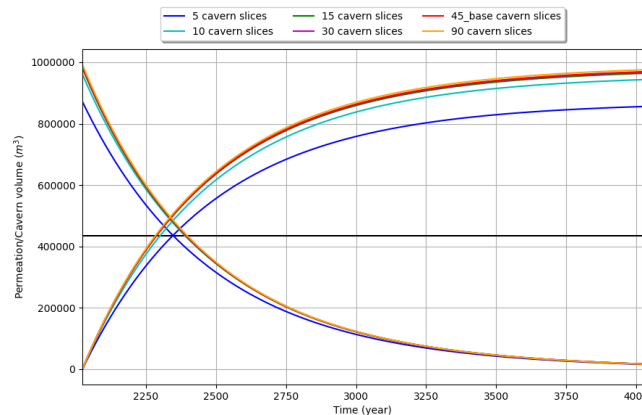


Figure 4.1 Cavern squeeze and permeation of slice thickness analysis

## Slice Width

As shown in table 4.2 the volumes are slightly different. This does lead to different permeation rates as can be seen in figure 4.2. The time before 0.11 million m<sup>3</sup> to permeate changes slightly as well.

Case (multiplication factor slice width)	Cavern volume (start, m <sup>3</sup> )	Time to reach 50% cavern volume (years)	Time for 0.11Mm <sup>3</sup> to accumulate (years)	Permeation rate at start (m <sup>3</sup> per year)
0.97	927,997	314	57	2,075
0.985	956,920	314	55	2,140
1 (base case)	986,287	314	53	2,206
1.015	1,016,097	314	51	2,272
1.03	1,046,352	314	50	2,340

Table 4.2 Results of Slice Width sensitivity analysis.

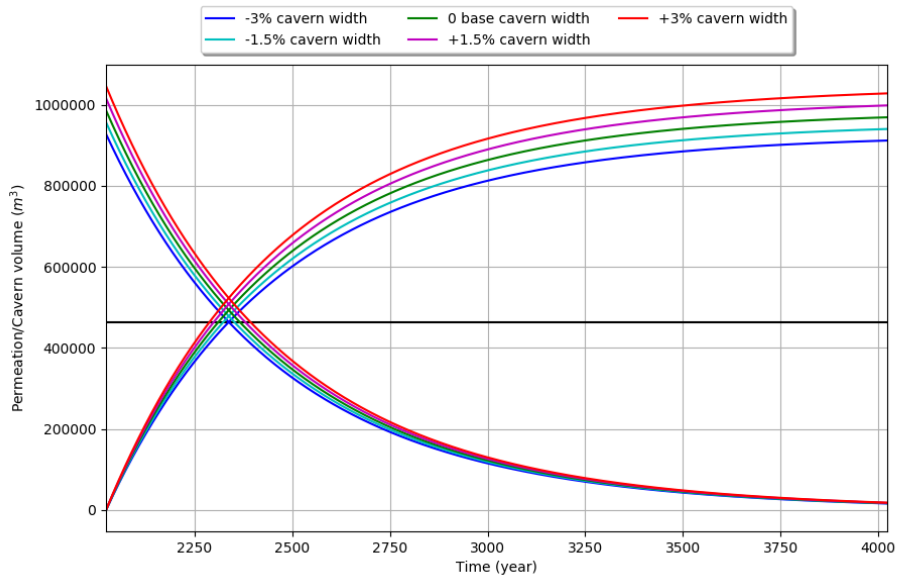


Figure 4.2 Cavern squeeze and permeation of slice width analysis

## Pressure deficit

The pressure deficit is proven to be a key factor as an input of the model. If the pressure deficit is 0 at the top, the squeeze is mainly driven from the lower parts of the cavern. A pressure deficit at the top of the cavern adds to this bottom driven squeeze, this effect can be seen in table 4.3 and figure 4.3.

Therefore, a lower pressure deficit significantly increases the permeation rate of a cavern. A pressure loss in the cavern could thereby significantly increase the permeation rates of the cavern. However, this is an unlikely scenario since the pressure of the cavern stays below the lithostatic pressure and any induced fractures are therefore unlikely. It is important however to accurately know what the pressure deficit is at the time of abandonment.

Case (pressure deficit %)	Pressure deficit top cavern (MPa)	Years to reach 50% cavern volume (years)	Time for 0.11Mm <sup>3</sup> to accumulate (years)	Permeation rate at start (m <sup>3</sup> per year)
0%	0	682	110	1,073
0.5%	0.26	525	86	1,356
1%	0.52	428	71	1,639
1.5%	0.79	362	61	1,922
2% (base case)	1.05	314	53	2,206
2.5%	1.3	278	47	2,489
3%	1.5	249	42	2,772

Table 4.3 Results of Pressure Deficit sensitivity analysis.

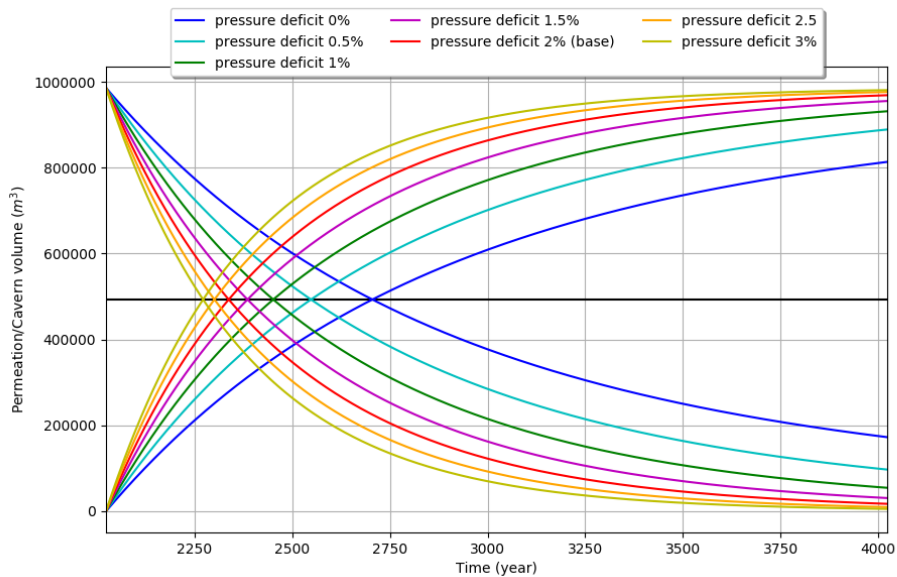


Figure 4.3 Cavern squeeze and permeation of pressure deficit analysis

## Specific weight lithosphere

The specific weight is well known from numerous drilling operations in the area. It could be that the actual value of the specific weight of the lithosphere is slightly different. The results of the sensitivity analysis (table 4.4 and figure 4.4) show that a slight change does not influence the cavern permeation rates by a significant amount.

Case (specific weight)	Years to reach 50% cavern volume (years)	Time for 0.11Mm3 to accumulate (years)	Permeation rate at start (m <sup>3</sup> per year)
2.15	317	54	2,183
2.16	315	53	2,199
2.164 (base case)	314	53	2,206
2.17	313	53	2,215
2.18	311	52	2,232

Table 4.4 Results of specific weight lithosphere sensitivity analysis

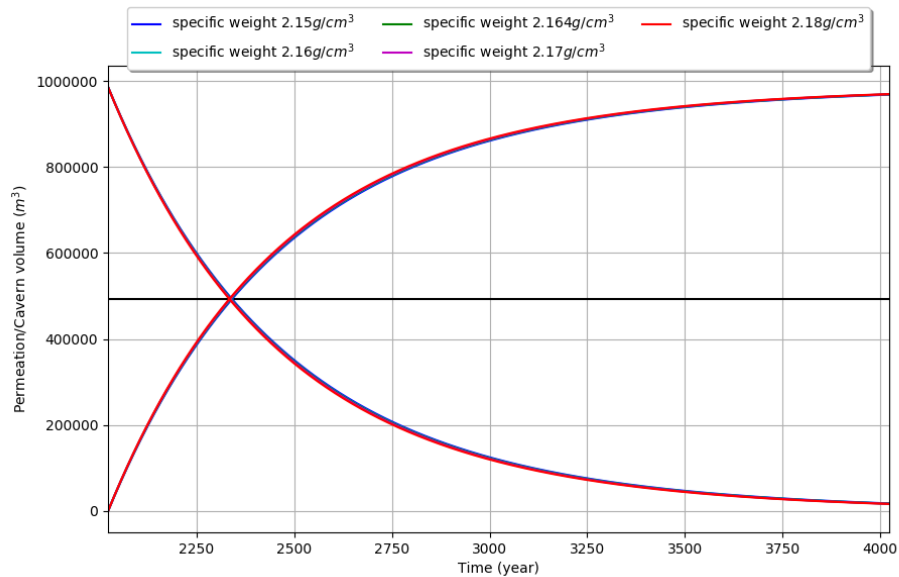


Figure 4.4 Cavern squeeze and permeation of specific weight lithosphere analysis

## Specific weight brine

The specific weight of the brine is an important factor as well, this is used as one of the inputs to calculate the pressure deficit at a slice. The results of the sensitivity analysis show that the slight change is not that significant, this can also be seen in table 4.5 and figure 4.5. Here it can be seen that a slight change in the density of brine does not have a big influence on the model output.

Case (specific weight)	Years to reach 50% cavern volume (years)	Time for 0.11Mm3 to accumulate (years)	Permeation rate at start (m <sup>3</sup> per year)
1.19	313	53	2,217
1.20 (base case)	314	53	2,206
1.21	316	53	2,194

Table 4.5 Results of specific weight brine sensitivity analysis.

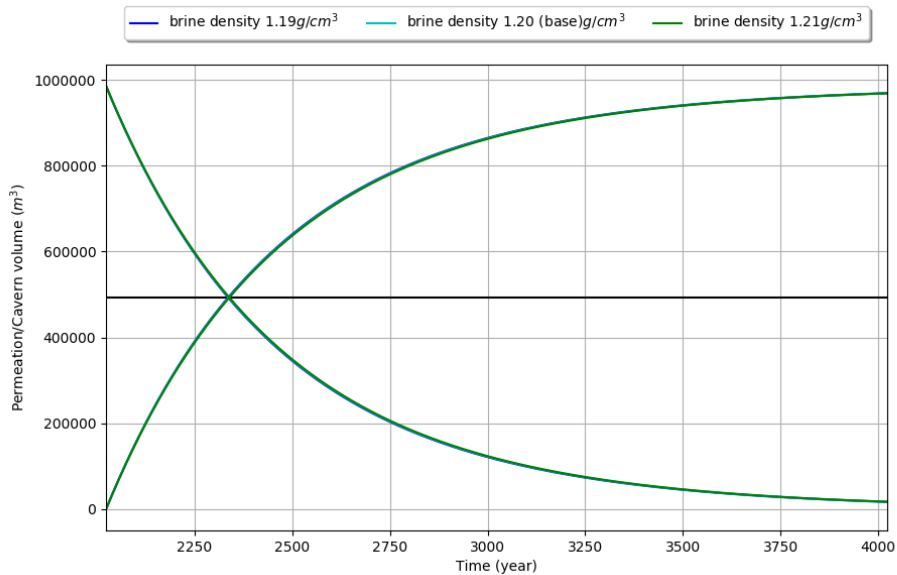


Figure 4.5 Cavern squeeze and permeation of specific weight brine analysis

## Nonlinear part squeeze model

In chapter 3 the linear and nonlinear parts of the model were already investigated and it was shown that the nonlinear part of the WEP creep model is not significant in low pressure deficits. To evaluate out if changes in this nonlinear part had any effect a sensitivity analysis was done on these parameters. As shown in table 4.6 and figure 4.6 (different scenarios are plotted over each other) these analyses have no effect on the permeation.

Case (specific weight in)	Years to reach 50% cavern volume (years)	Time for 0.11Mm3 to accumulate (years)	Permeation rate at start (m <sup>3</sup> per year)
-20%	314	53	2,206
0 (base case)	314	53	2,206
+20%	314	53	2,206

Table 4.6 Results of nonlinear part squeeze model sensitivity analysis

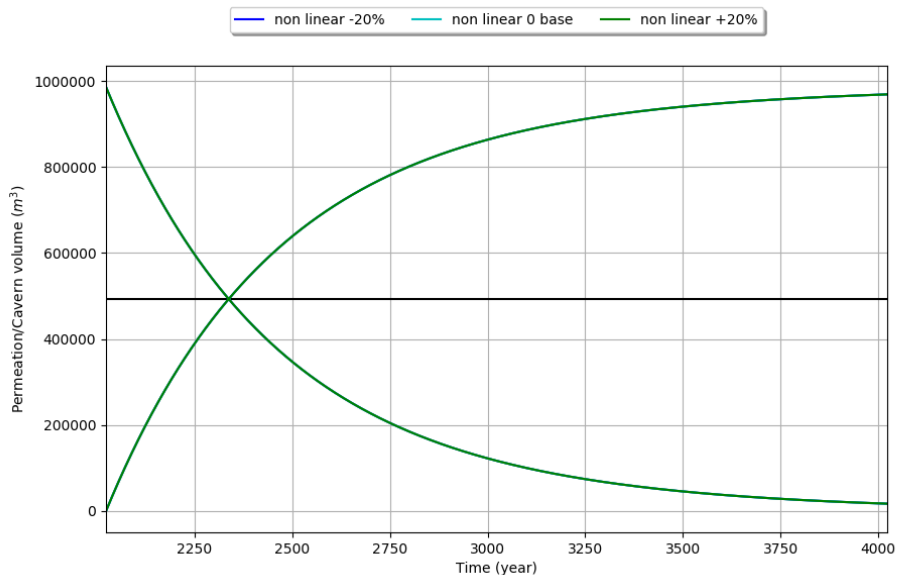


Figure 4.6 Cavern squeeze and permeation of nonlinear part squeeze model analysis

## Linear part squeeze model

As shown in chapter 3.2 the most important part of the model in lower pressure deficits is the linear part of the squeeze model. With the sensitivity analysis it is shown that the squeeze is dominated by this factor directly, previous research discussed the value of this parameter as well. A good understanding of this part is essential for accurate modelling.

Case (Value for $A_2$ )	Years to reach 50% cavern volume (years)	Time for 0.11Mm3 to accumulate (years)	Permeation rate at start ( $m^3$ per year)
$5 \cdot 10^{-6}$	188	32	3676
$3 \cdot 10^{-6}$ (base case)	314	53	2206
$1 \cdot 10^{-6}$	943	159	735
$7 \cdot 10^{-7}$	1,348	227	515
$4.2 \cdot 10^{-7}$	2,247	379	309
$1.4 \cdot 10^{-7}$	6,740	1,136	103
$7 \cdot 10^{-8}$	13,481	2,272	51
$4.2 \cdot 10^{-8}$	22,469	3,786	31
$1.4 \cdot 10^{-8}$	69,652	11,359	10
$7 \cdot 10^{-9}$	139,298	22,717	5
$5 \cdot 10^{-9}$	174,132	31,804	4

Table 4.7 Results of linear part squeeze model sensitivity analysis

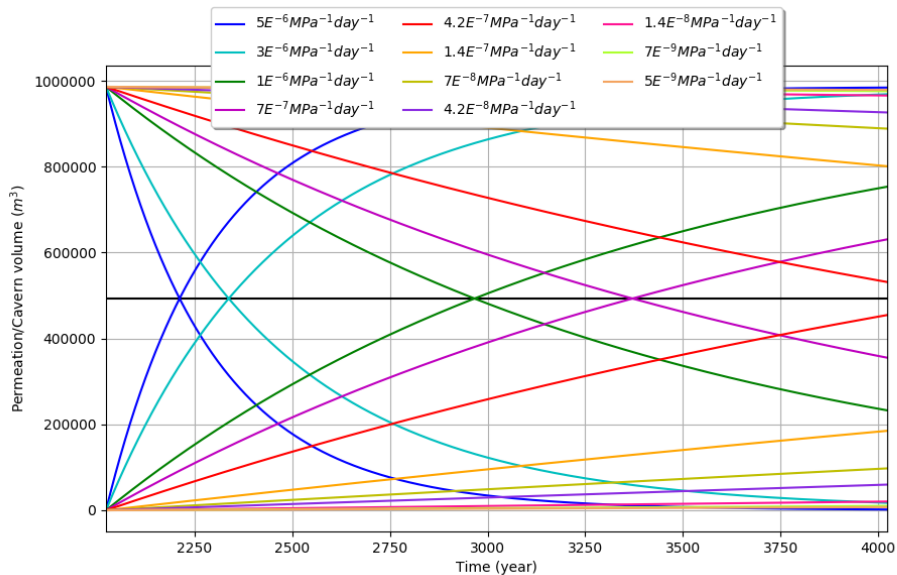


Figure 4.7 Cavern squeeze and permeation of linear part squeeze model analysis

### 4.3 Discussion of sensitivity analysis

This chapter will provide an interpretation of the results and explains their significance. Each tested parameter will be discussed separately.

#### **Slice thickness**

The sensitivity analysis showed that when drastically lowering the number of slices and increasing the thickness the model becomes inaccurate and this changes the output of the convergence model significantly. More slices give a more accurate representation of the cavern volume, but more importantly, it gives a more accurate representation of the squeeze rates. Each slice has a different pressure deficit and its own contribution to the cavern squeeze. In this case the cavern is big, so a slice thickness of at least 12 meters (15 slices) is needed for accurate modelling. The average width of a sonar measurement is given with an accuracy of around 2 meters. Ideally the input for the slice thickness should be given in this order of magnitude to keep the model as accurate as possible.

#### **Slice Width**

The slice width is an important factor to consider. An inaccuracy from the sonar measurement can give different permeation rates and therefore a brine breakthrough difference of  $\pm 15$  years. Next to this is the interpretation of the cavern measurement. In here the average width at a certain height is taken for the calculation of the volume of a slice. As was seen before the initial cavern volume was offset by 1.5%. The inaccuracies of the sonar measurement itself and its interpretation influences the starting volume of a cavern. This should be considered when performing a cavern convergence and permeation study.

#### **Pressure deficit**

The pressure deficit is one of the leading causes of cavern squeeze and is therefore important to consider. A good understanding of the pressure deficit and its development in the future is needed as an input of the model. A slight change can give a significant difference in brine permeation rates. However, data from the BAS-2 cavern (appendix 1) shows that the cavern stabilizes at this pressure in around 10 years. It changes slightly between caverns but it is expected to do so by 0.1-0.2% from the brine pressure that is at 98% of lithostatic pressure.

#### **Specific weight lithosphere**

It should be noted that the pressure deficit is taken from a percentage of the change in specific weight, a change in lithospheric pressure doesn't change the pressure in the cavern, however. A change in the specific weight might lead to bigger changes in the pressure deficit. However, the specific weight of the lithosphere is quite well known. Therefore, the value used is good enough and a slight change in this value does not influence the cavern processes much. It is recommended to use a specific weight of  $2.164 \text{ g/cm}^3$  as an average of the overlying lithosphere.

#### **Specific weight brine**

The specific weight of the brine is less significant and quite well known as well, specific weight doesn't change much within the cavern where the brine pressure and temperature are at an equilibrium in this phase of the cavern. As shown by the analysis, a small change in the specific weight of the brine has little effect on the cavern convergence processes.

## Nonlinear part squeeze model

The nonlinear part of the WEP squeeze model is not significant at all in the low-pressure deficit region, therefore this value using the WEP model can stay as it is and doesn't need to be considered.

## Linear part squeeze model

As seen by the results of the sensitivity analysis the squeeze part has a large influence on the permeation rate. When doubling the  $A_2$  factor the permeation rate at the start doubles as well. This high fluctuation in the linear part of the squeeze model gives a big uncertainty. What the actual value for this factor is should be better investigated. These measurements are very hard to conduct on macroscale in a Frisia cavern since the rates in a shut in/abandoned cavern are so low and the measurements possibly show a higher uncertainty. Next to this laboratory experiments could be done, but it is questionable until what extend these can be extrapolated to cavern scale.

### 4.4 Conclusion on sensitivity analysis

A few points stand out. Starting with the insignificant variables tested. Changes in the specific weights of the lithosphere and brine have shown to be less significant. On top of that comes that these values do not have a big uncertainty in themselves. From multiple drilling operations in the Barradeel concession the lithostatic pressure gradient is quite well known. Same goes for the specific weight of the brine, from laboratory tests this value is quite well known and any inaccuracies from these tests have shown to be insignificant by the sensitivity analysis.

As shown in chapter 3.2 the nonlinear part of the squeeze model is dominant in the production phase of the cavern. Changing the values of the nonlinear model has shown to still be insignificant. Since there is always a combination of linear and nonlinear behaviour in caverns this should be left in. When for instance in future research it is discovered that the linear part is extremely low, the nonlinear part can still become significant. Especially at a higher-pressure deficit.

More significant are the slice thickness and width. If the cavern is simplified a lot by too thick slices the modelling of the cavern becomes inaccurate. This is because the lower parts of the cavern experiences a higher squeeze due to the bigger pressure deficit between the cavern brine and walls. A sonar measurement measures the cavern in intervals between 1 to 4 meters depending on the requirements of the operations. If possible, this range should be used as well for slice thickness. The slice width is important as well. A higher slice width leads to a larger cavern volume at the start of modelling and therefore higher convergence rates. Inaccuracies from the interpretation or limitations of the sonar measurements can lead to these different slice widths. This should be considered during the modelling of post abandonment processes.

Lastly the 2 most significant parts of the convergence model, the pressure deficit and the linear part of the squeeze model. Changing the pressure deficit has a big effect on the convergence rates of the cavern. From data of roughly the last 10 years, the pressure of the brine in the cavern have shown to stabilize in pressure at a pressure of 98% of lithostatic pressure. This holds true for all the caverns at Frisia. A change in pressure could happen in the longer term. These scenarios will be modelled in chapter 6 and 7. The linear part of the model is an important factor to consider, this has the biggest influence on the model. A range of values should be considered in modelling of a cavern.

## 5. Intermediate conclusions and recommendations convergence model

### 5.1 Conclusions convergence model

This chapter will summarize the main findings of the convergence model and will answer the research questions related to the convergence model. The research questions of the convergence model are shown again below:

- What are the current concepts and techniques for measuring cavern convergence?
- How does the Norton-Hoff based model perform in low pressure deficits?
- What is the impact of varying model inputs on the output of the convergence model?

The objective of the first part of the research was to create a convergence model to model a salt cavern after abandonment and test its performance. During the production phase of a cavern, a squeeze model is used to keep track of the cavern convergence processes. This squeeze model is based on pressure and volume data from production and shut-in periods. The squeeze model was then used on the convergence model for post abandonment modelling. Next to the squeeze model another important input was the cavern itself. An initial cavern volume is needed at the start of modelling to determine the cavern convergence rates over time. This volume was taken from the most recent sonar measurement available. With the sonar measurement the cavern's volume is measured in certain depth intervals. One issue with the squeeze model was that it is fitted on data during production at much higher-pressure deficits and lower brine pressures. After shut in the brine pressure rises to around 98% of lithostatic pressure and the convergence of the cavern is much lower. It is questionable if it is possible to extrapolate the current squeeze model to these ranges. In laboratory tests and modelling discussed in chapter 3.2 it is shown that in the lower pressure deficit regions the creep becomes mostly linear. If these tests/models can be extrapolated to this region is questionable as well since Frisia has its caverns at a high depth. So, the rate of convergence in this pressure region remains unclear. The main conclusion from the sensitivity analysis showed this as well. During the sensitivity analysis all the factors influencing the cavern convergence model were tested. The pressure deficit, the initial cavern volume and the linear part of the squeeze model have shown to be most significant. Of these, the pressure deficit is known quite well and shows to stabilize. The cavern volume has some influence at the beginning stages of the convergence model but as time passes by the different volumes at start will approach similar convergence rates eventually. This is because with a higher volume there is a higher permeation rate as well. Only the linear part of the squeeze model stays an unknown. Before drawing any major conclusions, the permeation model and mechanisms will be researched in the next chapters.

### 5.2 Recommendation on parameters and final cases.

As was discussed in the previous 2 chapters the outcome of the base model has its uncertainties. Before continuing to the permeation models a solid basis is needed from the convergence model. This is because the output of the convergence model consists among of, other things, the permeation rate and volume. Since the cavern is abandoned the only way for this brine to escape is through the surrounding rocks by means of permeation. Because the values of some parameters have a larger range, 3 cases will be considered. A P10, P50 and P90 case where these are percentiles from the given range of values of the sensitivity analysis in chapter 4. Not all parameters from the sensitivity analysis will be considered. Only the significant parameters and the parameters with a certain uncertainty in their value will be considered. The slice thickness, specific weight of lithosphere and brine, nonlinear part of the squeeze model and the pressure deficit will therefore not be considered as they have shown to be insignificant to

changes in their values or are well known. The ranges of the cavern width and linear part from the sensitivity analysis are used to calculate the according percentile values, these are shown in table 5.1.

Case	P10	P50	P90
Cavern width (multiplication to width)	-2.4%	+0%	+2.4%
Linear component (MPa <sup>-1</sup> day <sup>-1</sup> )	7*10 <sup>-9</sup>	1.4*10 <sup>-7</sup>	3*10 <sup>-6</sup>

Table 5.1 Changes in input values for the P10, P50 and P90 cases

The results of these scenarios are shown in table 5.2 and figure 5.1. As shown by the output of these cases there is a large difference between the different cases. This is mainly due to the variation in the A<sub>2</sub> (nonlinear part of squeeze model) component of the squeeze model. In the next chapters the permeation model will be made and tested. With this permeation model, the range of permeation rates outputted by the convergence model might be lowered as some scenarios might turn out to be unrealistic.

Case	Time for 0.11Mm3 to accumulate (years)	Permeation rate at start (m <sup>3</sup> per year)
P10	23925	5
P50	1136	103
P90	50	2313

Table 5.2 Time for 0.11 Mm<sup>3</sup> of brine to permeate and permeation rate for the P10, P50 and P90 cases

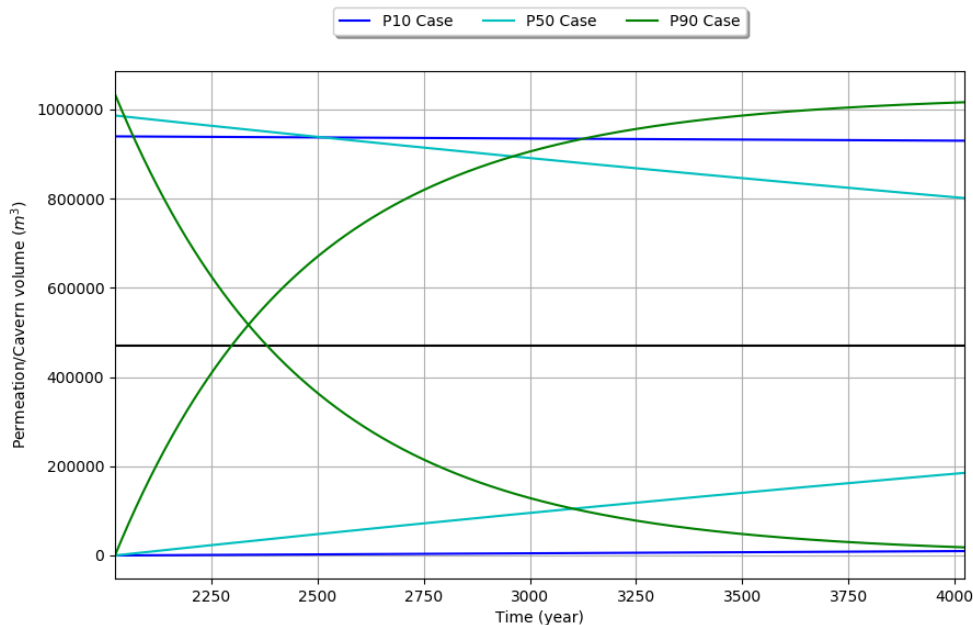


Figure 5.1 Cavern squeeze and permeation volume P10, P50 and P90 cases

## 6. Brine permeation model

### 6.1 Concepts review permeation

In this chapter the permeation model will be built. For a model that accurately represents the subsurface, a good understanding of the subsurface is needed. A short description of the geology was already given in the introduction. In this chapter each layer within the model will be discussed in detail. Next to this the overall geological structure and possible leakage mechanisms will be explained.

#### 6.1.1 Detailed description of geology, rock types and leakage mechanisms

The Zechstein salt was deposited over 250 million years ago. These layers of evaporates were deposited by the evaporation of sea water. When part of the sea gets closed off a small lake is formed and water evaporates allowing the evaporites to precipitate. A typical deposition sequence consists of the deposition of limestone first. This deposition happens under normal sea conditions already with the decay of calcium holding creatures. When the sea starts drying up the first evaporate to participate is anhydrite, followed by halite and lastly magnesium and potassium salts such as sylvite and carnallite are deposited. This cycle repeats and layers are formed. Back to the Zechstein in the north-western part of The Netherlands, the layer consists of mainly halite with small bandages of anhydrite. A few examples of the small anhydrite layers are shown by the red arrows in figure 6.1. At a later stage a roughly 40 m thick Zechstein-II Carnallite layer was formed and on top of that a Zechstein-II Anhydrite layer with a thickness of roughly 60 m was deposited. Between the Zechstein-II and III there is a thin layer of alternating carbonates and clays present as well. On top of the anhydrite is the Zechstein-III Halite layer. This halite is purer than the halite below the carnallite and anhydrite layers.



Figure 6.1 Core of BAS-1 at a depth of 2320m, red arrows point at thin anhydrite layers between the halite

After deposition deformation can occur. This is for instance the case in the eastern part of the Netherlands where massive diapirs were created as shown by the blue arrow in figure 6.2. This is not the case for the western part of The Netherlands as can be seen by the black arrow in figure 6.2. This black arrow points to where the BAS caverns are. The area where Frisia Zout is active the salt formation has a more uniform thickness. The layers are dipping slightly to the South-West at an angle of 20°, which is visible in the core in figure 6.1 as well. The red arrow in figure 6.2 shows the location of the Havenmond cavern, this cavern is situated in a basin and some more folds and faults are present here.

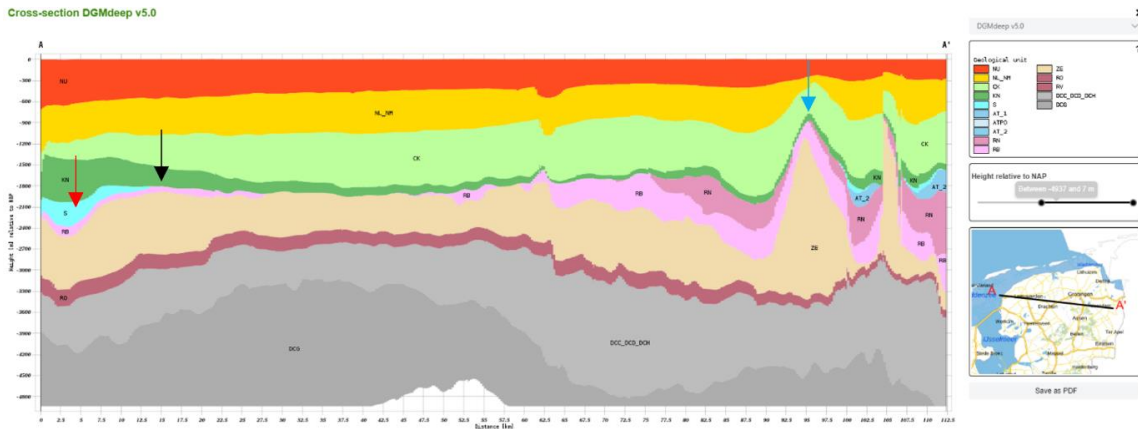


Figure 6.2 Cross section made with the DGMdeep v5.0 mode, retrieved from dinoloket.nl on 21-3-2023

Going back to the cavern abandonment phase. A model for cavern convergence was proposed in the previous chapter. The output of this model consists among other things of the permeation rate. The yearly permeating volume must go somewhere. That is where the permeation model comes in. As discussed in the literature review there are multiple ideas on how this brine can leak away from the cavern. There is no clear agreement on what processes are happening or in the case of multiple processes which is dominant. However the cases described in figure 6.3 are possible leakage mechanisms, these are derived from the KEM-17 report (Brouard Consulting, 2019c). From left to right it could be that (1) brine could leak away via the cement plug or cement around the casing, secondly (micro)fracturing could occur (2), a third option could be that the brine permeates very locally (3) and lastly (4) permeation over a large area could occur.

Applying these ideas on Frisia caverns gives a better insight. Since the brine pressure in the cavern equalizes at around 98% of the lithostatic pressure, the first 2 options can almost be ruled out. The brine pressure stays below lithostatic pressure and comes back to 98% of lithostatic pressure, so fracturing is not likely to occur (WEP, 2021). After drilling a leak off test is performed to check if the well is sealing and at abandonment the same is done to make sure the well is properly abandoned. Over the production period (10-20 years) micro fractures can develop around the cavern where the brine could find a way to permeate locally, this is in line with the proposal from the KEM-17 report where the brine finds very specific paths (figure 6.3 (3)). Lastly the brine could fill up the (secondary) pore space in the halite (4). This is in line with the permeation models made before (Lux, 2010; WEP, 2010).

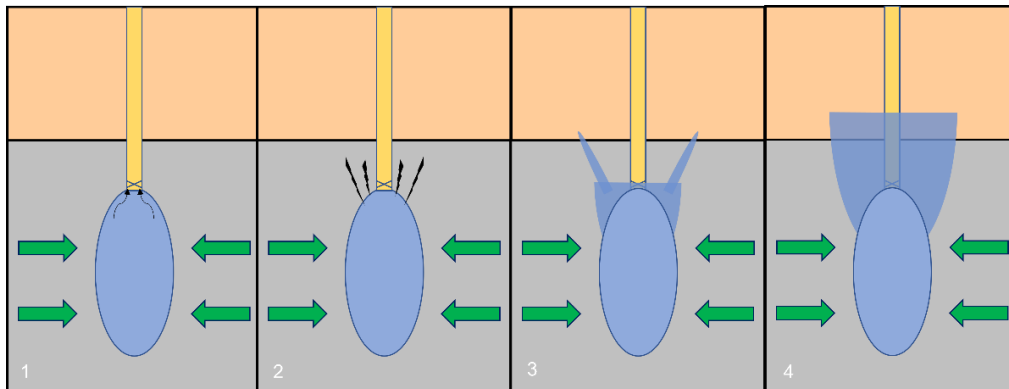


Figure 6.3 Different possible brine leakage mechanisms implemented from (Brouard Consulting, 2019b; Lux, 2010; WEP, 2010, 2021)

Taking the different possible permeation mechanisms into account, it is important to consider the rock types around the cavern. The different rock types were already mentioned in the introduction but understanding the properties and the reaction to brine is important to consider. There are multiple layers the brine must permeate through before entering a more permeable zone. They are described in chronological order from deep to shallow, the descriptions are mainly from the geological and core analysis of the BAS-1 well (KBB, 1994):

### **Zechstein-II Halite**

The Zechstein-II Halite is where the cavern is situated. It is a thick layer with a grain size ranging between 5-20mm. On the Mohs hardness scale halite has a rating of 2-2.5. Within the salt there are thin Anhydrite alterations from 1 to 3mm thickness, with around 4 to 15 stripes per meter. As discussed before this is the layer where the cavern(s) are situated. The porosity of the layer is not well known, in modelling this is taken between 0.2-1%, from the drilling report a much lower value is assumed (0.001%). It is important to differentiate between primary and secondary porosity. The drilling report only talks about primary porosity while the models assume a sum of the primary porosity and the secondary porosity. The integrity of this layer might be affected by the production phase of the cavern where microfractures might have formed due to the loading cycles.

### **Zechstein-II Carnallite**

Previous research already considered the Carnallite layer (WEP, 2012). In this research lab tests on the carnallite and its reaction to brine was done. The brine can partly dissolve the carnallite layer and a volume expansion takes place. During the dissolution of carnallite a brine conversion from halitic brine to carnallitic brine takes place and other minerals precipitate. 2 scenarios were tested. One with 55% carnallite and one with 30% carnallite. The 55% carnallite test resulted in a net volume increase of 0.15 m<sup>3</sup> per cubic meter of brine. The 30% carnallite showed a 0.12 m<sup>3</sup> volume increase per cubic meter of brine. Next to this there is more free volume present, some of this volume is trapped in the newly created pores. The 55% scenario (most conservative) has 1.65m<sup>3</sup> of free carnallitic brine per 1m<sup>3</sup> halitic brine (WEP, 2021). This volume expansion will be considered during the modelling. Furthermore it is important to mention that the carnallite layer has a low tensile strength compared to the surrounding layers (around 0.1 MPa) (Fokker, 1995).

### **Intermediate Carbonates/Clays**

Some carbonates are present between the Zechstein-II and III, these dolomitic/limestone carbonates are alternated with clays in between them. In the Barradeel cavern area this layer is rather thin and will therefore not be considered in the modelling. In the Havenmond area this layer is slightly thicker. Any implications with this layer will be discussed later.

### **Zechstein-III Anhydrite**

The Anhydrite layer is a relatively pure and fine crystalline layer. There are some dolomitic and claystone alterations present. The Anhydrite is a hard and therefore a brittle layer. It can 'protect' the overlying Zechstein-III Halite from the cavern production processes as was shown by numerical modelling (WEP, 2021). The layer itself can be slightly impacted by the cavern mining processes.

## Zechstein-III Halite

The Zechstein-III Halite layer is a very uniform and thick layer. The halite crystals are fine crystalline at around 10mm with some exceptions of crystals with a size of 20mm. Very thin anhydrite (<1mm thick) stripes are present within the layer and are sometimes discontinued within the core. This layer is a purer layer compared to the Zechstein-II Salt. As discussed, this layer possibly is unaffected by the cavern because of the hard anhydrite layer below it.

## Zechstein-IV/Bundsandstein

The overlying layers form a transition zone. First a layer consisting mainly of clays is present, this is a low permeability zone as well. Above this layer there is a mix of sandy and clayey layers. If the brine reaches this layer it leaves the permeation system and can freely flow over a much larger area.

### 6.1.2 Permeation shapes

With the properties of each layer in mind the permeation shapes can be defined. These shapes determine where the brine flows and where not. It is assumed that the brine only stays within a shape with a volume determined by the type of shape and its volume multiplied by the porosity. The volumes will be calculated per layer to visualize the storage capacity for each layer and to better simulate the expected behaviour of each layer according to its properties.

As discussed in the literature review, in previous modelling a knotted cone with an angle of 45° was fitted on the cavern with a porosity of 0.2% for the overlying layers was taken. The formula for a knotted cone volume is as follows:

$$V = \frac{1}{3} * \pi * h(a^2 + ab + b^2)$$

Equation 10

Where V is the volume in m<sup>3</sup>, h is the height of the cone in meter, a is the bottom width of the cone in meter and b is the top width of the cone in meter. A descriptive figure of the permeation cone is shown in figure 6.4. In here the blue square represents the cavern and the green shape on top of that the permeation shape. It is the side view of a cylindrical shape with the horizontal axis in x and the vertical axis y. This model will be run but will not be discussed in detail because this was already done in previous modelling (WEP, 2010).

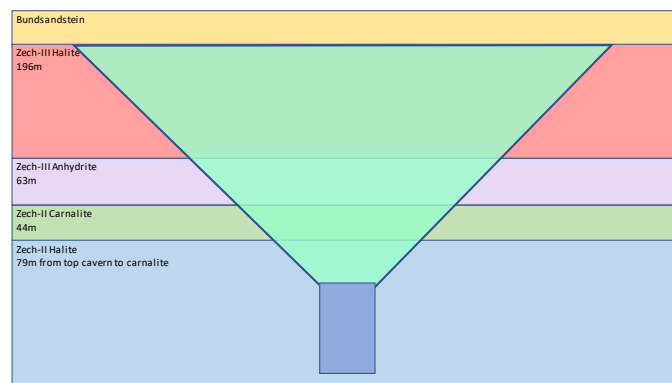


Figure 6.4 Impression of knotted cone permeation model

However, this model does not consider each layer individually. One issue with the model is the volume. This is governed by the volume in the cone multiplied by the porosity. A cone with an angle of 45° has a large volume increase with small increase in height. Secondly the cone model only assumes brine permeating from the top of the cavern. Next to permeating from the top the brine permeates through the wall of the cavern as well. This is not considered in the knotted cone model.

To better simulate the behaviour of brine permeation around the cavern, a paraboloid shape is proposed. This model can be sunk into the cavern and can be given a more natural shape to model the brine permeation paths around the cavern. An impression of the paraboloid model is given in figure 6.5, here it is visualized how the paraboloid shape can be sunk into the cavern and how the volume with height follows a more natural shape.

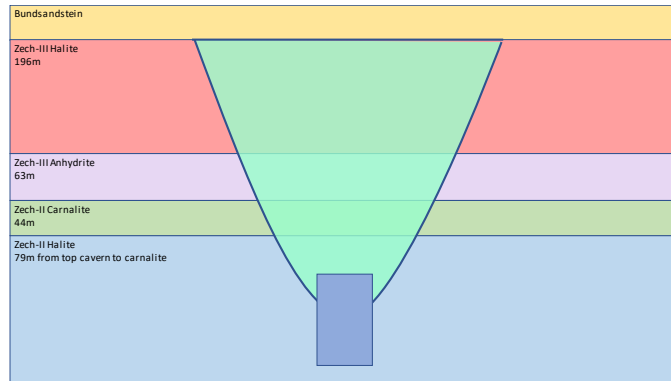


Figure 6.5 Impression of sunken paraboloid model

The equation for a parabola is the following:

$$y = ax^2 + b$$

Equation 11

Where y is the vertical axis, x is the horizontal axis, a is a shape factor and b defines the bottom of the paraboloid from the y axis. The parabola is centred around the vertical (y) axis, same as with the cavern. The volume of a paraboloid can be considered as half the volume of a cylinder. However, it would be easier for the model to integrate the parabola as a function from the y component since the top of the layers are defined that way. To evaluate the volume of a paraboloid in this way, the paraboloid can be considered as a bunch of stacked cylinders with a radius of  $\sqrt{y}$ , limiting the height ( $\Delta y$ ) to 0 gives the following integral to solve which will then give the volume of a paraboloid.

$$V = \int_{H_1}^{H_2} \pi y dy$$

Equation 12

Where  $H_2$  is the top height in meters of a paraboloid and  $H_1$  the bottom height in meters. Solving this integral gives the following formula for the volume of a paraboloid.

$$\frac{\pi y^2}{2} \Big|_{H_1}^{H_2}$$

Equation 13

Including the a and b factors gives the final formula for calculating the volume of a paraboloid. Note that the unit of a is 1/meter and b is in meter.

$$\frac{\pi y^2}{2a} + b \Big|_{H_1}^{H_2}$$

Equation 14

The base paraboloid model has its limitations as well. Looking at the geology it is expected that the brine will move more horizontally in the carnallite layer before entering the anhydrite layer. When the brine enters the carnallite a brine conversion and volume expansion occurs. This brine then enters the anhydrite layer. The anhydrite is a significantly harder layer compared to the layers around, therefore is more brittle than other layers. What could happen is that the volume expansion in the carnallite layer creates extra pressure in the carnallite layer which pushes on the anhydrite layer. This could induce microfractures in the anhydrite layer. This would make it easier for the brine to permeate through the anhydrite layer before entering the Zechstein-III Halite. As discussed in chapter 6.1.1 this salt layer has a low grain size and is very homogenous. The anhydrite alterations are thinner and sometimes discontinued. As shown by the numerical simulations of the layers (WEP, 2021), this layer is protected by the hard anhydrite layer. So, it is not likely that many microfractures have formed in this layer. The salt could again move in multiple directions. Taking all the previous considerations into account an 'adjusted paraboloid' model is proposed as shown in figure 6.6. In this model a paraboloid shape is defined for each layer separately. Thereby making it more adjustable to the properties of each layer.

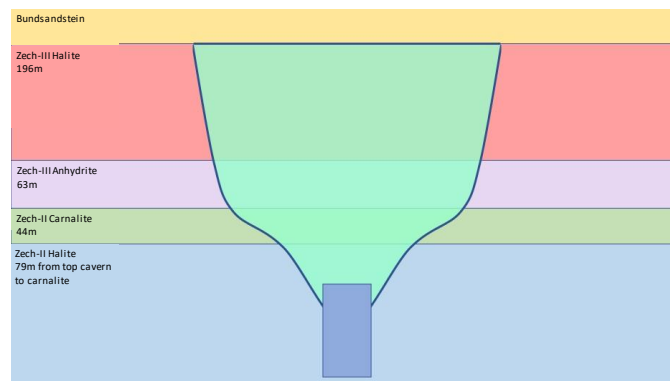


Figure 6.6 Impression of adjusted paraboloid model

## 6.2 Model description

The previous chapter explained which shapes will be tested and how they are defined. In this chapter the model will be described the final shape of each model will be presented.

The permeation model has 2 inputs. The first input is the permeation volume. As discussed in the introduction and literature review, the principle of the cavern system after abandonment is that as the cavern converges the brine within the cavern permeates through the overlying and surrounding layers. One of the outputs of the convergence model are the permeation volumes, this output of the convergence model will be used as one of the inputs of the permeation model. All the brine volume from the cavern will permeate out of the cavern through the salt formations.

Next to this input, another input file is used for different parameters. In this file the model type, the top of the different layers and porosities of each layer can be defined. For the cone model the cone angle can be adjusted and for the paraboloid models the shape parameters (a and b) can be defined. For the carnallite layer the carnallitic conversion factor can be defined.

With these files in place the model can be run. The first step in the model is to define the volumes of each layer, the volumes are calculated using the formulas described in the previous chapter. The volumes are calculated by the top and bottom each layer and is defined in the input file. The volume of each layer is then multiplied by the porosity of that layer.

The tops of each layer and cavern are defined as described in table 6.1. These are the same for each model type. The tops of each layer were extracted from the drilling report of BAS-4, in this report the boundaries of each layer were defined by the end of well report (WEP, 2004).

Zechstein III Halite	Zechstein III Anhydrite	Zechstein II Carnallite	Zechstein II Halite	Top Cavern
2086m	2282m	2345m	2389m	2468m

Table 6.1 Top of layers and cavern

The porosities can be defined for each layer as well, for the base case each porosity is set at 0.2%, similar to a previous model (WEP, 2010). The porosities ( $\phi$ ) can be seen in table 6.2. The permeation model considers the impact of fluid that has permeated into newly formed porosity, also referred to as secondary porosity. This porosity is created by the expansion of the rock at near lithostatic conditions. Additionally, there is a minimal amount of porosity within the salt rock itself (in between the grain boundaries). And in the case of Zechstein-II Halite, some micro fractures may have formed during production which could have created extra pore space. The porosity (0.2%) that is inputted to the model is the sum of the primary and secondary porosity. How the model output changes under different porosities for a layer will be tested in the sensitivity analysis.

$\phi$ Zechstein II Halite	$\phi$ Zechstein II Carnallite	$\phi$ Zechstein III Anhydrite	$\phi$ Zechstein III Halite
0.2%	0.2%	0.2%	0.2%

Table 6.2 Porosity inputs for each layer in base case

Lastly the parameters for the different models can be defined. For the cone model the cone angle can be defined. For the paraboloid model, the a and b factors can be defined and for the adjusted paraboloid model the a and b factor for each layer can be defined for the adjusted paraboloid model. For the

paraboloid models the paraboloid can be partly sunk into the cavern. Meaning the cavern volume needs to be subtracted from the volume of the paraboloid. This is done in the volume calculation as well.

With all the parameters in place and the volumes calculated the model will fill up each layer starting with the Zechstein-II Halite. Once this layer is full the next layer, the Zechstein-II Carnallite, will be filled. As discussed in chapter 6.1, when halitic brine meets carnallite rock a brine conversion to carnallitic brine will take place. With this brine conversion there is a volume expansion. This is considered in the model, all halitic brine passing the carnallite layer will be converted to carnallitic brine with a volume expansion. In the laboratory testing a 30% and 55% carnallite concentration sample were tested (WEP, 2012). To model the most conservative scenario the 55% carnallite concentration will be used, in this case the free brine volume created is 2.09 m<sup>3</sup> per 1 m<sup>3</sup> of brine. Not all this fluid will escape since some minerals precipitate and trap fluids as well. This creates some pore space where the converted brine is trapped, this is assumed to be 28.5% (WEP, 2021). In total the amount of free carnallitic brine that can escape the system is 1.65 m<sup>3</sup> per 1 m<sup>3</sup> of halitic brine.

The outputs of the model can be further analyzed, a plot with the final shape and the volumes of each model are described in the next sub chapters.

### 6.2.1 Cone model

An example of the output of the cone model is shown in figure 6.7, the yellow lines are the boundaries of the models shape. In this permeation model the cone angle is set at 45°. The cone is knotted at the top of the cavern. Note that this is a 2D presentation of a 3D volume. The top of the layers are assumed perfectly horizontal, in reality the layers are slightly tilted as discussed in chapter 6.1.1. The tops are defined according to the input file discussed in chapter 6.2. The top of the Zechstein II Halite layer is at 2086 meters, the Carnalite on top is at 2282 meters followed by the Zechstein III Anhydrite at 2345 meters and the last Halite layer with a top at 2086 meters. This can be seen in figure 6.7 as well. After the brine reached the top of the Zechstein III Halite it can freely flow into the overlying bundsandstein layer with a significantly higher permeability and porosity.

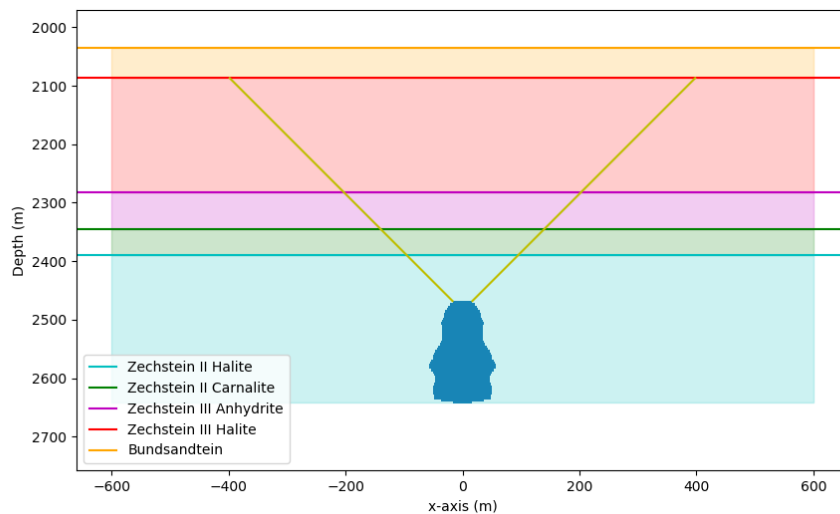


Figure 6.7 Cone model on cavern BAS4

The volumes of each layer are shown in table 6.3. Here both the rock volumes and pore volumes are shown. The brine can accumulate in the pore volume of each layer. To compare the storage capacities in each layer the percentage of volume per layer is shown together with the total storage capacity. As discussed in chapter 6.1.1 the cone model rapidly expands in volume with height. This is seen as the Zechstein-III Halite contains 85% of the total storage capacity while the other layers contain the other 15% with only 1% in the Zechstein-II Halite. The total pore volume is around 130 thousand cubic meters. This is 13% of the total cavern volume, meaning that if the cavern squeezes fully the other 87% of the cavern volumes would flow into the overlying layers.

	Zechstein II halite	Zechstein II Carnallite	Zechstein III Anhydrite	Zechstein III Halite	Total Volume
<b>Total volume (m<sup>3</sup>)</b>	792,319	1,721,689	7,593,839	55,150,188	65,258,035
<b>Porosity volume (m<sup>3</sup>)</b>	1,584	3,443	15,187	110,300	130,514
<b>Volume %</b>	1%	3%	12%	85%	

Table 6.3 Brine storage capacity and rock volume per layer cone model

### 6.2.2 Paraboloid model

The base paraboloid model is a simple model. The a factor can be reduced to create a wider permeation paraboloid and thereby bigger volume. The volume doesn't rapidly expand with height as was the case in the cone model. As was described in chapter 6.1.1 the brine can permeate along the cavern walls as well and can accumulate around the cavern. This is not taken into consideration with the cone model. The depth by how much the permeation shape can sink into the cavern is determined by the b factor in the paraboloid model. For the base case the a factor is taken at 0.15 and b at 100 m. This is done because the lower middle part of the cavern has a thicker radius. It could be that the volume starts permeating from that height. The effect of changing this height will be tested in the sensitivity analysis.

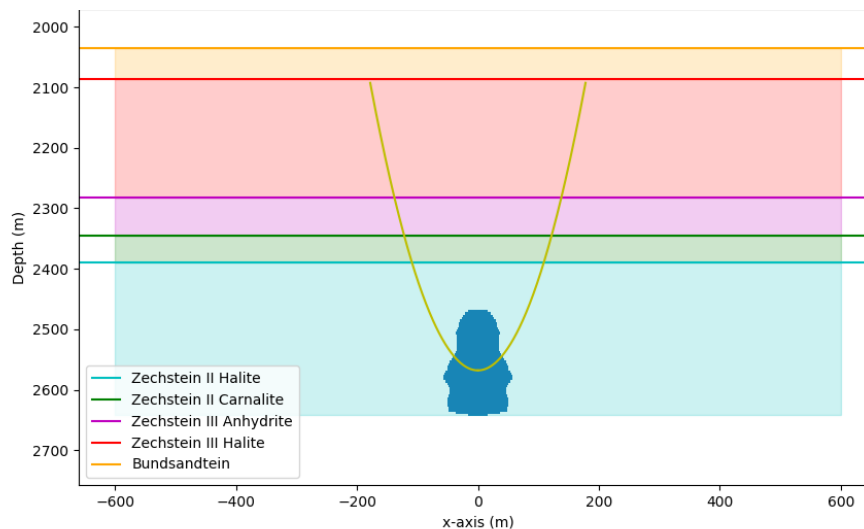


Figure 6.8 Paraboloid model on BAS-4 Cavern

Looking at the volumes (table 6.5), the largest storage capacity is within the Zechstein-III Halite at 66%. The Zechstein-II Halite has a more significant volume compared to the cone model and like the Carnallite and Anhydrite layers. The total permeation volume is much lower compared to the cone model at only 5% of the cavern volume.

	Zechstein II halite	Zechstein II Carnallite	Zechstein III Anhydrite	Zechstein III Halite	Total Volume
<b>Total volume (m<sup>3</sup>)</b>	3,041,217	1,852,283	3,358,048	15,763,255	24,014,803
<b>Porosity volume (m<sup>3</sup>)</b>	6,082	3,704	6,716	31,526	48,028
<b>Volume %</b>	13%	8%	14%	66%	

Table 6.4 Brine storage capacity and rock volume per layer paraboloid model

### 6.2.3 Adjusted paraboloid model

In the adjusted paraboloid model each layer has its own paraboloid which can be adjusted accordingly to best simulate its characteristics. The base shape and its parameters of the adjusted paraboloid model are fitted using the knowledge about the layers as described in chapter 6.1.

	Zechstein-II Halite	Zechstein-II Carnallite	Zechstein-III Anhydrite	Zechstein-III Halite
a	0.015	0.005	0.01	0.003
b	100	-10	100	-100

Table 6.5 Base case a and b factors of adjusted paraboloid model

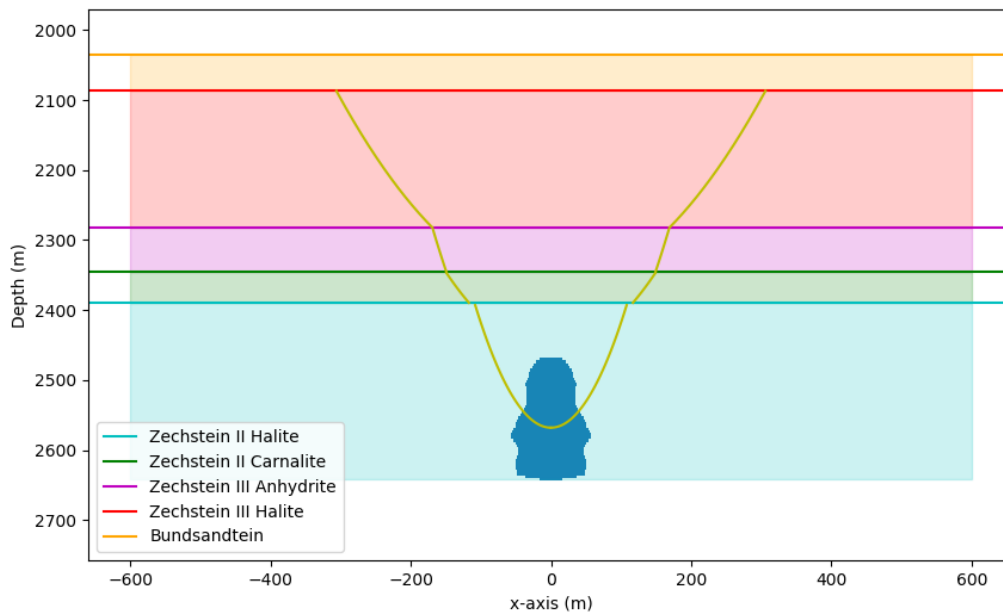


Figure 6.9 Adjusted paraboloid model on BAS-4 Cavern

The adjusted paraboloid model volumes are shown in table 6.8. Still a significant percentage of the volume is stored in the Zechstein-III Halite. The total permeation space is around 96 thousand cubic meters. This is roughly in between the cone and paraboloid model. Like the base paraboloid model, this model is sunk slightly into the cavern as well.

	<b>Zechstein II halite</b>	<b>Zechstein II Carnallite</b>	<b>Zechstein III Anhydrite</b>	<b>Zechstein III Halite</b>	<b>Total Volume</b>
<b>Total volume (m<sup>3</sup>)</b>	3,041,217	2,515,787	5,037,073	37,766,132	48,360,209
<b>Porosity volume (m<sup>3</sup>)</b>	6,082	5,031	10,074	75,532	96,719
<b>Volume %</b>	6%	5%	10%	78%	

*Table 6.6 Brine storage capacity and rock volume per layer adjusted paraboloid model.*

### 6.3 Modelling results for BAS-4

The adjusted paraboloid model is assumed to be the base model since it considers each layer separately. Still, in this chapter all the 3 previous models will be presented to give an overview of different outcomes. Each model ran 3 times with the P10, P50 and P90 outputs from the convergence model. Resulting in 9 outputs on breakthrough times for the specific layers. The permeation rates vary a lot as was concluded from the convergence model. Since this is used as the main input on the permeation model the outputs in the permeation models P10, P50 and P90 cases vary a lot as well.

#### 6.3.1 Cone Model

As discussed in chapter 6.2 the cone model has the largest volumes. This leads to the cone model giving the longest permeation times for the different convergence scenarios as shown in table 6.7. The large range has to do with the linear part of the squeeze model. The differences in the linear part of the squeeze model between the P10, P50 and P90 cases are roughly a factor of 20 each. This directly translates to the output of the permeation model. The difference between the P10 and P90 is roughly a factor of 400. A better understanding of the permeation mechanisms using different methods will try to lower this range in the next sub chapters.

Case	Zechstein II halite	Zechstein II Carnallite	Zechstein III Anhydrite	Zechstein III Halite
P10	324	623	2516	16885
P50	15	30	120	802
P90	1	1	5	36

Table 6.7 Time in year for each layer to fill up in cone model.

#### 6.3.2 Paraboloid model

The paraboloid model has much lower breakthrough times compared to the cone model, in the P90 analysis this is already after 19 years. This is because this model has a much lower volume since the permeation shape gets more vertical with less depth. If the brine can reach this layer after 19 years will be assessed in the next sub chapters.

Case	Zechstein II halite	Zechstein II Carnallite	Zechstein III Anhydrite	Zechstein III Halite
P10	1245	1245	2052	6035
P50	59	59	98	287
P90	3	3	4	13

Table 6.8 Time in year for each layer to fill up in paraboloid model.

### 6.3.3 Adjusted paraboloid model

As discussed in chapter 6.2 this model sits in between the other 2 models in terms of volume. The times for each layer to fill up is in between the other 2 models as well. This model will be used as reference in the next sub chapter and tested in the sensitivity analysis.

Case	Zechstein II halite	Zechstein II Carnallite	Zechstein III Anhydrite	Zechstein III Halite
P10	1,245	1,379	2,638	12,363
P50	59	66	126	588
P90	3	3	6	26

*Table 6.9 Time in year for each layer to fill up in adjusted paraboloid model.*

All 3 models were run to give an idea of the different permeation volumes and times. As presented the adjusted paraboloid model is the base case since it considers each layer separately and will be used for testing in the sensitivity analysis.

These models present a simplification of reality. In the model there are only 4 layers considered within the salt, these layers are considered as pure layers as well. There are many more thinner layers in between the different layers and some thicker as well. Next to the assumption of pure homogenous layers the model uses permeation through salt as a means of transport through the layers. Before drawing any conclusions from these model results some other aspects will be considered to further validate or compare these model outputs. These will be discussed in the following sub chapters.

## 6.4 Permeability of halite

To assess the different permeation paths the permeability of halite is investigated in this section. Salt formations are mostly seen as impermeable rocks, when enough pressure is applied the salt becomes slightly permeable. The flow rate of fluids through porous media can be calculated with the following formula.

$$Q = \frac{kA}{\eta} \frac{\Delta P}{\Delta x}$$

Equation 15

Where  $Q$  is the flow in  $\text{m}^3/\text{s}$ ,  $k$  is the permeability in  $\text{m}^2$ ,  $A$  is the surface area in  $\text{m}^2$ ,  $\eta$  is the viscosity of the fluid in  $\text{Pa s}$ ,  $\Delta P/\Delta x$  is the pressure gradient. The permeability of rock salt is very low, however by modelling and laboratory testing this permeability is defined. (Rokahr et al., 2002) did modelling on different permeability in relation to the effective pressure. The effective pressure can be calculated by the following formula:

$$\sigma_{teff} = P_{cavern} - \sigma_t$$

Equation 16

Where  $\sigma_{teff}$  is the effective pressure,  $P_{cavern}$  is the brine cavern pressure and  $\sigma_t$  is the local in situ pressure (assumed to be isotropic). 3 permeability criteria were defined, the LMS, IUB and the Generalized Stormont Criterion. The 3 criteria are plotted with the effective pressure against the permeability is shown in figure 6.11.

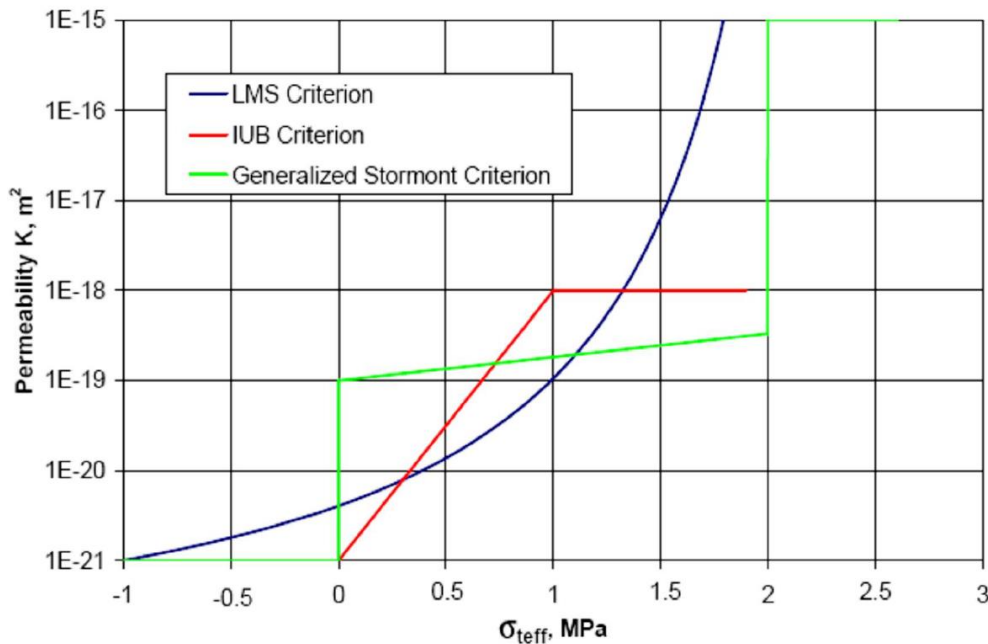


Figure 6.10 Criteria for permeability of rock salt (Rokahr et al., 2002)

Another study did laboratory tests on hollow salt spheres (Brouard et al., 2001). Not all tests succeeded but in general a permeability between  $10^{-19}m^2$  and  $10^{-21}m^2$  is seen in the tests. A slight increase of permeability above the range is seen when the pressure in the spheres comes to around 1.5 MPa, shortly after a fracture develops.

To give an idea on yearly permeation volumes looking at the perspective of permeability the following cases shown in table 6.11 will be calculated. In this table the permeabilities (in  $m^2$ ) according to the different models at different pressures are shown. These were extracted from the graph in figure 6.10.

Pressure MPa	-1	0	0.5	1	1.5
LMS Criterion	$1*10^{-21}$	$7*10^{-21}$	$2*10^{-20}$	$1*10^{-19}$	$9*10^{-18}$
IUB Criterion	$1*10^{-21}$	$1*10^{-21}$	$5*10^{-20}$	$1*10^{-18}$	$1*10^{-18}$
Generalized Stormont Criterion	$1*10^{-21}$	$1*10^{-19}$	$2*10^{-19}$	$3*10^{-19}$	$4*10^{-19}$

Table 6.10 Permeabilities for models and corresponding effective pressures (permeabilities in  $m^2$ )

The Darcy flow equation can be applied to a cavern filled with brine. Where A is the surface area of the cavern walls and roof. The viscosity of saturated brine at normal conditions is around  $1.2 * 10^{-3} Pa * s$ . However, in the cavern the brine is at a temperature of around  $95^\circ$  and a pressure of around 51 MPa. Correcting the viscosity for these factors gives a viscosity of  $0.7 * 10^{-3} Pa * s$ . The pressure gradient is calculated from the specific weight of the lithosphere ( $0.0212 MPa/m$ ). Note that here the pore pressure in the halite is assumed to be the same as the lithostatic pressure. Q is taken as  $m^3/year$ . Looking at the permeation model it was assumed that the brine flows around roughly the top half of the cavern out to the surrounding rock. Therefore, for the surface area 2 cases are considered, one where only the top half of the cavern is considered ( $19,537m^2$ ) and one case where the whole cavern is considered ( $46,184m^2$ ). These areas are calculated from the model at year 0 using the top (as a circle) and the sum of the disks as cylinder area. It should be noted that the cavern walls are highly heterogenous and have a larger surface area than the cylinder and circle shape that is used for calculation of the area. Note as well that pressure is dependent on depth. For BAS-4 the pressure difference between the cavern and the surrounding rock is around 1 MPa at the top of the cavern and 2.7 MPa at the bottom of the cavern. Note that as an effective pressure these are negative. The calculation made here is done to get an idea of permeation rates possible out of the cavern and does not accurately represent reality. Table 6.12 shows the results for the top half of the cavern, table 6.13 shows the results for the whole cavern. All results in table 6.12 and 6.13 are the flows in  $m^3/year$ .

Pressure MPa	-1	0	0.5	1	1.5
LMS Criterion	$1.87*10^{-2}$	$1.31*10^{-1}$	$3.74*10^{-1}$	$1.87E*10^0$	$1.68*10^2$
IUB Criterion	$1.87*10^{-2}$	$1.87*10^{-2}$	$9.35*10^{-1}$	$1.87*10^1$	$1.87*10^1$
Generalized Stormont Criterion	$1.87*10^{-2}$	$1.87*10^0$	$3.74E*10^0$	$5.61*10^0$	$7.48*10^0$

Table 6.11 Cavern permeation rates using permeability for top half of cavern in  $m^3/year$ .

Pressure MPa	-1	0	0.5	1	1.5
LMS Criterion	$4.42 \cdot 10^{-2}$	$3.09 \cdot 10^{-1}$	$8.84 \cdot 10^{-1}$	$4.42 \cdot 10^0$	$3.98 \cdot 10^2$
IUB Criterion	$4.42 \cdot 10^{-2}$	$4.42 \cdot 10^{-2}$	$2.21 \cdot 10^0$	$4.42 \cdot 10^1$	$4.42 \cdot 10^1$
Generalized Stormont Criterion	$4.42 \cdot 10^{-2}$	$4.42 \cdot 10^0$	$8.84 \cdot 10^0$	$1.33 \cdot 10^1$	$1.77 \cdot 10^1$

Table 6.12 Cavern permeation rates using permeability for whole of cavern in  $m^3/year$ .

Looking at current conditions in a Frisia cavern where the brine pressure equalizes to 98% of lithostatic pressure meaning an effective pressure in the top of the cavern at around -1 MPa. At these conditions the permeation rates are between  $1.87 \cdot 10^{-2} m^3/year$  for the top half of the cavern and  $4.42 \cdot 10^{-2} m^3/year$  for the whole cavern. To give an idea of this number it would mean a volume equivalent of 18 to 44 liters brine per year. This is low compared for a cavern with a volume of around  $1Mm^3$ . The P10, P50 and P90 cases have a permeation rate of 5, 103,  $2313m^3/year$ , respectively. The permeability of the cavern is a factor 250 smaller compared to the P10 case, let alone the P50 and P90 case. This indicates that the permeability of salt is not the dominating permeation process and that there are other permeation mechanisms present around the cavern.

It could be that in decades to centuries other permeation processes and the cavern pressure rises. At this point, the permeation process could become more significant again. Taking the average of the 3 models at an effective pressure of 0 MPa the permeation rate could become  $0.67 m^3/year$  for brine permeating from the top half of the cavern. At an effective stress of 1 MPa this would mean  $8.7 m^3/year$  and at 1.5 MPa it would mean a permeation rate of  $64 m^3/year$ . At an over pressure of 1 MPa the permeability is like the P10 convergence case. However, this would mean an overpressure throughout the top half of the cavern and the effective pressure in the cavern can never go above 0 MPa because only the lithostatic pressure creates pressure on the cavern. One way the effective pressure in a cavern can become positive is of temperature effects. When a cavern is just taken out of production the cavern brine is at a lower temperature compared to the surroundings. Volume expansion because of a rise in temperature can cause an overpressure. This is not the case for abandonment since these timescales are much longer than it takes for the brine temperature to equalize with its surroundings. Another way would be at large cavern volumes where the squeeze is driven purely by the bottom part of the cavern. Here a positive or 0 pressure deficit could be created at the top of the cavern. This is not in line with the current data where the pressure in the cavern equalizes at 98% of lithostatic pressure in the top of the cavern.

Since the permeability of the cavern is so low compared to the results of the convergence model there must be other permeation methods/systems at play at the time of abandonment. Other possible migration paths will be discussed in chapter 6.7 and tested in the sensitivity analysis in chapter 7.

## 6.5 Discussion on other permeation mechanisms

The permeation model made in section 6.2 assumed a combination of the filling of pore spaces within the salt and preferential flow paths such as micro fractures created during production. The permeability of virgin halite was assessed in section 6.4. It turned out that the permeability of halite is much lower compared to what the output of the convergence and permeation model suggests. It could therefore be that other permeation mechanisms are much more dominant around the cavern. Different mechanisms are discussed in this section. These will then be tested in the sensitivity analysis in chapter 7.

### 6.5.1 Threshold pressure deficit for cavern convergence

As discussed in the literature review (chapter 2.2) and the concept review of squeeze models (chapter 3.2) the pressure solution creep is mostly dominant within the lower pressure deficit region. (Van Oosterhout et al., 2022) made a model for a threshold pressure deficit where the pressure solution creep would stop, a very low dislocation creep comes in again; resulting in a significant slow down of creep. In older models this was believed to be at a pressure deficit in the range of 1-10 MPa. (Van Oosterhout et al., 2022) proposed a much lower boundary. In the model made for a depth up to 3 km the pressure solution creep is believed to come at halt at a deficit somewhere between 0.07 and 0.7 MPa. The threshold value was tested in numerical modeling (Hunfeld et al., 2022). In these models it showed that the threshold pressure is significant and should be considered. However, there is no evidence on the stopping of creep below a certain stress in field tests.

### 6.5.2 Preferential flow due to heterogeneities

#### 6.5.2.1 Permeation via anhydrite alterations

The cavern, at the start of production, is well below the last cemented casing. The space between the top of the cavern and the last cemented casing is called the neck and is filled with blanket fluid. Through the cavern's life the cavern slowly moves upwards. This has multiple reasons as discussed in chapter 3.1. One of the reasons is that during production it sometimes happens that part of the roof is collapsing. This could be due to the loss of tensile strength in the anhydrite bands between the halite as the blanket fluid slowly permeates through the layer. This could also be a leakage path at time of abandonment.

In the cavern there are then a lot of thin anhydrite bands in direct contact with the brine. It could be that the brine permeates horizontally through the salt layers before permeating upwards. This could lead to a much wider permeation front.

#### 6.5.2.2 Micro fractures created during production

When a cavern experiences multiple loading cycles micro fractures occur. These microfractures can increase the permeability of salt. How far and how much of these fractures develop is not known. This could be another preferential flow path for the brine and could give the salt more vertical permeability than what the models predict.

### 6.5.3 Stringers/floaters in salt formations

Stringers are layers within salt formations which contain some porosity, these are well investigated since they can pose a risk during the drilling of a well. Floaters are smaller unconformities within a salt layer. These can be pieces of anhydrite that have sunk into the salt formation because of their higher density. These floaters can trap fluids (brine, oil or gas) and still store them under high pressures for longer time periods.

## 6.6 Comparison to other models

In the past, 2 other models were prepared to model the cavern convergence rates after abandonment of a cavern. One model was prepared by professor Lux of the Technical University of Clausthal (Lux, 2010) the other was prepared by (WEP, 2010). These models were prepared on the BAS-3 cavern, a cavern half the size of the BAS-4 cavern meaning that the cavern convergence rates are roughly half that of BAS-4 as well since the squeeze model is volume based. However, the BAS-4 cavern is situated slightly deeper compared to the BAS-3 cavern meaning a higher volume in the permeation model.

The Lux model uses an alternative permeation model based on the Lubby-2 salt creep law and Darcy flow through porous rock. The speed of outflow in this model is determined by how much can flow into the overlying layers and not by the cavern convergence rate as in the WEP model. This permeation model creates an expanding balloon like shape above the cavern where the brine accumulates. The WEP model modelled the permeation as an upside-down knotted cone above the cavern and the permeation rate was purely governed by the cavern convergence. The Lux model assumed that the total porosity in the permeation zone is 1%, in the WEP model a porosity of 0.2% was assumed. The Lux model predicts that it will take approximately 55,000 years for the permeation front to reach the Bundsandstein in the BAS-3 scenario. The WEP model applied on BAS-3 predicts a faster time of 1,300 years, which is around 40 times faster than the Lux model. The faster infiltration time in the WEP model is due to the lower secondary porosity, a different permeation shape and a different approach to the permeation process. The Lux model considers the energy needed to create the new micro-migration paths between the salt crystals, which slows down the permeation rate and cavern convergence. Whereas the WEP model is from the perspective of the cavern convergence and the brine permeates out of the cavern and fills up the cone. A slower convergence rate in the future will be assessed in chapter 7, this will be achieved by lowering the pressure deficit within the cavern.

Both models have their simplifications. The main simplification of the WEP model is that it does not take into account the permeability of the surrounding layers and the Lux model assumes homogenous halite layers around the cavern. The permeation model in this research predicts times in the range of these models (26, 588 and 12,363 years for the P10, P50 and P90 convergence models respectively). The permeability of halite was discussed in chapter 6.4. Here it was shown that this permeability is much lower than the convergence model predicted. Other permeation paths were discussed in section 6.5, a number of these will be tested in the sensitivity analysis in chapter 7.

## 6.7 Subsidence bowl

Previous models (WEP, 2010, 2014) discussed how the permeation of brine affects the volume of underground caverns and the potential for subsidence. Initially, the displacement of volume caused by permeation occurs in a near-constant volume system that includes the cavern, surrounding areas, and the permeation volume above the cavern. The theory is that if there is no reduction in volume underground, there will be no surface subsidence.

However, if fluid escapes from the system and flows into permeable zones (e.g., Bundsandstein), it can cause a decrease in the volume of the system and lead to subsidence. This is like the production phase of a cavern where salt is mined and thus volume gets removed from the system. For the production phase a subsidence model is made and calibrated from subsidence measurements on the surface (WEP, 2021). The subsidence will not occur only above the cavern since the salt that is mined comes from the surrounding area around the cavern. Therefore, the subsidence is in the form of a bowl with the deepest point above the cavern. For the subsidence model it is assumed that the volume exiting the system equals the volume of the bowl as shown below.

$$\text{Permeation volume} = \text{Volume bowl}$$

Equation 17

The subsidence prediction model for after abandonment assumes that all fluid leaving the cavern and surrounding permeation volume thereby leaving the system will result in subsidence. Once this brine permeates out of the system it can freely flow over a larger area (in the Bundsandstein above the salt). To model the subsidence bowl, some formulas are used, first is the subsidence with distance from the cavern is shown in equation 16 below.

$$w_{(x,y)} = w_{max} e^{-\gamma r^\delta}$$

Equation 18

Where  $w_{(x,y)}$  is the subsidence in mm at a certain distance from the deepest point (the cavern),  $w_{max}$  is the deepest point in the subsidence bowl directly above the cavern (mm), the parameter  $\gamma$  defines the flattening of the subsidence bowl,  $r$  is the distance from the cavern in meters and  $\delta$  defines the steepness of the subsidence bowl. The base values for  $\gamma$  and  $\delta$  are  $3.35 \cdot 10^{-7}$  and 1.96, respectively.

The volume of the subsidence bowl can be defined by equation 17 below.

$$\text{Volume bowl} = 2\pi w_{max} * 1/\delta * \left( \gamma^{-2/\delta} * \text{Gamma}(2/\delta) \right) / 1000$$

Equation 19

Where  $\text{Volume bowl}$  is the total volume of the subsidence bowl in  $\text{m}^3$  and  $\text{Gamma}$  is the gamma function. This is then corrected for the conversion from mm to m. To calculate the deepest point of subsidence over time the formula needs to be rewritten as follows.

$$w_{max} = \text{Permeation volume} / Z$$

Equation 20

Where Z equals:

$$Z = 2\pi * 1/\delta * (\gamma^{-2/y} * \text{Gamma}(2/\delta)) / 1000$$

Equation 21

The volume of the bowl can be substituted for the permeation volume since it is assumed that all the volume that permeates out of the cavern system will lead to subsidence.

Different publications with predictions of subsidence until 2050 in The Netherlands were made (*Bodemdaling, 2023; Bodemdalingsvoorspellings-kaarten, 2022*). Looking at the North-Western part of The Netherlands, caverns subsidence levels of around 10-20cm are expected. Going more to the east of Friesland, the subsidence is expected to be even higher (20-30cm). 20 cm until the year 2050 means around 6 mm/year of subsidence unrelated to solution mining processes.

After production is stopped, subsidence data shows some residual subsidence after shut-in of a cavern and shortly after there is no subsidence linked to the caverns anymore. Once the system fills up and brine can freely flow over a larger area. For the adjusted paraboloid P50 case model it takes around 588 years for all the layers above the cavern to fill up before entering the Bundsandstein. Implementing the previously mentioned formulas and inserting the permeation rate (of converted carnallitic brine) into the formula gives the results shown in table 6.10 (for the adjusted paraboloid P50 model). The subsidence rates mentioned in the table are at the deepest point in the subsidence bowl directly above the cavern, the subsidence farther from the cavern can be calculated from equation 16. An example of the subsidence with distance to the cavern in year 589 is shown in figure 6.10.

According to the adjusted paraboloid model there might be some subsidence after 588 years when the brine reaches the Bundsandstein. The subsidence rate is shown at various times, it is possible to see that the rate is decreasing over the years. This is because the cavern gets smaller and thereby the permeation rate drops as well. The permeation rate is linked to the subsidence rate in the formula discussed in this chapter. After 588 years the subsidence rate is roughly 0.016 mm/year, a negligible amount looking at subsidence rates in the near future unrelated to the mining processes of Frisia.

After 588 years the subsidence that could start to occur because of permeation processes is several magnitudes lower compared to the yearly subsidence unrelated to the mining activities. Because these potential subsidence rates are so small it is impossible to measure it in the current time scale. Looking at the P10 and P90 cases, in the P10 case the adjusted paraboloid model is full after 12,363 years. At this time, the potential subsidence will be in an order  $7 \cdot 10^{-4}$  mm/year. A negligible amount. Looking at the P90 case the adjusted paraboloid model fills up after 26 years and potential subsidence will occur. This is in the range of 0.36mm/year. This is much higher compared to the other cases but still a factor 15 smaller than the expected subsidence in that area unrelated to the caverns.

Year	Subsidence rate (mm/year)	Permeation rate (m <sup>3</sup> /year)
589	0.016	159
600	0.016	159
1,000	0.015	152
2,000	0.013	136
5,000	0.010	99
10,000	0.005	58
20,000	0.002	21

Table 6.13 Subsidence predictions P50 case together with permeation rates (converted brine)

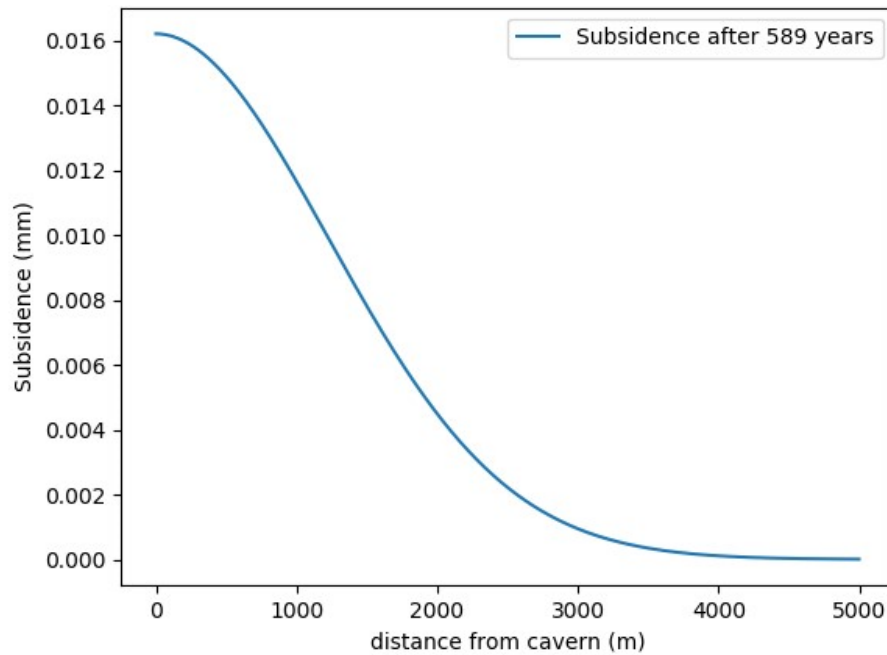


Figure 6.11 Subsidence with distance from the cavern

## 7. Sensitivity analysis of brine permeation model

### 7.1 Base case and deviations

A sensitivity analyses will be performed on the adjusted paraboloid model together with the P50 convergence model. There are several different inputs to the permeation model as discussed in chapter 6.2, the values of these parameters can be slightly inaccurate for multiple reasons. The sets of sensitivities can be divided into 2 parts. The first set of sensitivity analyses are about testing the base case. Here the variability in the top of the layers themselves and their porosities will be tested. The second set of cases will test different permeation shapes and mechanisms proposed in chapter 6.7.

#### 7.1.1 Variability base case model

In this chapter the top heights of the different layers will be tested. In the area around the BAS caverns there is a small dip of around 20 degrees present. Depending on the width of the adjusted paraboloid at a certain height a 20° angle has a different influence on the top of a layer. The higher and wider a layer the larger volume effect there is on a certain angle. However, assuming the layers are perfectly even, the dip angle evens out over a distance. A lower top of a layer in the South-West means a higher top of a layer in the North-East. Therefore, this should not matter much. To study the effect of a change in the tops of a layer, an analysis will still be performed. Using the tangent rule ( $\text{tangent} = \text{opposite}/\text{adjacent}$ ), the top width of a certain layer and using an angle of 10 to 20 degrees for the different cases. The following changes in top height are assessed:

#### **Top height Zechstein-II Halite**

The width of the paraboloid is still quite small over here. -30, -15, 15 and 30m will be added and subtracted from the top height of this layer.

#### **Top height Zechstein-II Carnallite**

This layer sits slightly higher than the previous one. -50, -25, 25 and 50m will be added and subtracted from the top height of this layer.

#### **Top height Zechstein-III Anhydrite**

Again, the anhydrite layer only has a thickness of around 60m, next to this it was proposed that the brine permeates quite vertically through this layer in the adjusted paraboloid model. The following values will be tested: -60, -30, 30 and 60m will be added and subtracted from the top height of this layer.

#### **Top height Zechstein-III Halite**

The Zechstein-III Halite has a much larger thickness and a wider width; therefore, the following cases will be evaluated: -100, -50, 50 and 100m will be added and subtracted from the top height of this layer.

## Porosity of each layer.

The porosity is an important input within the permeation model. After a permeation volume gets calculated, this volume is then multiplied with the porosity. This then gives the volume of brine a layer can hold. For these scenarios, the porosities presented in table 7.1 will be assessed for each of the 4 layers.

1.00%
0.50%
0.20%
0.10%
0.01%
0.001%

*Table 7.1 Porosities tested in sensitivity analysis.*

### 7.1.2 Variations on base case model

The cavern system will always try to find an equilibrium between cavern convergence and brine permeation. Currently this equilibrium is met at a cavern brine pressure at 98% of lithostatic pressure. This could change in the future when the brine filled cavern reaches a certain layer by means of permeation and enters a new layer and a new way of permeation. When this happens the permeation rates could change, to model this potential effect the following 2 scenarios will be modelled where a change in cavern pressure will occur.

#### **Cavern pressure increase when Zechstein-III Anhydrite is reached.**

As discussed in chapter 6.1 the Anhydrite layer is a very hard layer. Because of this it could be that the permeating brine finds a larger resistance when this point is reached. Therefore, the cavern must find a new balance between the permeation and convergence. Since there is more resistance, the cavern convergence rates must go down. The only way for the convergence rates to go down is by a pressure increase in the cavern. This is modelled by setting the pressure deficit on the top of the cavern at 0 MPa. Since it is assumed that the temperature is stabilized in the cavern the only factor that can put pressure on the cavern is the lithostatic pressure. The pressure of the brine in the cavern can thereby never exceed lithostatic pressure. Thus, a maximum pressure deficit of 0 MPa in the top of the cavern is only possible. Since the brine has a lower specific weight (approximately a difference of  $1\text{g/cm}^3$  compared to the surrounding salt rock) there will still be a pressure deficit in the bottom of the cavern as discussed in chapter 3.3. So, when there is no pressure deficit in the top of the cavern, the cavern convergence is purely driven from the bottom parts of the cavern.

As discussed in section 7.1 in this scenario the adjusted paraboloid P50 case will be considered. According to the modelling results it takes 66 years for the Halite-II and Carnallite-II layers to fill up. For the first 66 years the pressure in the cavern will stay at the 98% pressure compared to the lithostatic pressure, after that time the brine pressure will increase to 100%.

### Cavern pressure increase when Zechstein-III Halite is reached.

Another scenario could be that the cavern pressure increases when the Zechstein-III Halite is reached. In the adjusted paraboloid P50 case this happens after 126 years.

As discussed in chapter 6.1, a brine conversion takes place in the carnallite layer. In this process a volume expansion takes place, during this volume expansion there will be a lot of pressure exerted on the anhydrite layer. Next to this as discussed in chapter 6.1, the anhydrite layer could have been affected during the production phase as well. These things could induce microfractures in the anhydrite layer and the brine can easily flow to the Zechstein-III Halite. Once this halite layer is reached, there could be a large resistance in flow and the cavern convergence rates drop as well because of an increase in pressure in the cavern. So, this scenario will be like the previous scenario but in this case the pressure will increase slightly later when the anhydrite layer is filled and the last halite layer is reached.

### Horizontal flow in the Zechstein-II Halite

As discussed in chapter 6.1 the Zechstein-II Halite has experienced more stress changes over time causing microfractures in the layer, next to this there are a lot of horizontal anhydrite alterations in the layers. Since the cavern brine has direct access to these horizontal layers it could be that the horizontal permeability is much larger and easier accessible by the brine. In this scenario an adjusted paraboloid is fitted that is much wider to accommodate this volume. The model of this analysis is shown in figure 7.1, the model parameters and volumes are shown in appendix 9.

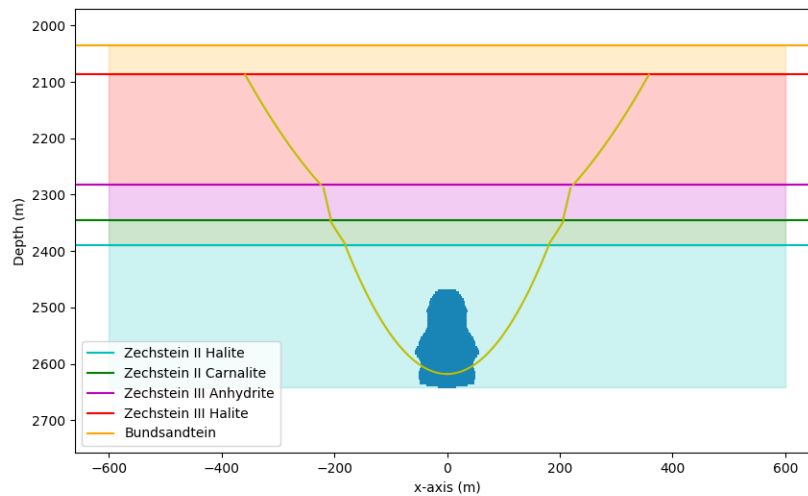


Figure 7.1 Sensitivity analysis horizontal flow Zechstein-II Halite

## Horizontal flow in the Zechstein-II Carnallite

As discussed in chapter 6.1 when halitic brine meets carnallite a brine conversion takes place and a precipitation of minerals happens together with a volume expansion. The potential creation of a cavern was already widely discussed in previous research (WEP, 2010). An actual calculation on the larger spreading of this front was not considered however since the only shape used was a cone. In this scenario, like the previous, a larger spread in the carnallite will be made as shown in figure 7.2. This then has its effects in a wider spread in the overlying layers as well. Model parameters and volumes are shown in appendix 9.

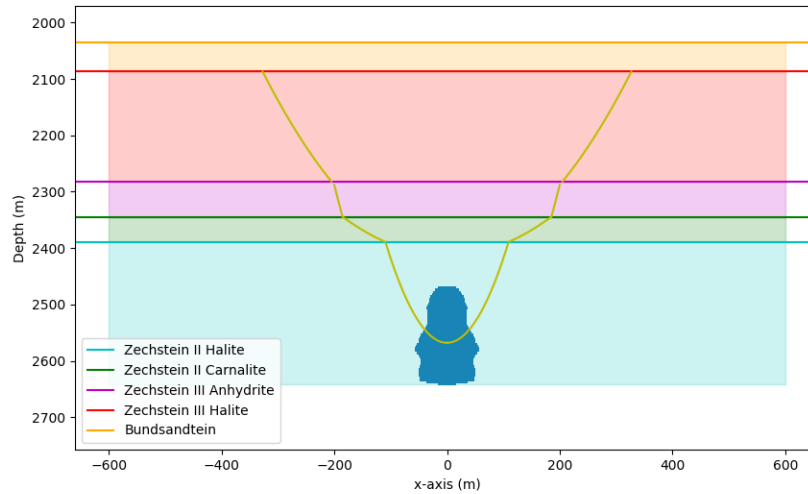


Figure 7.2 Sensitivity case horizontal flow Carnallite

## 7.2 Results sensitivity analysis

### 7.2.1 Variability base case model

The results of the top height variations and porosity variations can be found in appendix 8.

Looking at the sensitivity analysis of the top heights, the variations of the first 3 layers (the Zechstein-II Halite and Carnallite and the Zechstein-III Anhydrite) do not matter much. The total time for the entire system to fill up only varies with a few years for the different scenarios.

This is because the total thickness of the system (between the top of the cavern and the top of the Zechstein-III Halite) stays the same. Only the thickness of certain layers changes and thereby the volume of that layer. Since each layer has its own shape, the volume gets influenced by this change in height and so the times for a layer to fill up. But only slightly since the total thickness of the system stays the same and on top of that comes that the Zechstein-III Halite has the biggest storage volume.

The times for the Zechstein-III Halite to fill up do change significantly with different top heights. A 50 m drop in top height results roughly in a 250-year change in breakthrough time to the overlying Bundsandstein. It should be noted that even though there is a slight dip of the layers in the area, these scenarios are unrealistic since the layers stay quite uniform in thickness and dip, so a lower top height west means a higher top height east. So, the volume only changes slightly over a larger area.

Similar results can be seen for porosity cases. As discussed in chapter 6.6 the previous WEP Modelling and the Lux model used different porosities. A good understanding of secondary porosity created is needed since a doubling in porosity means that the time for a layer to fill up doubles as well. This is especially important for the Zechstein-III Halite since this layer contains 78% of the storage volume. So, a slight change in porosity in this layer changes the breakthrough time significantly.

### 7.2.2 Variations on base case model

The different scenarios on the base case shape and cavern pressure over time of the adjusted paraboloid model were tested as well. The results are discussed in the next subsections.

#### **Cavern pressure increase when Zechstein-III Anhydrite is reached**

The results for the case where a pressure increase happens once the bottom of the Anhydrite layer is reached is shown in table 7.2. Once the brine fills up the Zechstein-II Carnallite layer and reaches the bottom of the Zechstein-III Anhydrite the pressure deficit at the top of the cavern becomes 0. When this happens the squeeze of the cavern is purely driven from the bottom parts of the cavern and the permeation rates slow down. Without a pressure increase the permeation rate after 66 years is around 100 m<sup>3</sup>/year. With the pressure increase the permeation rate slows down to around 49 m<sup>3</sup>/year after 66 years. So, when the pressure of the brine in the top of the cavern becomes equal to the lithostatic pressure the permeation rate is around half the original permeation rate. This has its effect on the permeation model as well as the time for the rest of the system to fill up doubles.

Case	Zechstein II halite	Zechstein II Carnallite	Zechstein III Anhydrite	Zechstein III Halite
Base case	59	66	126	588
Pressure increase Anhydrite	60	66	192	1165

Table 7.2 Case for pressure increase when Zechstein-III Anhydrite is reached.

### Cavern pressure increase when Zechstein-III Halite is reached

A similar scenario was run with a pressure increase once the Anhydrite filled up and the Zechstein-III Halite is reached. The results of this scenario are shown in table 7.3 below. The permeation rates show similar behaviour as in the previous case. But since the cavern pressure increase is later (126 years), the total time for the system to fill up is slightly shorter compared to the previous case.

Case	Zechstein II halite	Zechstein II Carnallite	Zechstein III Anhydrite	Zechstein III Halite
Base case	59	66	126	588
Pressure increase Halite III	60	66	126	1100

Table 7.3 Case for pressure increase when Zechstein-III Halite is reached.

### Horizontal flow in the Zechstein-II Halite

In these cases, a different permeation shape was fitted to the permeation model. The shape, parameters and volumes are shown in appendix 9. In this case it was assumed that the brine migrates more horizontally in the Zechstein-II Halite since the layers are layered horizontal and are in direct contact with the cavern. In this model the volume in the Zechstein-II Halite is much larger (around 4 times). This results in a wider top width of the paraboloid and a wider permeation system throughout the other layers resulting in a much longer time for the system to fill up as shown in table 7.4 below.

Case	Zechstein II halite	Zechstein II Carnallite	Zechstein III Anhydrite	Zechstein III Halite
Base case	59	66	126	588
Sensitivity	214	214	300	997

Table 7.4 Results case for more horizontal flow in the Zechstein-II Halite

### Horizontal flow in the Zechstein-II Carnallite

In this case a similar scenario to the previous one was run; however, the Zechstein-II Halite was left the same as the base case and the Carnallite had a wider spread in this case. This resulted in a lower change but still takes around 150 years longer for the system to fill up as shown in table 7.5 below.

Case	Zechstein II halite	Zechstein II Carnallite	Zechstein III Anhydrite	Zechstein III Halite
Base case	59	66	126	588
Sensitivity	59	74	162	730

Table 7.5 Results case for more horizontal flow in the Zechstein-II Carnallite

## 7.3 Discussion on sensitivity analysis

### 7.3.1 Variability base case model

In these scenarios there were 2 things tested. First the top heights of the system and secondly the porosity of different layers were tested.

First the variability of the top height of the different layers was tested. What stood out from the sensitivity analysis is that the volume of the layers in between the top of the cavern and the top of the Zechstein-III Halite did not change significantly with a change in top height of those layers. This has multiple explanations. For one the volume of the Zechstein-III Halite is the most significant in terms of volume and a change in that height will be seen the most. Another reason is that the changes in the heights of layers between the top of the cavern and the top of the Zechstein-III Halite do not change the total height of the system. Only the volume of a specific paraboloid changes.

To show how the layers are dipping 2 cross sections over BAS-4 of the DGM-Deep model are shown in figure 7.3 below. The left part is a plot from west to east and the right plot shows a cross section from north to south. Here it is shown how the layers dip to the South-West. More specifically it can be seen that the dip is more West-South-West. The top of the adjusted paraboloid has a width of around 600 m. Over 600m the top of the Zechstein dips between around 50 m (north-south) and 100m (west-east). It could be that parts of the permeation model reach the overlying layers faster compared to other parts. This will not change the total volume of the system that much, however. The average top height will be like the top height obtained from drilling data of the BAS-4 well.

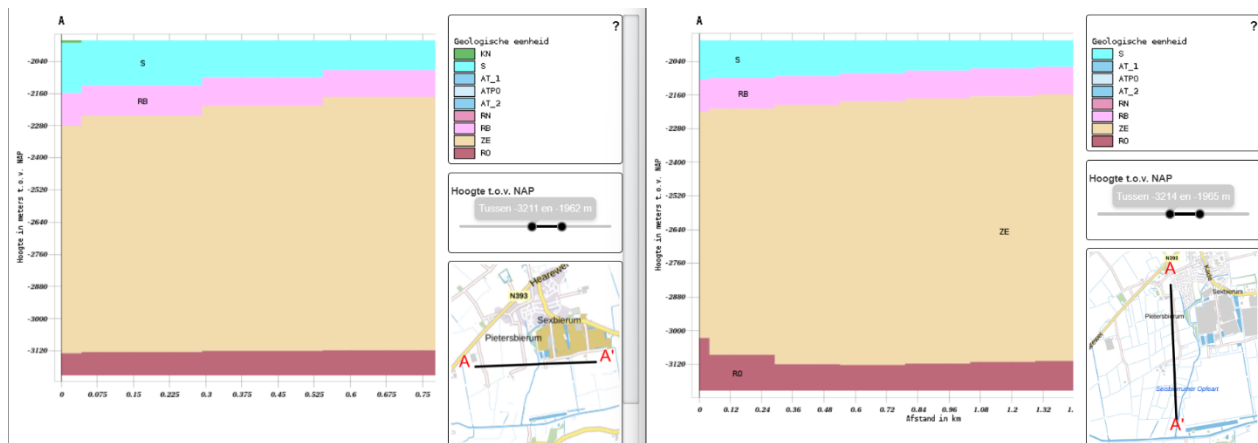


Figure 7.3 West-East (Left) and North-South (Right) cross section of Zechstein over BAS-4 cavern (DGM-Deep model, extracted 2-5-2023).

Next to the tops heights the porosities were investigated as well. The porosity of a layer has shown to be especially important in the modelling. Especially within the Zechstein-III Halite since this layer has the largest permeation volume. There is not much research done on porosities the porosities of the different layers. Especially on secondary porosities. What is known is that these porosities are low. And a porosity of 1% is on the high side, even if it is created secondary porosity due to permeation. The actual total porosity of most likely in in the lower ranges around or lower than 0.2%.

### 7.3.2 Variations on base case model

On the variations 2 things were tested, first the effect of a pressure increase in the cavern at different times were tested. Secondly different shapes were tested to see how different permeation mechanisms performed.

By changes in the pressures a significant drop in the permeation rates were seen. In this scenario the pressure on the top of the cavern was raised from the situation at abandonment (a deficit of around 1MPa in comparison to the local lithospheric pressure) to a pressure equal to the lithospheric pressure (a pressure deficit of 0 MPa in the top of the cavern). What was seen from this is that the permeation rates roughly halve since there is still a larger pressure deficit with depth. This gives a good understanding on the convergence/permeation model itself but it is questionable on how this data is usable in the field.

Currently the brine probably has not reached the carnallite yet. Let stand the anhydrite and halite above. If and by how much the cavern pressure would rise at what time might never be known since these processes happen over such a long time. More research into the processes within the carnallite layer is needed to get a better understanding of the interactions between and the halite carnallite and anhydrite layers and within those layers to brine.

How the brine will permeate exactly might never be known. Since the shape parameters determine volume and thereby the times for each layer to fill up, it does matter. Looking at the geology there are a lot of horizontal anhydrite alterations in between the halite layers around the cavern. As was discussed in chapter 7.1 this was the main motivation to model a larger spread in the Zechstein-Halite layer. This resulted in a 70% increase in time for the total system to fill up. The results could look like one of the models or could be somewhere in between these models.

## 8. Intermediate conclusion on permeation model

To conclude the permeation model, the research questions need to be answered. These are repeated below.

- What are the aspects of the current permeation model and what does previous research suggest about permeation fronts of brine?
- What variations can be made on parameters in the permeation model and how do these variations impact the outputs of the permeation model?
- At what time and rate is the outflow of brine into the sandstone layer above?
- What is the final additional surface subsidence and subsidence rate in the different models?

In previous models the permeation front was modelled as a cone above the cavern (WEP model) and as an 'expanding balloon' above the cavern in numerical modelling by Lux (Lux model). Other research proposed different paths for brine to escape the cavern. This can be summarized in 4 systems, leakage through the abandoned well, fracturing, micro fracturing and local permeation or lastly pure permeation of brine through the permeability of salt. Fracturing and well leakage can almost be ruled out since before the cavern is abandoned there is a shut-in phase where the temperature in the cavern can equalize and the pressure of the brine has shown to stabilize at 98% of lithostatic pressure. At these under pressures fracturing is not possible. At the time of abandonment, the well is sealed and tested, therefore this is not a likely scenario. The main way for brine to escape the cavern is by some way of permeation.

For this the permeation model was built. Once the base case was presented the model was tested with a sensitivity analysis. 2 types of analyses were done, first the model itself was tested and the influence of a change in porosity or top height of different layers were evaluated. Secondly different cavern pressure scenarios over time and different permeation shapes were tested.

The conclusion from the first set of scenarios is that the top height influences the permeation times but that the influence is not super big, only by varying the top height of the Zechstein-III Halite the times change significantly. Since the top height are quite well known, it will not change that much. The porosity is a more important factor because this determines how much volume can be stored. A good understanding of the primary and secondary porosity is needed.

According to the model outputs it takes 26 years for all layers to fill up according to the P90 case. 588 years for the P50 cases and 12,363 years for the P10 case. Looking at the permeation mechanisms it's more realistic that the range will be somewhere between the P10 and P50 cases and the P90 case seems unrealistically fast. From recent testing and modelling it was shown that the salt creep is probably much lower than in the P90 case (Bérest et al., 2019; van Oosterhout et al., 2022). Next to this the permeability of halite is much lower than the convergence rates of the P90 model. Still the permeability of halite is much lower compared to the P10 case meaning there must be other permeation paths as well.

Lastly in terms of subsidence, this was assessed in chapter 6.7. The subsidence would be  $7 \cdot 10^{-4}$  mm/year after 12,363 years, 0.016 mm/year after 588 years and 0.36 mm/year after 26 years for the P10, P50 and P90 cases respectively. Compared to unrelated subsidence processes in the area, the potential additional subsidence from the cavern when it would reach overlying layers is negligible.

## 9. Discussion

The main objective was to build a convergence and permeation model for a salt cavern after abandonment. The output of the convergence model, the convergence rate, is used as an input for the permeation model since there is an equilibrium between the cavern convergence and the permeation of brine.

The convergence model proposed high convergence rates, this had mainly to do with the linear part of the squeeze model. The linear part is probably much lower in the low-pressure deficit region where the cavern is at abandonment. 3 cases, a P10, P50 and P90, were made where these are the respective percentiles from the range of the sensitivity analysis. Where in the P90 case the linear squeeze parameters were like the production parameters but in the P50 and P10 the linear parameters were much lower and like creep rates of salt under low-pressure deficits. The permeability of salt is very low, compared to the P10 case it is a factor 250 lower. Therefore, there must be other permeation mechanisms or the cavern convergence is lower than the model predicts.

Lower convergence rates could be because of a lower linear component of the squeeze model. However, the P10 case already uses parameters very favourable for low salt squeeze. Another option could be that there is a threshold pressure for salt creep to occur (van Oosterhout et al., 2022). In this case the cavern convergence would mainly be from the bottom parts of the cavern only since there is a higher-pressure deficit compared to the upper parts which might have no convergence at all. The pressure deficit is determined by the lithostatic pressure, therefore any inaccuracies in the specific weight of the lithosphere could change the pressure deficit at the top of the cavern. Since the convergence rates are quite high it could be that the pressure deficit is lower and the cavern convergence rates are lower because of this.

A discussion on other permeation paths were held as well focusing on the halite around the cavern. In here, 2 other probable permeation paths were found. One was the permeation through anhydrite layers in between the halite and one was permeation through micro fractures created during production. These heterogenous flow paths were incorporated in the model and tested in the sensitivity analysis.

The P90 convergence model used as an input on the permeation model suggested extremely fast times for the layers in the permeation model to fill up. The brine would reach more permeable layers almost 400 meters higher after 26 years. This is a highly unlikely scenario as the permeability of halite is much lower. Next to this, testing and modelling of salt sample under low-pressure deficits (Bérest et al., 2019; van Oosterhout et al., 2022) showed much lower creep rates.

The convergence model, with the right input variables, is a good model for calculating cavern convergence after the abandonment of a cavern. The model has its assumptions but considering the timescale where the model is run these are not that significant. The main question in this model is the value of the linear part of the squeeze model and if there is a threshold pressure deficit for salt creep to occur. Next to this a change in the pressure deficit changes the output significantly as well, a good understanding of this deficit is needed.

The permeation model is more limited. The paraboloid shapes were best fitted on each layer to describe their potential permeation behaviour. The shape in the Zechstein-II Halite is probably accurate. The cavern has direct access to anhydrite alterations between the halite. And it could be that the brine flows along the interfaces of these small layers resulting in a higher horizontal permeability. The halite has

some microfractures created during production as well, where the brine could flow more upwards through these created pore spaces. These scenarios were tested in chapter 7.

Once the brine reaches the carnallite layer a dissolution of the carnallite will happen where more brine volume will be created. In the model it was assumed the upwards movement of this brine would be wider. What will happen with this layer remains an unknown and requires more research. Not knowing exactly what happens with the carnallite layer limits the knowledge of the layers overlying the carnallite.

The Zechstein-III Anhydrite is a hard layer that could have been slightly deformed by the production phase of the cavern. Together with the brine expansion there could be some microfractures created in the anhydrite that makes its permeability much higher and the Zechstein-III Halite is reached quite fast. On the other hand, the Anhydrite could largely still be intact and the brine has a hard time permeating through this layer. The actual permeability of the anhydrite remains difficult to predict and requires more research.

Lastly the brine could reach the Zechstein-III Halite, a roughly 200-meter-thick virgin salt (almost not influenced by the cavern) with less and discontinuous anhydrite alterations. If the brine reaches this layer, it must permeate purely by the permeability of halite. Because this permeability is so low it is questionable if this brine front will reach the overlying more permeable zone. At least within geological timescales. The Zechstein-III Halite has the largest volume in the permeation model (around 78% assuming equal porosities for each layer). The time for the brine to reach this layer is quite fast in all the scenarios. What would happen in this layer and how much brine it can store is therefore an important question for future research.

## 10. Conclusion and recommendations

### 10.1 Conclusion

The research started with a research question; this is again stated below.

- What are the cavern convergence rates in an abandoned cavern and in what timeframe will the brine permeate through the salt layers above the cavern and permeate out of the Zechstein to the overlying layers?

The cavern convergence model showed that the pressure solution creep is most significant at low pressure deficits. This is the linear part of the squeeze model and the value of this component in the WEP model is most likely on the high side or the halite around the cavern experiences a threshold pressure for salt creep to occur. What the actual creep rates are remains a question and more lab tests in the low-pressure deficit region need to be conducted to create more certainty of the behaviour of halite in low-pressure deficits. Still, it is questionable if and how these results can be extrapolated to cavern scale convergence rates. In the permeation model the permeability of halite was assessed. This turned out much lower than the cavern convergence rates predicted. Assuming the convergence model cases are correct there must be other permeation mechanisms present. These were investigated as well

The magnitude of the cavern convergence rates in an abandoned cavern is narrowed down but there remains a large uncertainty. From the ranges of the sensitivity analysis of the convergence model 3 scenarios, a P10, P50 and P90 case, were prepared with different convergence rates. The P50 convergence model in combination with the adjusted paraboloid permeation model predicted 588 years for all the Zechstein layers to fill up and reach more permeable layers. This would mean a much larger permeability in the halite compared to testing and modelling have shown. So, the cavern convergence is lower than predicted or there must be other permeation paths for the brine. The P10 convergence model assumed favourable conditions for a low linear component of the squeeze model and gives much lower convergence rates than the P90 base case model. Applying the P10 model on the adjusted paraboloid permeation model showed that it would take 12,363 years for the system to fill up. Still the permeability of halite is much lower than the permeation rate of the P10 case.

Especially in the last, Zechstein-III Halite layer, which isn't affected by the cavern production period so little to no micro fractures are present and has less and discontinuous anhydrite alterations as alternative permeation paths. Therefore, in this layer the brine must find its way by filling up the porosity of the halite. This process will most likely take longer than the P10 permeation model predicts.

To conclude, the convergence model has its assumptions, but with the right linear creep component it's accurate enough for modelling long term cavern convergence. The P10 and P50 convergence models applied on the permeation model are accurate for the layers in the Zechstein-II. Since there is some uncertainty in the carnallite it is hard to predict what happens in the Zechstein-III layers. Looking at the permeability of halite and the fact that these layers are not much affected by the cavern mining processes, the models probably are very conservative and it would take much longer for the layers to fill. The P90 convergence case gives high cavern convergence rates compared to the creep rate of halite under low-pressure deficits. Next to this the permeation of brine through layers is fast compared to the permeability of halite and is therefore an unlikely scenario.

This MSc thesis continued research done 13 years ago. It tried to combine all research done in between then and now to give an updated version of the cavern convergence and permeation processes. To a certain extent the research was a success. New models were built and tested. This gave more questions which were tried to be answered in the research. However, in the future several things could be investigated as well. These will be discussed in section 10.2.

## 10.2 Recommendations

The models made in this research tried to give a more updated version of previous models. In this time a lot of new research is done on the behaviour of salt and salt caverns during operation and after abandonment. This gave a lot of new insights and knowledge on salt cavern behaviour after abandonment. This research tried to apply the knowledge specifically on Frisia caverns. From this there are still a few unknowns, the most important ones will be highlighted in this chapter.

First in terms of the convergence model. As discussed, there is a volume balance between brine exiting the cavern and storing it in the surrounding layers. Recently there were new models made on a pressure threshold for salt creep to occur. Previously it was believed this was somewhere 1-10 MPa, a new model proposed a range of 0.07 and 0.9 MPa where below this pressure no creep would occur (van Oosterhout et al., 2022). However, evidence for this phenomenon is yet to be found in laboratory or field tests. Laboratory low-pressure creep test on salt samples from the BAS caverns could give a better understanding of the strain rates of the salt. Currently the pressure deficit is determined by the well head pressure, validating this pressure and the pressure throughout the cavern by for instance wire lining would be recommended as this influences the model significantly.

Another important aspect is the (secondary) porosity. Previous research and modelling did investigate the permeability of salt under pressure. But the porosity that is created in this process is not investigated. It could be helpful to investigate what porosity the salt has since the porosity has a substantial influence on the modelling, in different models the porosity is ranging a lot which gives a big range in the output of the models.

One thing all the models assume is that the salt around and on top of the cavern is homogenous and that there are only a few distinct layers. This is not true as discussed. For example, in the Halite layers there are small anhydrite bands present and in between the Zechstein-II and III there are carbonates and clays present. This could be a way of migration as well. Another option could be permeation via the micro-fractures created during production, question here is how many are there and to what distance do they extend? Fluids always like to go in the path of least resistance. Determining what this path is for instance laboratory testing on salt samples could clarify these dominant permeation processes.

## 11. References

Bérest, P., Bergues, J., Brouard, B., Durup, J. G., & Guerber, B. (2001). A salt cavern abandonment test.

*International Journal of Rock Mechanics and Mining Sciences*, 38(3), 357-368.

[https://doi.org/10.1016/S1365-1609\(01\)00004-1](https://doi.org/10.1016/S1365-1609(01)00004-1)

Bérest, P., Gharbi, H., Brouard, B., Brückner, D., DeVries, K., Hévin, G., Hofer, G., Spiers, C., & Urai, J.

(2019). Very Slow Creep Tests on Salt Samples. *Rock Mechanics and Rock Engineering*, 52(9),

2917-2934. <https://doi.org/10.1007/s00603-019-01778-9>

*Bodemdaling*. (Extracted on 2023, april 20). [Overzichtspagina]. Bodem+.

<https://www.bodemplus.nl/onderwerpen/bodem-ondergrond/bodemdaling/>

*Bodemdalingsvoorspellings-kaarten*. (2022, februari 10). ArcGIS StoryMaps.

<https://storymaps.arcgis.com/stories/89c12cdd9f54453ead3b9d85e71f8bdc>

Brouard, B., Bérest, P., & Karimi-Jafari, M. (2017). Deep salt-cavern abandonment. In M. Wallner, K.-H.

Lux, W. Minkley, & H. R. Hardy (Red.), *The Mechanical Behavior of Salt – Understanding of THMC*

*Processes in Salt* (1ste dr., pp. 445-452). CRC Press. <https://doi.org/10.1201/9781315106502-53>

Brouard, B., Greef, V. D., & Berest, P. (2001). *SALT PERMEABILITY TESTING RFP 98-*.

Brouard Consulting. (2019a). *KEM-17 Cavern scale*. [https://www.sodm.nl/binaries/staatstoezicht-op-de-](https://www.sodm.nl/binaries/staatstoezicht-op-de-mijnen/documenten/rapporten/2020/02/11/onderzoek-langetermijnrisicos-afsluiten-zoutcavernes/KEM-17+Cavern-scale.PDF)

[mijnen/documenten/rapporten/2020/02/11/onderzoek-langetermijnrisicos-afsluiten-](https://www.sodm.nl/binaries/staatstoezicht-op-de-mijnen/documenten/rapporten/2020/02/11/onderzoek-langetermijnrisicos-afsluiten-zoutcavernes/KEM-17+Cavern-scale.PDF)

[zoutcavernes/KEM-17+Cavern-scale.PDF](https://www.sodm.nl/binaries/staatstoezicht-op-de-mijnen/documenten/rapporten/2020/02/11/onderzoek-langetermijnrisicos-afsluiten-zoutcavernes/KEM-17+Cavern-scale.PDF)

Brouard Consulting. (2019b). *KEM-17 conclusions and recommendations*.

[https://www.sodm.nl/binaries/staatstoezicht-op-de-](https://www.sodm.nl/binaries/staatstoezicht-op-de-mijnen/documenten/rapporten/2020/02/11/onderzoek-langetermijnrisicos-afsluiten-zoutcavernes/KEM+17+Conclusions+and+Recommendations.PDF)

[mijnen/documenten/rapporten/2020/02/11/onderzoek-langetermijnrisicos-afsluiten-](https://www.sodm.nl/binaries/staatstoezicht-op-de-mijnen/documenten/rapporten/2020/02/11/onderzoek-langetermijnrisicos-afsluiten-zoutcavernes/KEM+17+Conclusions+and+Recommendations.PDF)

[zoutcavernes/KEM+17+Conclusions+and+Recommendations.PDF](https://www.sodm.nl/binaries/staatstoezicht-op-de-mijnen/documenten/rapporten/2020/02/11/onderzoek-langetermijnrisicos-afsluiten-zoutcavernes/KEM+17+Conclusions+and+Recommendations.PDF)

- Brouard Consulting. (2019c). *KEM-17 Microscale*. <https://www.sodm.nl/binaries/staatstoezicht-op-de-mijnen/documenten/rapporten/2020/02/11/onderzoek-langetermijnrisicos-afsluiten-zoutcavernes/KEM-17+Micro-scale.pdf>
- Fokker, P. A. (1995). *The behaviour of salt and salt caverns*. s.n.].
- KBB. (1994). *Geological and core report BAS 1*. Kavernen Bau- und Betriebs-GMBH.
- Lux, K.-H. (2010). *Untersuchung der konvergenzinduzierten zeitlichen und räumlichen Soleinfiltration aus der Kaverne BAS-3 in das anstehende Steinsalzgebirge*. Technische Universität Clausthal.
- Pruiksma, J. P., & Luger, H. J. (2005). *Shut-in gedrag en stabiliteit Frisia caveerne FEM berekeningen kruipgedrag*. GeoDelft (Deltares).
- Rokahr, R. B., Hauck, R., Staudtmeister, K., Zander-Schiebenhöfer, D., Crotogino, F., & Rolfs, O. (2002). *High Pressure Cavern Analysis. 2002*.
- Thoraval, A., Lahaie, F., Brouard, B., & Berest, P. (2015). A generic model for predicting long-term behavior of storage salt caverns after their abandonment as an aid to risk assessment. *International Journal of Rock Mechanics and Mining Sciences*, 77, 44-59. <https://doi.org/10.1016/j.ijrmms.2014.10.014>
- van Oosterhout, B. G. A., Hangx, S. J. T., & Spiers, C. J. (2022). A threshold stress for pressure solution creep in rock salt: Model predictions vs. observations. In S. J. T. Hangx, A. R. Niemeijer, J. H. P. de Bresser, C. J. Spiers, M. R. Drury, M. Gazzani, & P. A. Fokker, *The Mechanical Behavior of Salt X* (1ste dr., pp. 57-67). CRC Press. <https://doi.org/10.1201/9781003295808-6>
- WEP. (2004). *End of well report BAS-4*. BECi (Well Engineering Partners (WEP)).
- WEP. (2010). *Frisia bas 3 cavern abandonment*. Well Engineering Partners (WEP). <https://www.sodm.nl/binaries/staatstoezicht-op-de-mijnen/documenten/wob-verzoek/2018/09/10/wob-verzoek/3.Rapport+24+december+2010%2C+Frisia+cavern+abandonment.pdf>

WEP. (2012). *Carnallitic Brine Conversion BAS-3*. Well Engineering Partners (WEP).

<https://www.sodm.nl/binaries/staatstoezicht-op-de-mijnen/documenten/wob-verzoek/2018/09/10/wob-verzoek/5.Rapport+19+september+2012%2C+Addendum+Carnallitic+Brine+Conversion+BAS-3.pdf>

WEP. (2014). *Definitieve afsluiting van caverne BAS-3*. Well Engineering Partners (WEP).

[https://www.sodm.nl/binaries/staatstoezicht-op-de-mijnen/documenten/wob-verzoek/2019/02/07/besluit-wob-verzoek-inzake-zoutwinning-frisia-februari-2019/Bas-3+-15066666+frisia\\_definitieve\\_afsluiting\\_caverne\\_%285+november+2014%29\\_Geredigeerd.pdf](https://www.sodm.nl/binaries/staatstoezicht-op-de-mijnen/documenten/wob-verzoek/2019/02/07/besluit-wob-verzoek-inzake-zoutwinning-frisia-februari-2019/Bas-3+-15066666+frisia_definitieve_afsluiting_caverne_%285+november+2014%29_Geredigeerd.pdf)

WEP. (2020). *Review of previously applied squeeze models and description of a revised WEP squeeze model applicable for Frisia operated caverns*. Well Engineering Partners (WEP).

WEP. (2021). *Havenmond Cavern Abandonment Risks*. Well Engineering Partners (WEP).

## 12. Appendices

### Appendix 1: BAS-2 wellhead data after shut-in of the cavern

Pressure trends of the BAS-2 injection and production tubing. Shut in happened in 2003, after this the well was monitored before abandonment in 2017. In 2007 and 2009 there is a drop in pressure, this was for compressibility testing. Afterwards the pressure slowly rose and stabilized at 98% of the local in situ pressure.

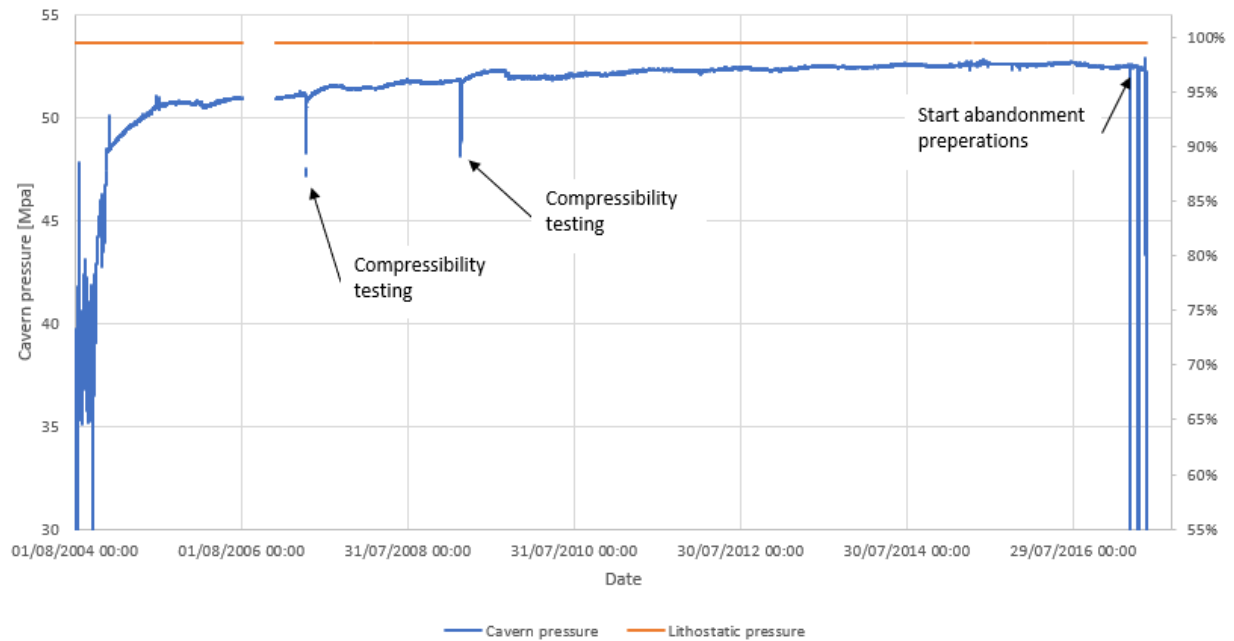


Figure 12.1 Shut in pressure data top BAS-2 cavern and lithostatic pressure at top of cavern

**Appendix 2: Comparison of WEP model and shut-in data**

*Figure 12.2 Comparison to WEP model and production data up to a deficit of 12 MPa*

### Appendix 3: High and Low linear squeeze parameters

Parameter	Low Linear	High Linear	Unit
$A_1$	$1.5 \cdot 10^{-7}$	$5.8 \cdot 10^{-8}$	$\text{MPa}^{-1}\text{day}^{-1}$
$n_1$	3.6	3.6	-
$A_2$	$1.0 \cdot 10^{-6}$	$5.1 \cdot 10^{-6}$	$\text{MPa}^{-1}\text{day}^{-1}$
$n_2$	1	1	-

Table 12.1 GeoDelft squeeze model parameters

### Appendix 4: WEP squeeze model used on Frisia operated caverns.

Parameter	WEP model	Unit
$A_1$		
$n_1$		
$A_2$		
$n_2$		
$\beta_t$ low (shape 1.5)		
$\beta_t$ high (shape 2)		

Table 12.2 WEP squeeze model parameters

# Appendix 5: Echo measurement BAS-4 17-10-2019

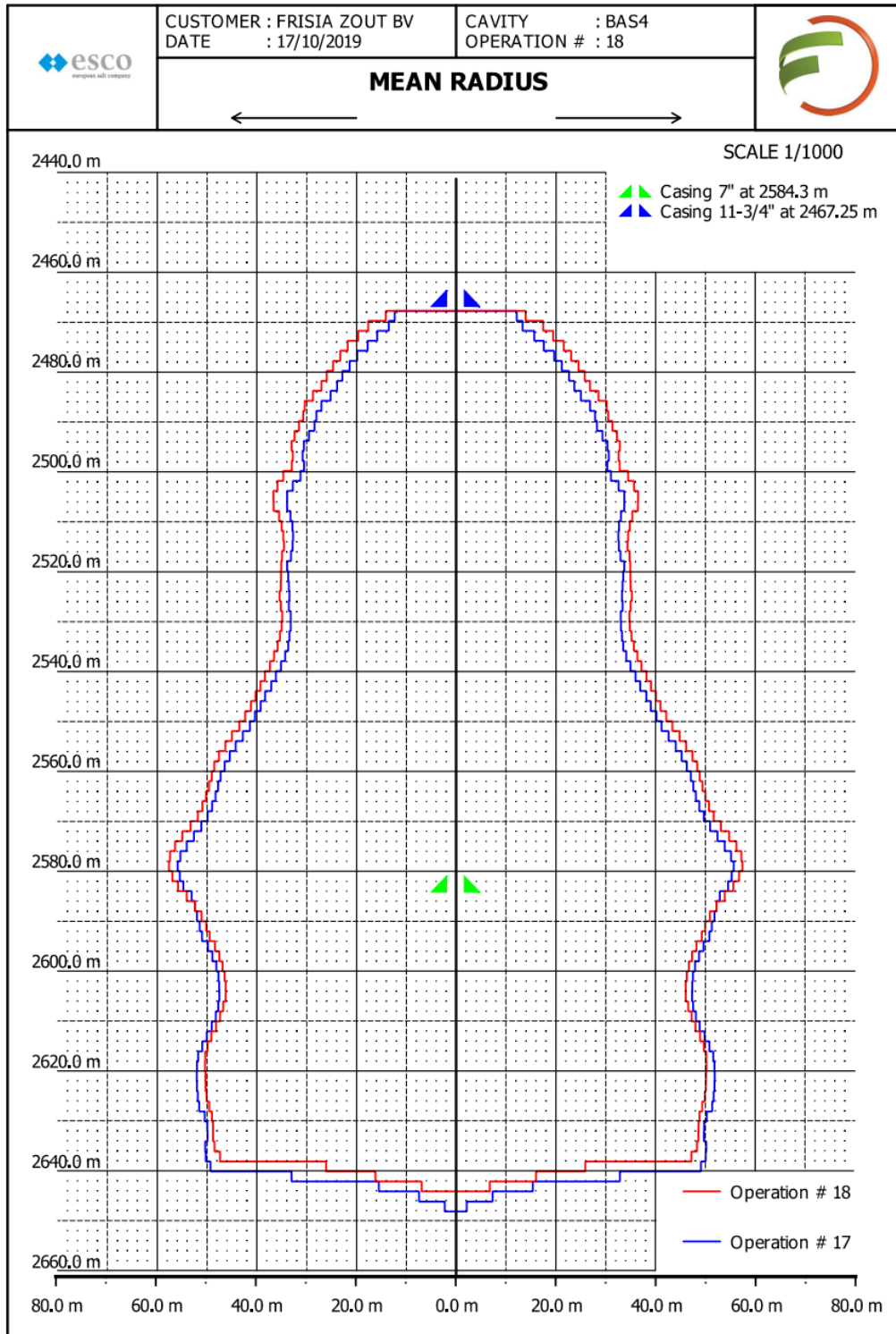
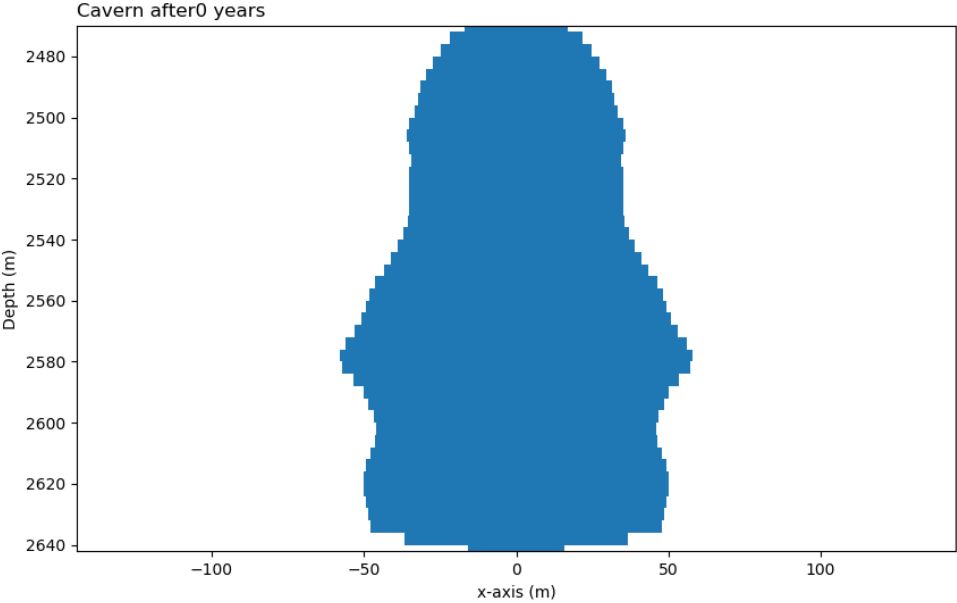
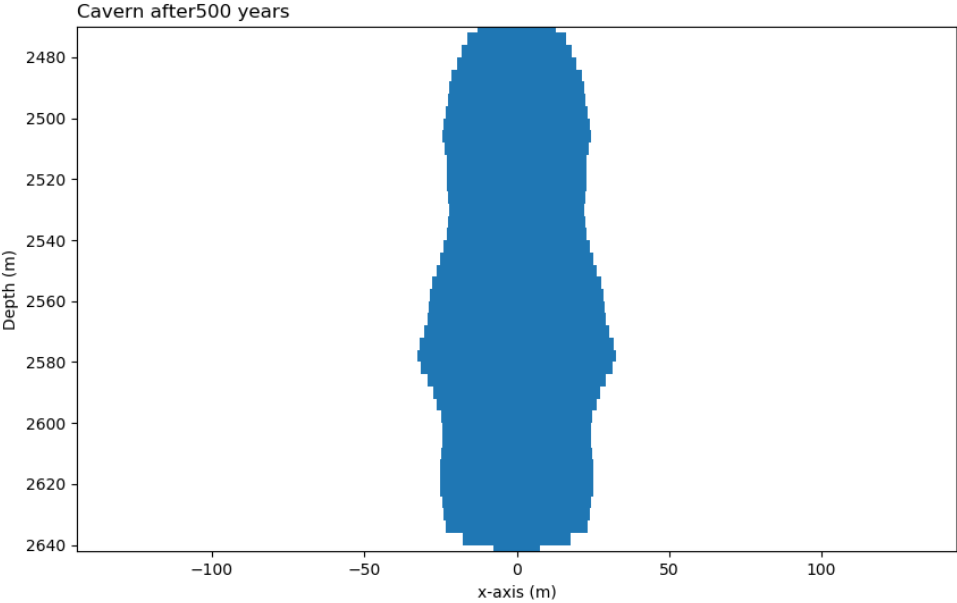


Figure 12.3 Recent echo measurement of BAS-4 Cavern

**Appendix 6: BAS-4 Base case convergence model results**



*Figure 12.4 BAS-4 Base case 2D cavern after 0 years*



*Table 12.3 BAS-4 Base case 2D cavern after 500 years*

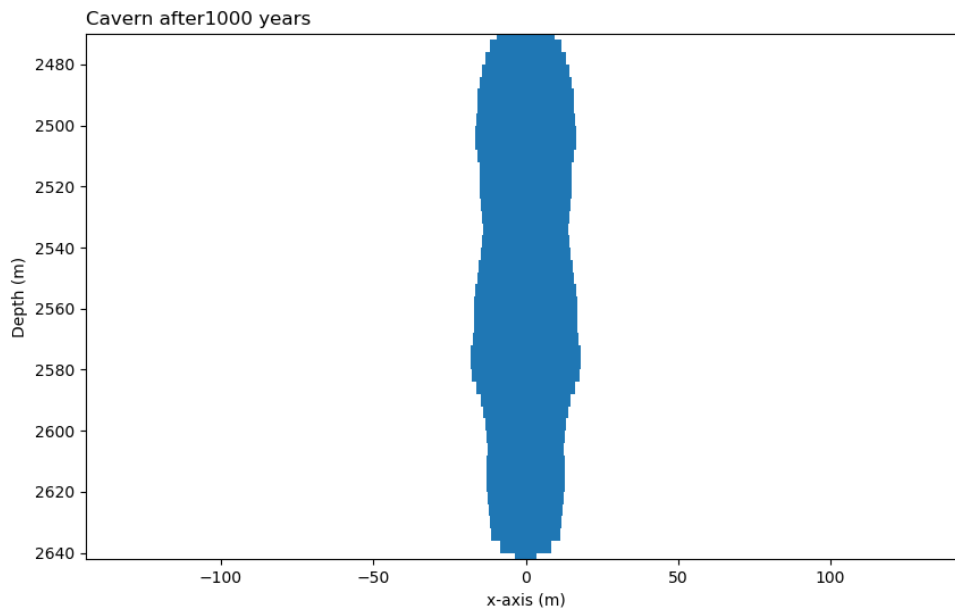


Figure 12.5 BAS-4 Base case 2D cavern after 1000 years

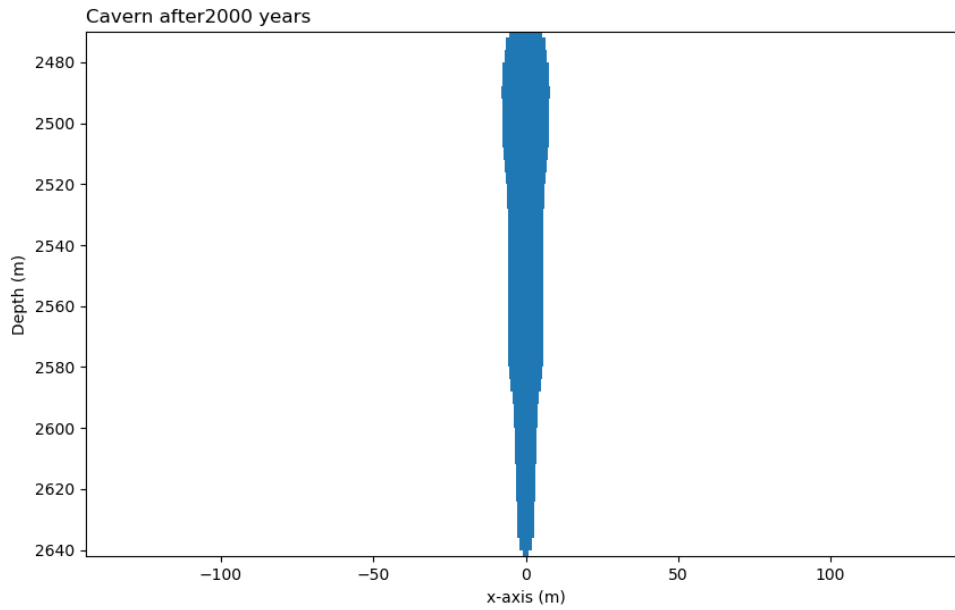


Figure 12.6 BAS-4 Base case 2D cavern after 2000 years

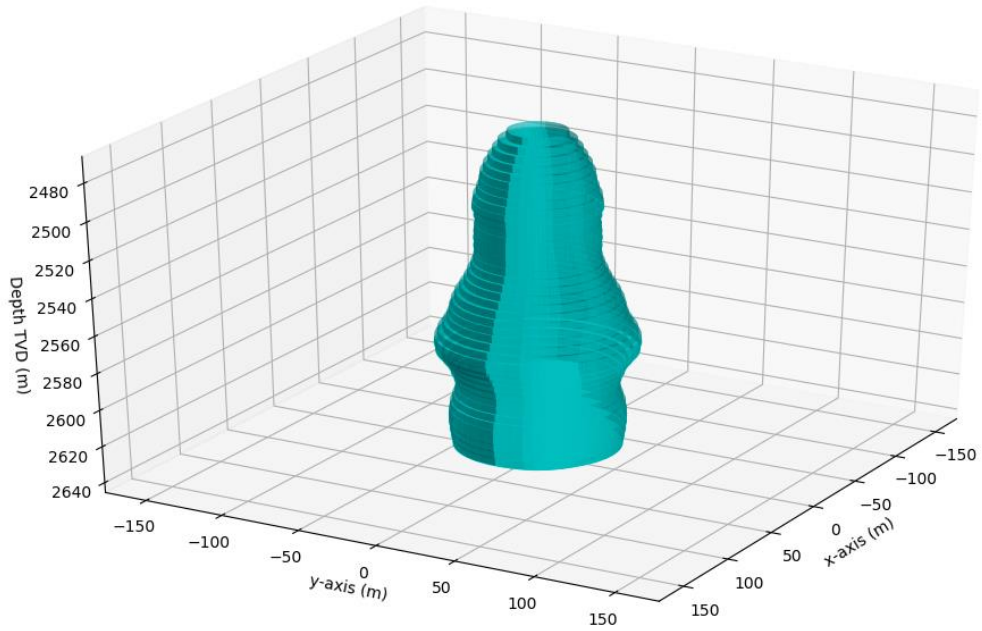


Figure 12.7 BAS-4 Base case 3D cavern after 0 years

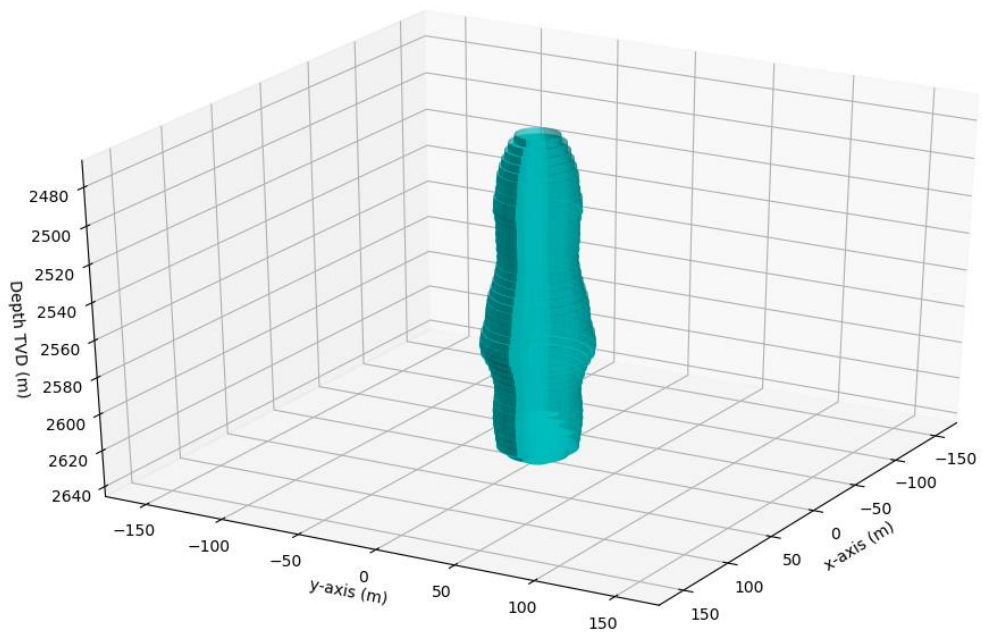


Table 12.4 BAS-4 Base case 3D cavern after 500 years

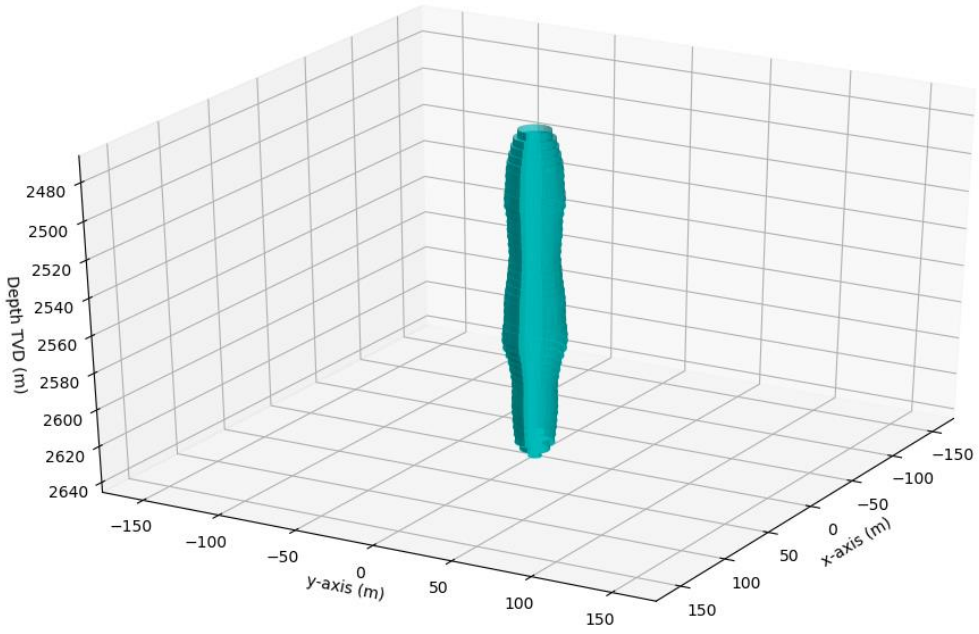


Figure 12.8 BAS-4 Base case 3D cavern after 1000 years

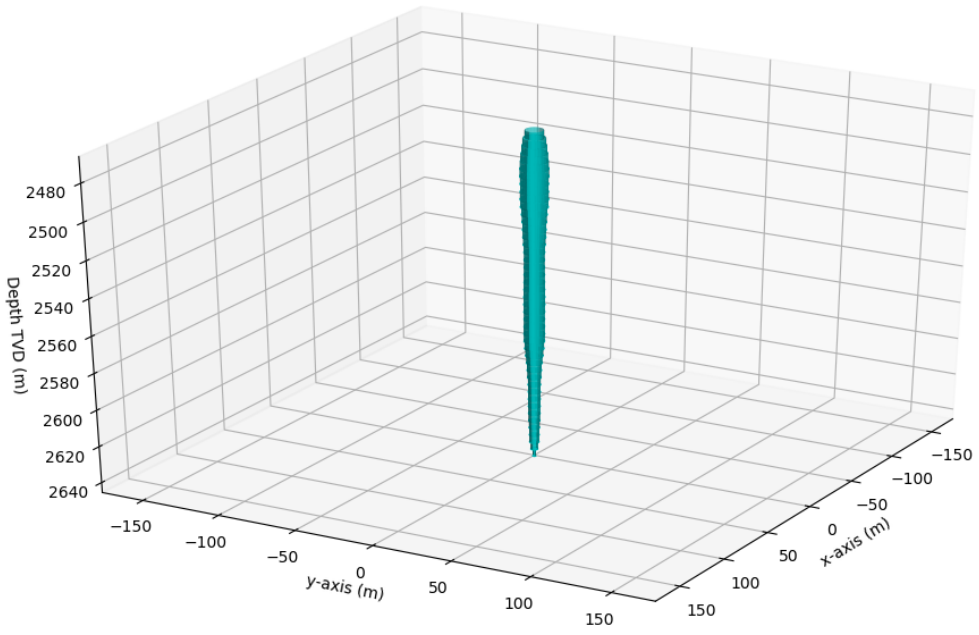


Figure 12.9 BAS-4 Base case 3D cavern after 2000 years

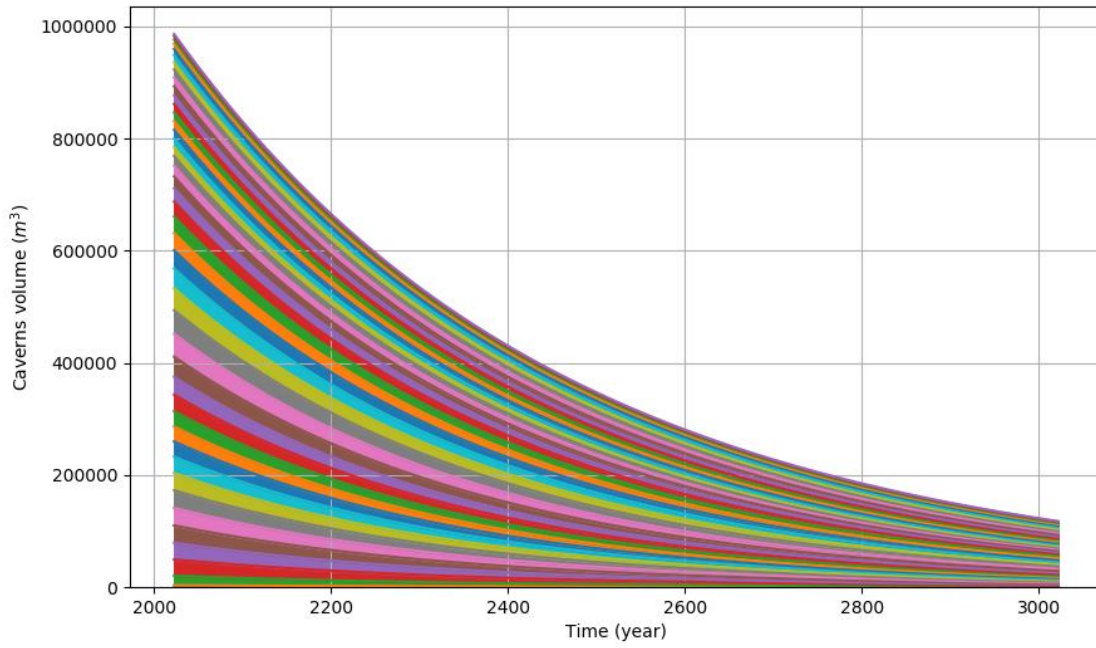


Figure 12.10 Stack plot of layers over the first 1000 years

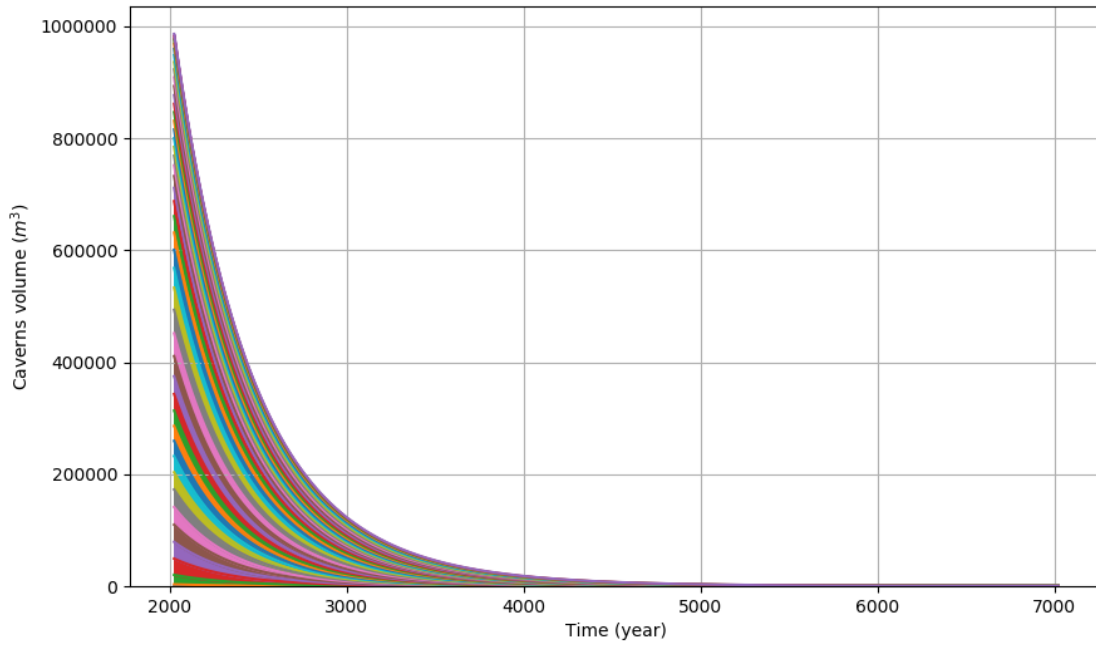


Figure 12.11 Stack plot of layers over 5000 years

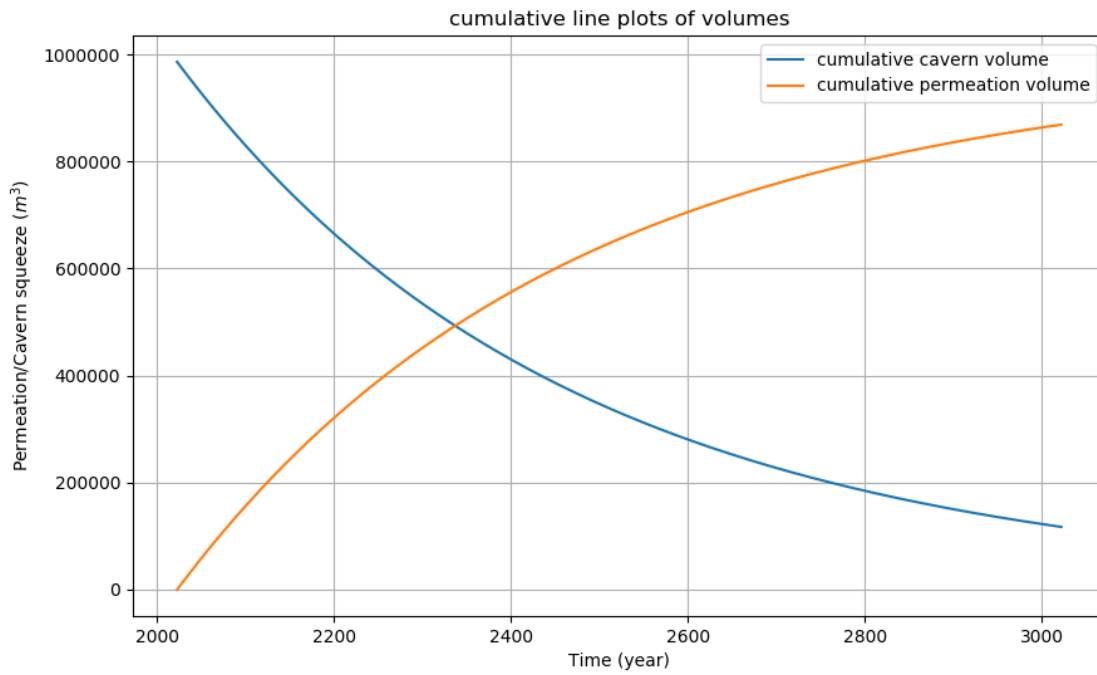


Figure 12.12 Line plot of layers over the first 1000 years

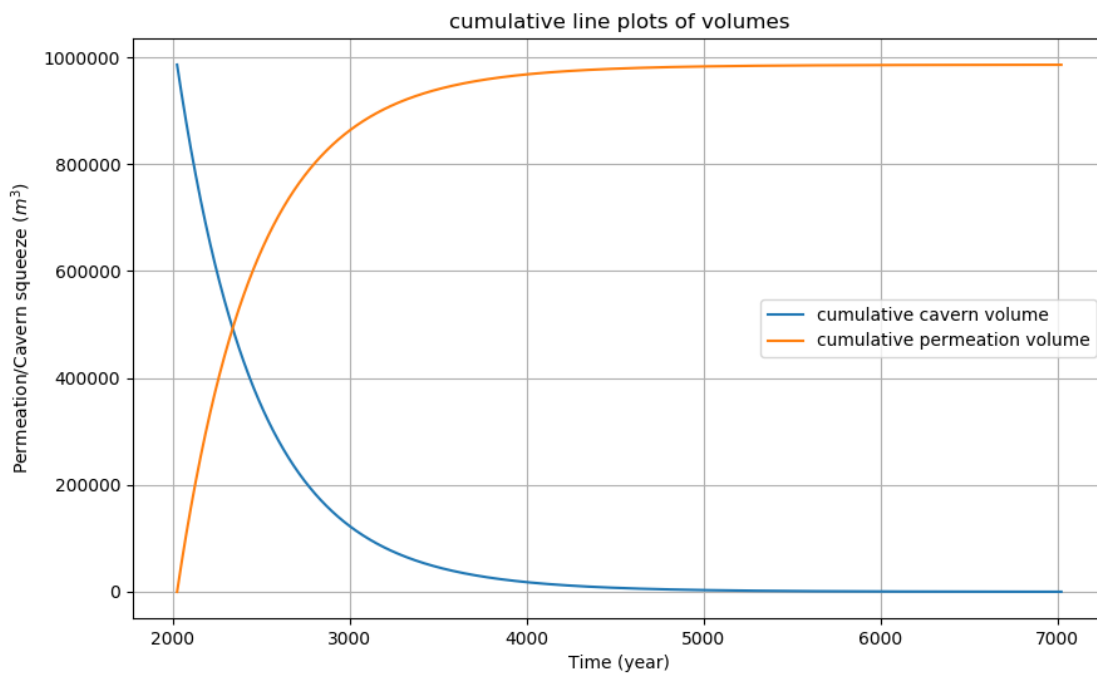


Figure 12.13 Line plot of layers over 5000 years

# Appendix 7: Sensitivity analysis convergence model

## Slice thickness

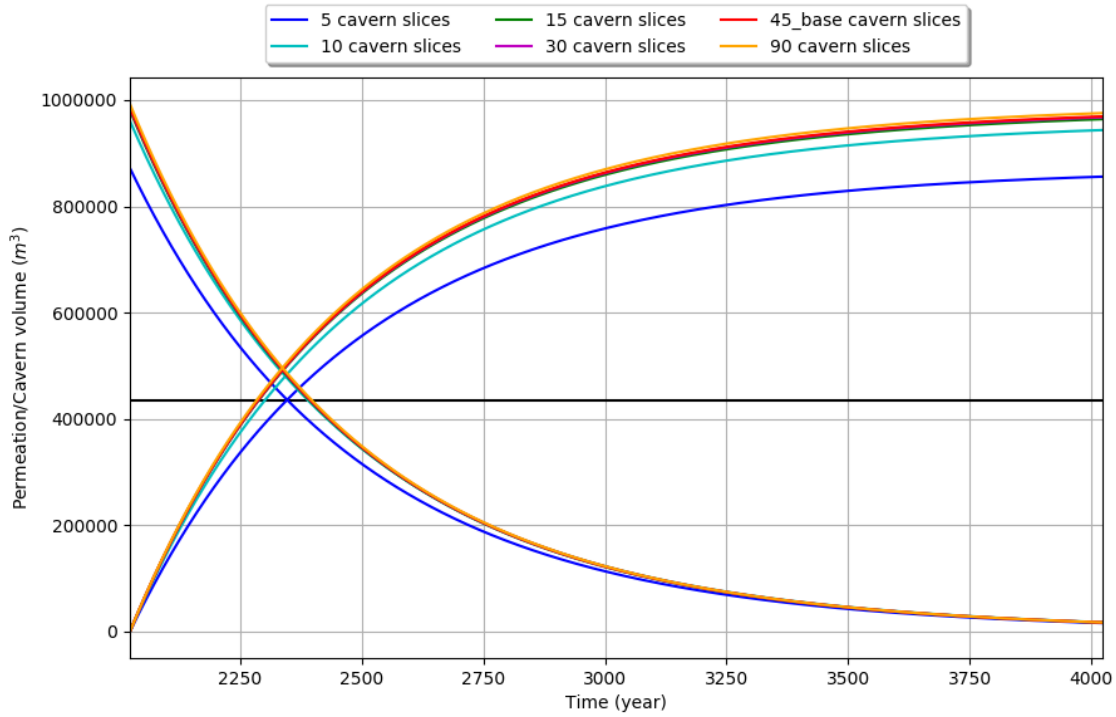


Figure 12.15 Cavern and permeation volume over time for slice thickness cases

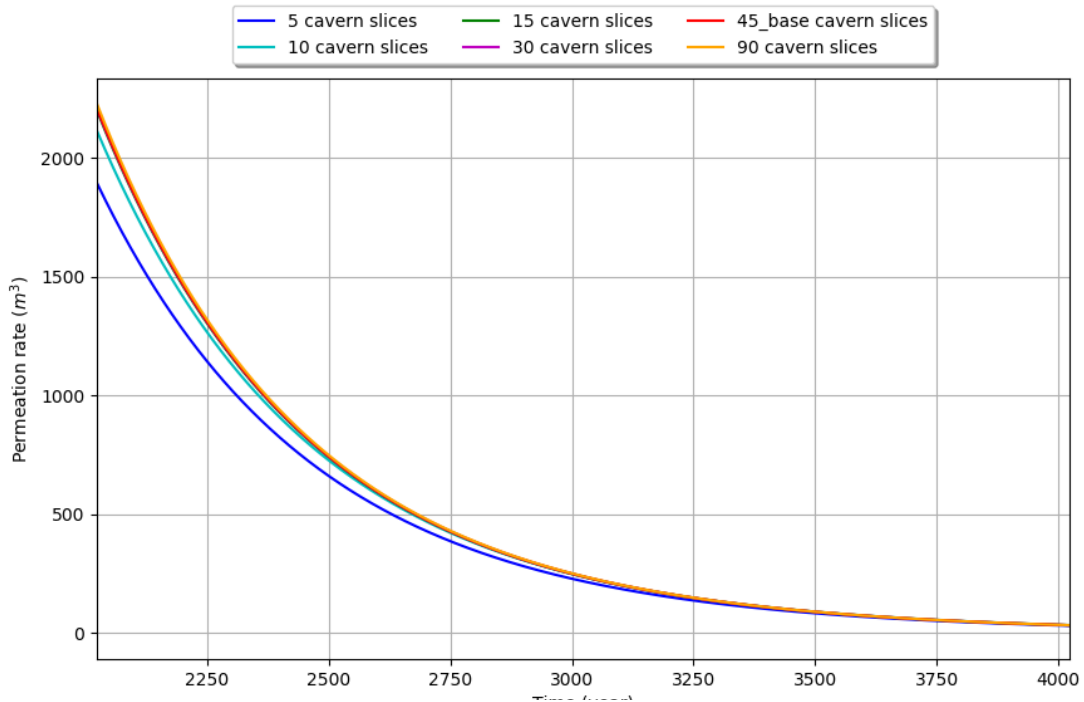


Figure 12.14 Cavern permeation rates over time for slice thickness cases

## Slice Width

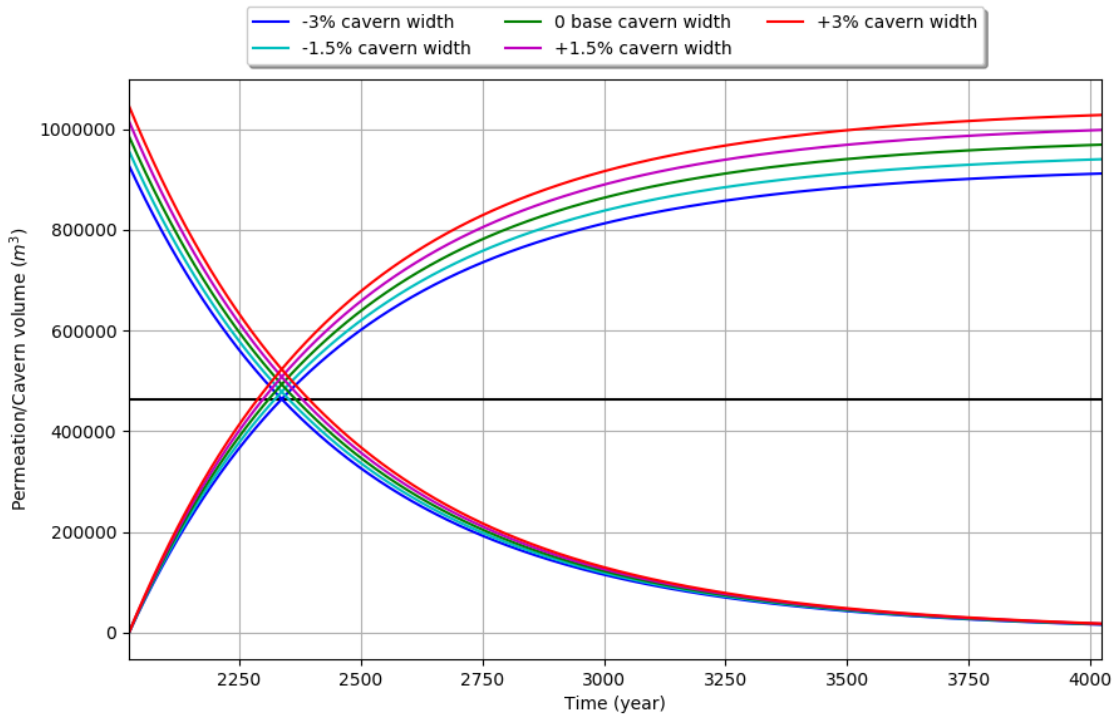


Figure 12.17 Cavern and permeation volume over time for slice width cases

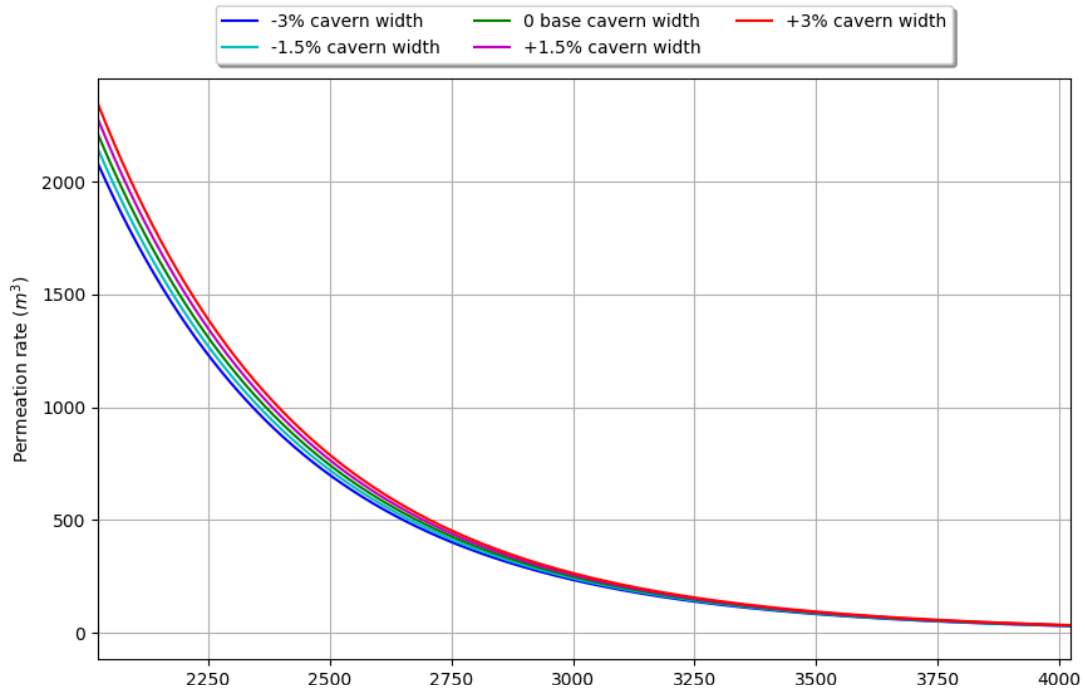


Figure 12.16 Cavern permeation rates over time for slice width cases

## Pressure deficit

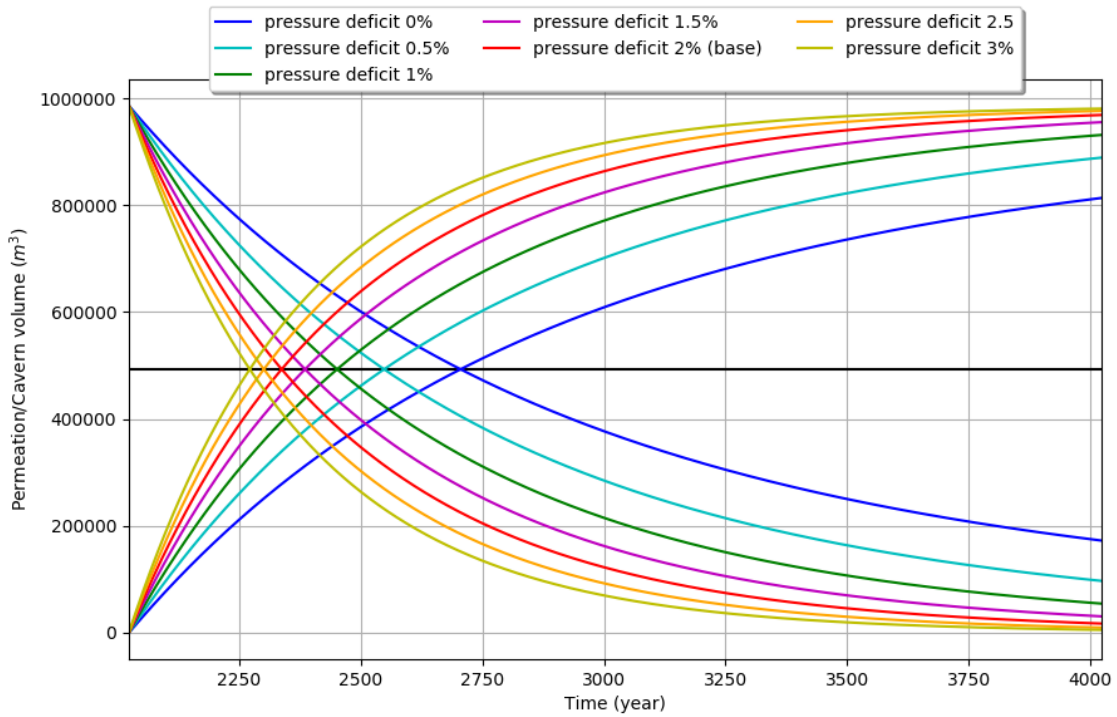


Figure 12.19 Cavern and permeation volume over time pressure deficit cases

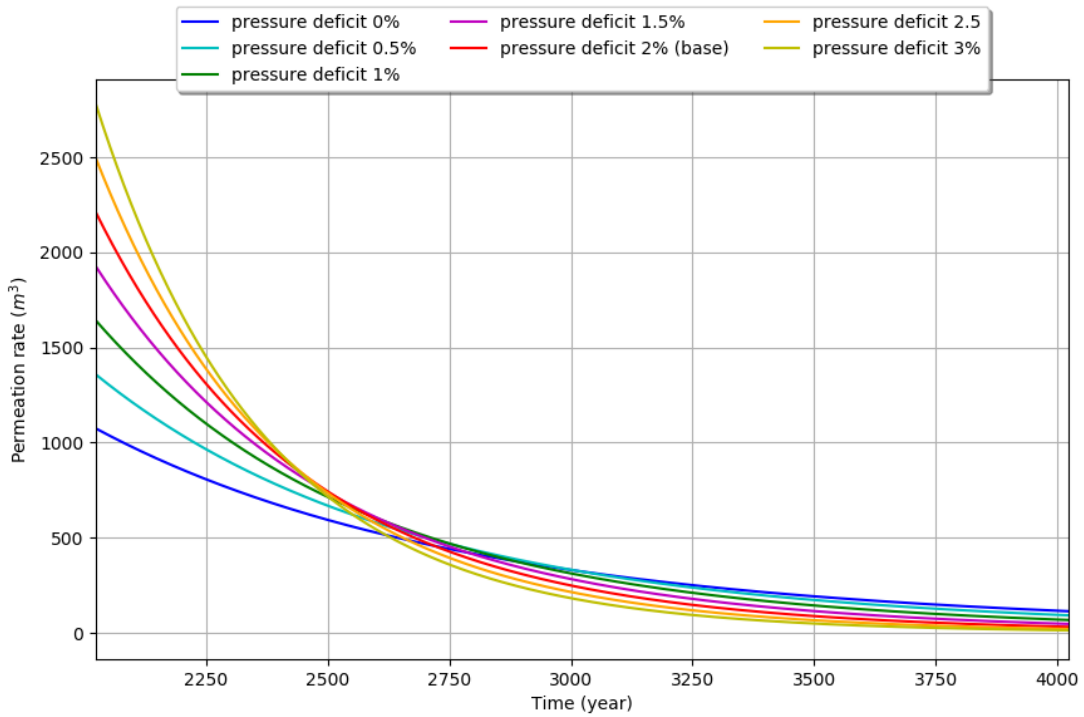


Figure 12.18 Cavern permeation rates over time for pressure deficit cases

## Specific weight lithosphere

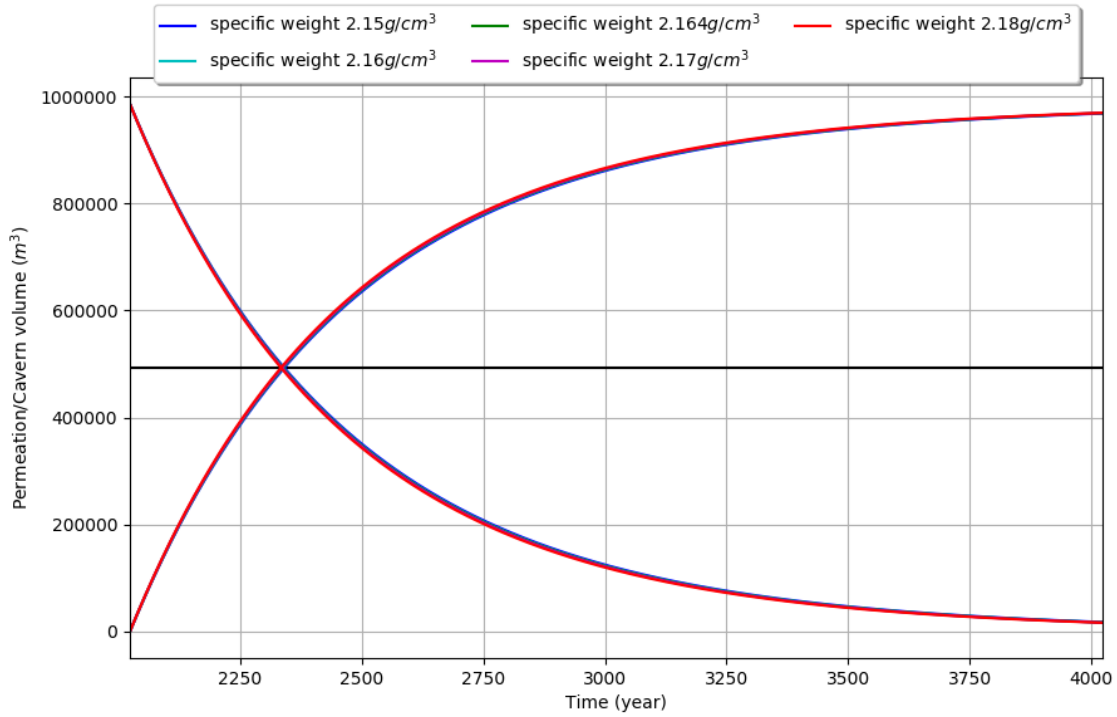


Figure 12.20 Cavern and permeation volume over time for specific weight lithosphere cases

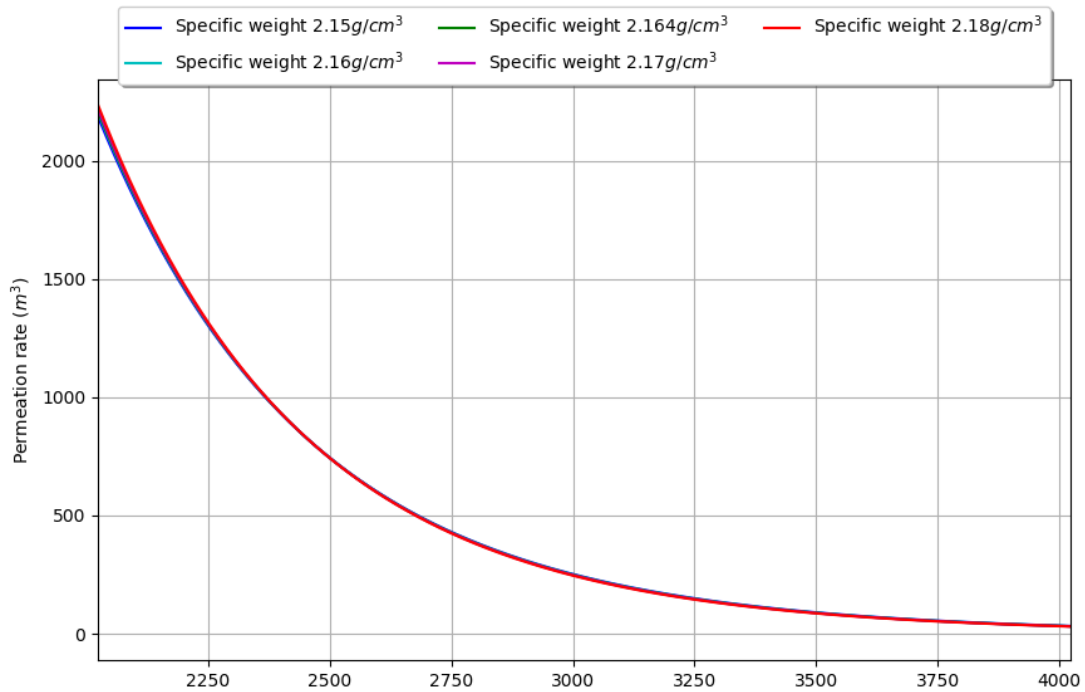


Figure 12.21 Cavern permeation rates over time for specific weight lithosphere cases

## Specific weight brine

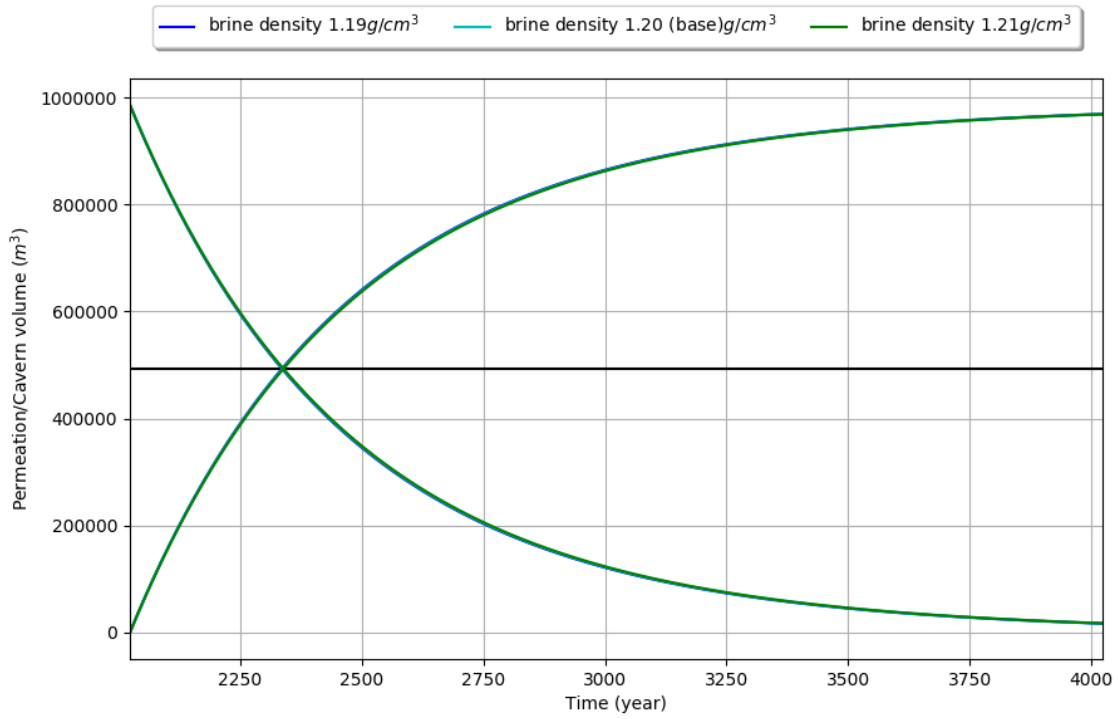


Figure 12.23 Cavern and permeation volume over time for specific weight brine cases

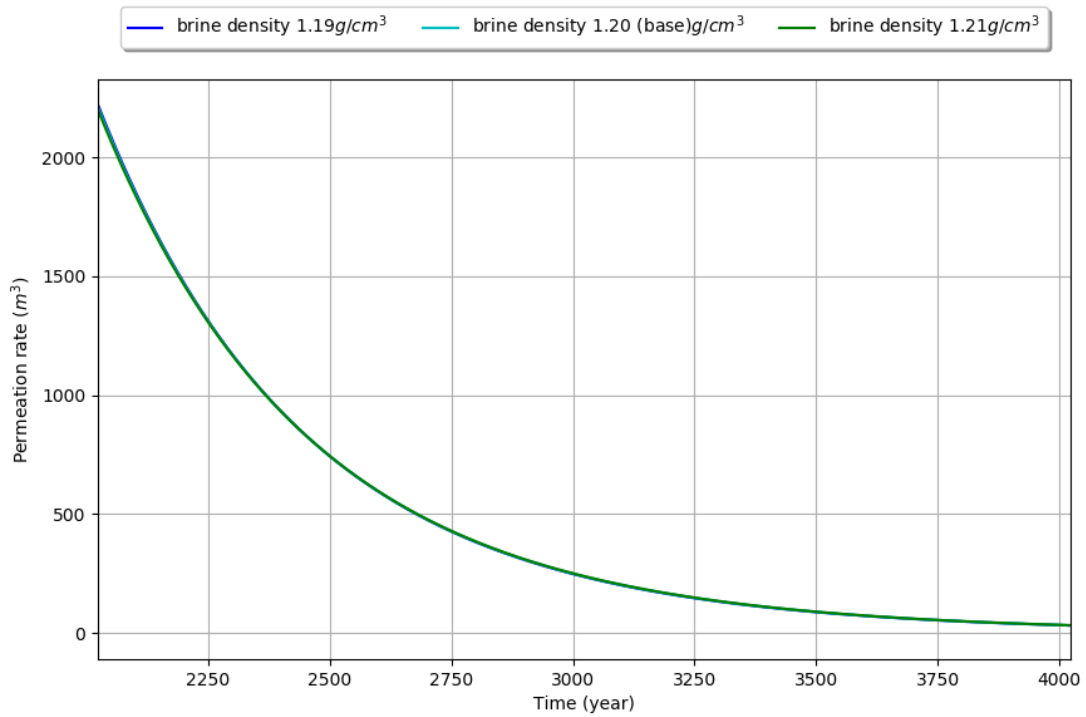


Figure 12.22 Cavern permeation rates over time for specific weight brine cases

## Nonlinear part squeeze model

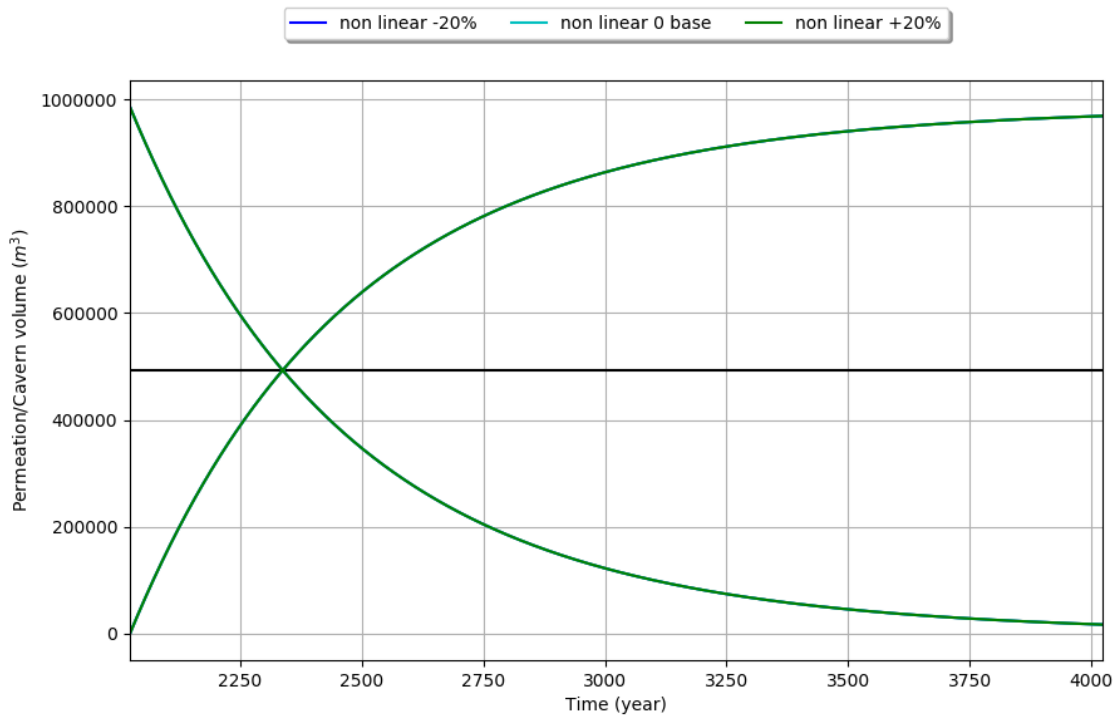


Figure 12.25 Cavern and permeation volume over time for nonlinear part squeeze model cases

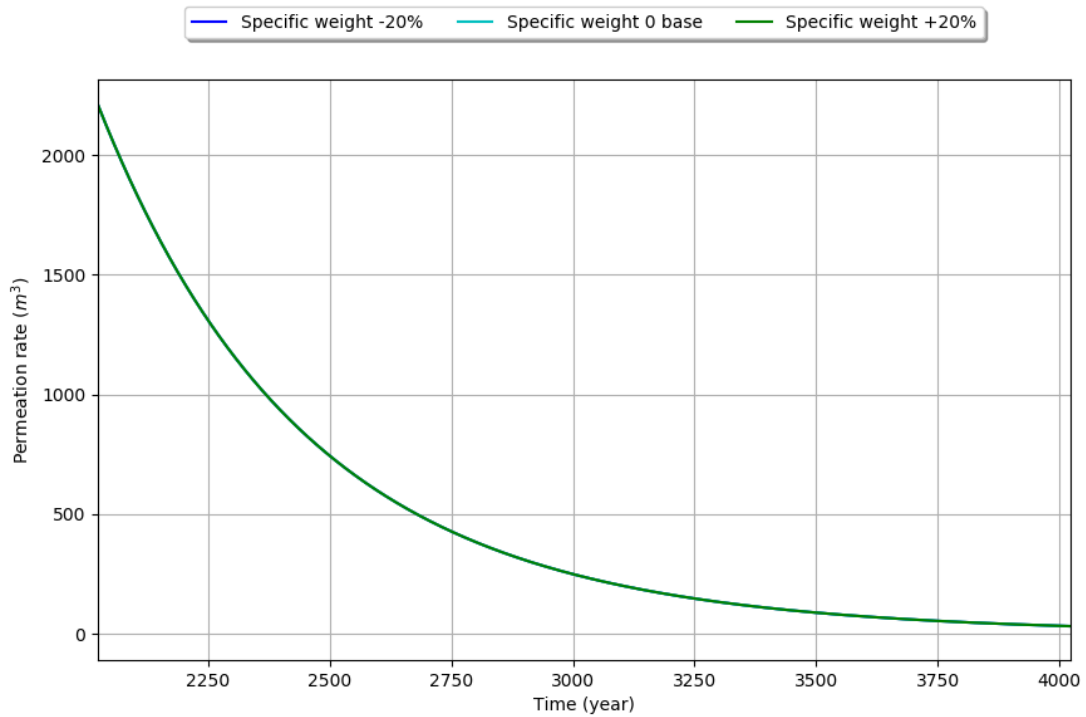


Figure 12.24 Cavern permeation rates over time for nonlinear part squeeze model cases

## Linear part squeeze model

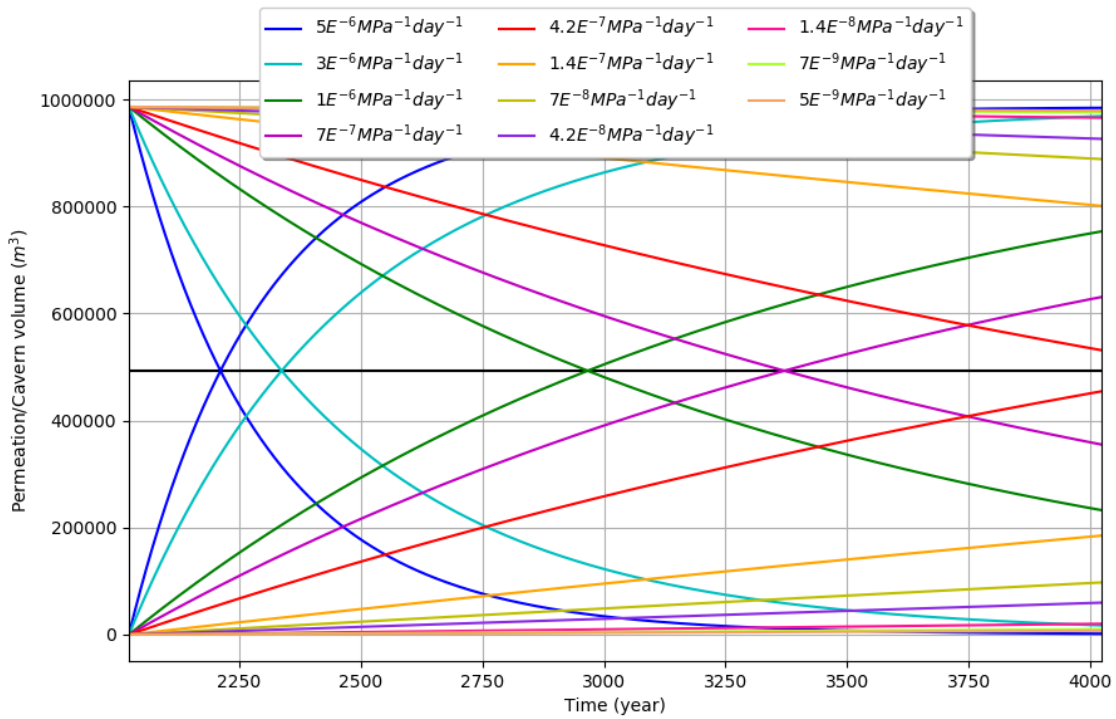


Figure 12.27 Cavern and permeation volume over time for linear part squeeze model cases

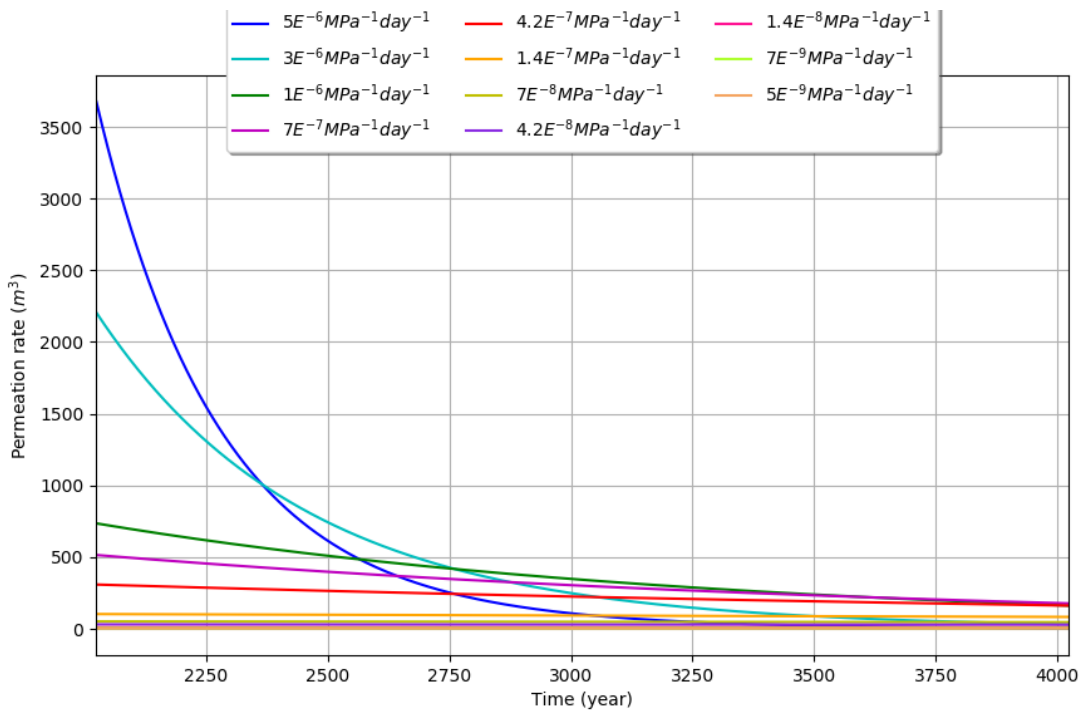


Figure 12.26 Cavern permeation rates over time for linear part squeeze model cases

## Appendix 8: Sensitivity analysis variability permeation model

Sensitivity analysis performed with P50 convergence model as an input

### Top height Zechstein-II Halite

Varying top height Zechstein-II Halite

Case	Zechstein II halite	Zechstein II Carnallite	Zechstein III Anhydrite	Zechstein III Halite
30	39	66	125	588
15	49	66	126	588
0	59	66	126	588
-15	71	71	124	586
-30	83	82	121	583

Table 12.5 Permeation model sensitivity analysis top height Zechstein-II Halite

### Top height Zechstein-II Carnallite

Varying top height Zechstein-II Carnallite

Case	Zechstein II halite	Zechstein II Carnallite	Zechstein III Anhydrite	Zechstein III Halite
50	59	54	130	592
25	59	58	126	589
0	59	66	126	588
-25	59	89	127	589
-50	59	117	131	593

Table 12.6 Permeation model sensitivity analysis top height Zechstein-II Carnallite

### Top height Zechstein-III Anhydrite

Varying top height Zechstein-III Anhydrite

Case	Zechstein II halite	Zechstein II Carnallite	Zechstein III Anhydrite	Zechstein III Halite
60	59	66	68	571
30	59	66	95	584
0	59	66	126	588
-30	59	66	160	584
-60	59	66	197	571

Table 12.7 Permeation model sensitivity analysis top height Zechstein-III Anhydrite

## Top height Zechstein-III Halite

Varying top height Zechstein-III Halite

Case	Zechstein II halite	Zechstein II Carnallite	Zechstein III Anhydrite	Zechstein III Halite
100	59	66	126	288
50	59	66	126	420
0	59	66	126	588
-50	59	66	126	792
-100	59	66	126	1035

Table 12.8 Permeation model sensitivity analysis top height Zechstein-III Halite

## Porosity Zechstein-II Halite

Varying porosity Zechstein-II Halite

Case	Zechstein II halite	Zechstein II Carnallite	Zechstein III Anhydrite	Zechstein III Halite
1.00%	300	299	300	742
0.50%	149	149	180	645
0.20%	59	66	126	588
0.10%	30	48	107	569
0.01%	3	31	91	552
0.001%	0	30	90	550

Table 12.9 Permeation model sensitivity analysis porosity Zechstein-II Halite

## Porosity Zechstein-II Carnallite

Varying porosity Zechstein-II Carnallite

Case	Zechstein II halite	Zechstein II Carnallite	Zechstein III Anhydrite	Zechstein III Halite
1.00%	59	186	247	715
0.50%	59	111	171	635
0.20%	59	66	126	588
0.10%	59	59	111	572
0.01%	59	59	97	558
0.001%	59	59	96	556

Table 12.10 Permeation model sensitivity analysis porosity Zechstein-II Carnallite

### Porosity Zechstein-III Anhydrite

Varying porosity Zechstein-III Anhydrite

Case	Zechstein II halite	Zechstein II Carnallite	Zechstein III Anhydrite	Zechstein III Halite
1.00%	59	66	369	844
0.50%	59	66	216	683
0.20%	59	66	126	588
0.10%	59	66	96	556
0.01%	59	66	69	528
0.001%	59	66	66	525

Table 12.11 Permeation model sensitivity analysis porosity Zechstein-III Anhydrite

### Porosity Zechstein-III Halite

Varying porosity Zechstein-III Halite

Case	Zechstein II halite	Zechstein II Carnallite	Zechstein III Anhydrite	Zechstein III Halite
1.00%	59	66	126	2710
0.50%	59	66	126	1328
0.20%	59	66	126	588
0.10%	59	66	126	354
0.01%	59	66	126	148
0.001%	59	66	126	128

Table 12.12 Permeation model sensitivity analysis porosity Zechstein-III Halite

## Appendix 9: Variations base case permeation model

	Zechstein II halite	Zechstein II Carnallite	Zechstein III Anhydrite	Zechstein III Halite	Total Volume
<b>Total volume (m<sup>3</sup>)</b>	3,041,217	2,515,787	5,037,073	37,766,132	48,360,209
<b>Porosity volume (m<sup>3</sup>)</b>	6,082	5,031	10,074	75,532	96,719
<b>Volume %</b>	6%	5%	10%	78%	

Table 12.13 Volumes of base case adjusted paraboloid model (for comparison)

### Case Horizontal flow in halite-II

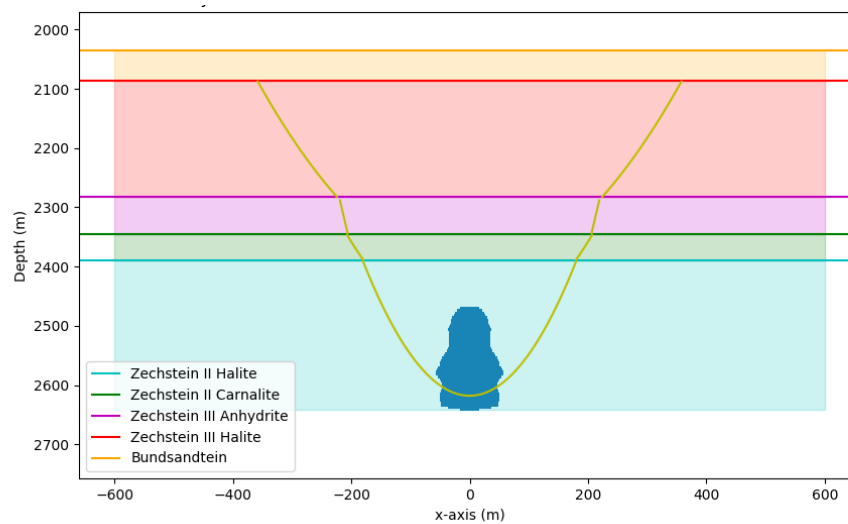


Figure 12.28 Permeation model vertical flow Zechstein-II Halite

	Zechstein-II Halite	Zechstein-II Carnallite	Zechstein-III Anhydrite	Zechstein-III Halite
a	0.007	0.004	0.01	0.0025
b	150	50	300	-60

Table 12.14 Model parameters sensitivity analysis vertical flow Zechstein-II Halite

	Zechstein II halite	Zechstein II Carnallite	Zechstein III Anhydrite	Zechstein III Halite	Total Volume
<b>Total volume (m<sup>3</sup>)</b>	10,876,392	5,218,185	8,995,479	55,171,394	80,261,450
<b>Porosity volume (m<sup>3</sup>)</b>	21,752	10,436	17,990	110,342	160,522
<b>Volume %</b>	14%	7%	11%	69%	

Table 12.15 Permeation volumes sensitivity analysis vertical flow Zechstein-II Halite

## Case Horizontal flow in Carnallite-II

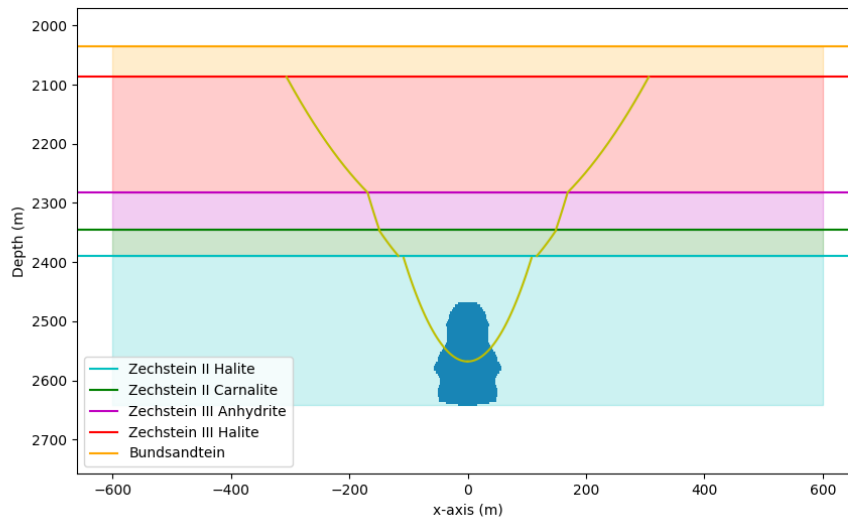


Figure 12.29 Permeation model vertical flow Zechstein-II Carnallite

	Zechstein-II Halite	Zechstein-II Carnallite	Zechstein-III Anhydrite	Zechstein-III Halite
a	0.015	0.002	0.01	0.003
b	100	-55	220	-60

Table 12.16 Model parameters sensitivity analysis vertical flow Zechstein-II Carnallite

	Zechstein II halite	Zechstein II Carnallite	Zechstein III Anhydrite	Zechstein III Halite	Total Volume
<b>Total volume (m<sup>3</sup>)</b>	3,041,217	3,179,292	7,412,117	45,976,161	59,608,786
<b>Porosity volume (m<sup>3</sup>)</b>	6,082	6,358	14,824	91,952	119,217
<b>Volume %</b>	5%	5%	12%	77%	

Table 12.17 Permeation volumes sensitivity analysis vertical flow Zechstein-II Carnallite